

CHARACTERIZATION OF STRESS-DEFORMATION BEHAVIOUR OF MUNICIPAL SOLID WASTE

**A Thesis Submitted to the
College of Graduate Studies and Research
in Partial Fulfillment of the Requirements for the
Degree of Doctor of Philosophy
in the
Department of Civil and Geological Engineering
University of Saskatchewan
Saskatoon, Canada**

**By
Manoj Kumar Singh**

PERMISSION TO USE

The author has agreed that the library, University of Saskatchewan, may make this thesis freely available for inspection. Moreover, the author has agreed that permission for extensive copying of this thesis for scholarly purposes may be granted by the professors who supervised the thesis work recorded herein or, in their absence, by the head of the Department or the Dean of the College in which the thesis work was done. It is understood that due recognition will be given to the author of this thesis and to the University of Saskatchewan in any use of the material in this thesis. Copying, publication, or any other use of the thesis for financial gain without approval by the University of Saskatchewan and the author's written permission is prohibited.

Requests for permission to copy or to make other uses of materials in this thesis in whole or part should be addressed to:

Head, Department of Civil and Geological Engineering

University of Saskatchewan,

Engineering Building

57 Campus Drive

Saskatoon, Saskatchewan,

Canada, S7N 5A9

ABSTRACT

Several catastrophic failures have occurred during the past two decades, both in engineered as well as non-engineered landfills. In addition, there are numerous instances of significant deformations, although not failure in the sense of significant and rapid downslope mass movement, which may cause sufficient damage to buried gas and leachate collection infrastructure. One such instance was observed in 1999 near the toe of a 75 m high 4H:1V slope at the Brock West Landfill in Ontario, Canada. Significant distortion of gas collection laterals was observed at this site. The present research is an in-depth study intended to examine deformation in landfills based on a detailed study of the mechanical properties of municipal solid waste.

Four research objectives were defined based on identified shortcomings and knowledge gaps in the existing literature pertaining to mechanical properties of MSW viz; (a) to develop a method for obtaining intact samples of MSW and to examine the significance of using intact and recompacted samples in characterizing the stress-deformation behaviour of MSW; (b) to characterize MSW shear strength and Young's modulus of elasticity from interpretation of triaxial test results and to determine the parameters of a non-linear elastic constitutive model as applied to MSW; (c) to measure the evolution of compressibility behaviour of MSW with degradation and verify the mechanism of secondary compression in waste; (d) to develop a simple design chart for predicting lateral deformations in landfills. A comprehensive research program was carried out to address various research objectives - field monitoring of deformations at the Brock West site; triaxial compression tests on large intact and recompacted samples

of waste; simulating waste degradation in a large laboratory compression cell; analyzing stress-strain data from various published studies and a numerical modelling study.

Interpretation of the effective stress paths followed during shearing in triaxial compression tests suggested that while recompacted samples may be sufficient to characterize shear strength parameters for use in stability analysis of landfill slopes, there might be a benefit in obtaining intact samples to evaluate the deformation characteristics of MSW. A hyperbolic model is proposed to describe the stress-deformation response of waste. The required parameters for this model were determined from evaluation of the results of numerous triaxial tests, both from this study and from the published literature.

Observations from the long-term degradation test suggested that degradation has a significant effect on the compressibility of waste and further verifies the mechanism of secondary compression in waste. The coefficient of at-rest lateral pressure was observed to maintain an essentially constant value during combined compression and degradation.

The results obtained from the experimental work were combined with the findings of a stochastic numerical modelling study and a statistical evaluation of published data and used to propose a simple design chart for estimating the maximum lateral displacement in a landfill slope. The design chart was developed using results of a finite element parametric study in which the behaviour of the municipal solid waste was modeled using a non-linear elastic hyperbolic model. The design chart incorporates non-linear variation in unit weight as well as Young's modulus with depth. The predictions from the design chart were compared with the results of field monitoring of lateral displacement in the instrumented slope at the Brock West landfill and were found to be in good agreement.

ACKNOWLEDGEMENTS

I would like to express my gratitude to my supervisor Dr. I. R. Fleming for his invaluable guidance, moral support and encouragement during the entire period of this research which cannot adequately be expressed in words in this acknowledgement. The interest and support provided by my co-supervisor Dr. J. S. Sharma especially in carrying out numerical modelling work and designing of compression cell is truly commendable. I would like to thank Dr. Fleming and NSERC for providing the financial support for this research work.

I would like to extend my acknowledgement to my advisory committee members Dr. S. L. Barbour, Dr. D. Pufahl and Dr. T. A. Fonstad for their valuable suggestions and feedback. The inputs provided by Dr. S.L Barbour, his interest and critical appraisal during the early stages of this research are invaluable. The time and support of my advisory committee chair, Dr. J. Peng is greatly acknowledged.

The help and support provided by technical staff Alex Kozlow, Doug Fisher and Brennan Pokoyoway with various equipments/instruments and analyzing samples during the entire research period is greatly appreciated. I am grateful to all my friends especially Patrick Schmidt and Chad Salewich for their support and encouragement. Their faith in me was a great source of inspiration for me.

Special thanks to my wife Seema and son Chitbhanu for their patience, understanding and constant support during the whole research program. Everything I am today and everything I have done, I owe to them. Thanks to my parents, parent-in-laws, my brothers and sisters for providing encouragement at difficult times.

TABLE OF CONTENTS

| | |
|---|-----------|
| PERMISSION TO USE | I |
| ABSTRACT | II |
| ACKNOWLEDGEMENTS | IV |
| TABLE OF CONTENTS | V |
| LIST OF TABLES | X |
| LIST OF FIGURES | XII |
| LIST OF SYMBOLS | XV |
| Chapter 1 Introduction..... | 1 |
| 1.1 Background | 1 |
| 1.2 Problem Statement..... | 7 |
| 1.3 Research Objectives | 7 |
| 1.4 Organization of this thesis | 8 |
| 1.5 References | 10 |
| Chapter 2 Literature Review..... | 12 |
| 2.1 Introduction | 12 |
| 2.2 Shear strength of MSW | 13 |
| 2.3 Compressibility characteristics of MSW | 19 |
| 2.4 Elastic Modulus | 21 |
| 2.5 Lateral stress and Poisson's ratio | 24 |
| 2.6 Types of sample and sampling techniques..... | 26 |
| 2.6.1 Laboratory vs. On-site testing and Intact vs. Recompacted samples | 26 |
| 2.6.2 Sampling Devices | 26 |
| 2.7 References | 28 |
| Chapter 3 Shear strength testing of intact and recompact samples of municipal solid waste..... | 34 |

| | | |
|------------------|---|-----------|
| 3.1 | Introduction | 35 |
| 3.2 | Equipment | 39 |
| 3.2.1 | Large Triaxial compression apparatus..... | 39 |
| 3.2.2 | Large scale Direct shear apparatus | 40 |
| 3.3 | Methodology | 41 |
| 3.3.1 | Collection of Intact MSW samples..... | 41 |
| 3.3.2 | Preparation of MSW samples for Triaxial testing | 44 |
| 3.3.2.1 | Intact samples | 44 |
| 3.3.2.2 | Recompacted samples | 44 |
| 3.3.2.3 | Consolidated undrained Triaxial tests on MSW | 45 |
| 3.3.2.4 | Direct shear test on MSW | 47 |
| 3.4 | Results and Discussions..... | 48 |
| 3.4.1 | Composition of MSW | 48 |
| 3.4.2 | Stress-strain response of MSW in Triaxial tests | 49 |
| 3.4.3 | Shear strength of MSW from Triaxial tests | 51 |
| 3.4.3.1 | Shear strength of Recompacted MSW | 51 |
| 3.4.3.2 | Shear strength of Intact MSW | 56 |
| 3.4.4 | Stress-strain behaviour of MSW from Direct shear test | 59 |
| 3.4.5 | Shear strength of MSW from Direct shear tests | 59 |
| 3.4.6 | Measured shear strength of MSW – Comparison with published literature..... | 61 |
| 3.5 | Conclusions | 63 |
| 3.6 | References | 65 |
| Chapter 4 | Application of a non-linear stress-strain model to municipal solid waste | 69 |
| 4.1 | Introduction | 70 |
| 4.2 | Review of hyperbolic stress-strain model | 72 |
| 4.3 | Methodology | 76 |
| 4.4 | MSW samples and Test equipment used in this study | 77 |
| 4.4.1 | Samples from Brock West landfill | 77 |

| | | |
|---|--|-----|
| 4.4.2 | Samples from Spadina Landfill..... | 78 |
| 4.4.3 | Method of estimating parameters for hyperbolic model from stress-strain data | 79 |
| 4.5 | Results and Discussion | 81 |
| 4.5.1 | Statistical analysis of estimated hyperbolic model parameters | 89 |
| 4.5.2 | Validation of proposed hyperbolic model parameters | 90 |
| 4.5.2.1 | Estimation of shear strength parameters | 91 |
| 4.5.2.2 | Fitting hyperbolic model to stress-strain data from triaxial tests..... | 92 |
| 4.6 | Conclusions | 95 |
| 4.7 | References | 96 |
| Chapter 5 Evolution of compressibility behaviour of municipal waste during degradation | | |
| 99 | | |
| 5.1 | Introduction | 100 |
| 5.2 | Compressibility and Elastic properties of MSW | 102 |
| 5.2.1 | Compressibility | 102 |
| 5.2.2 | Lateral stresses and At-rest lateral pressure..... | 105 |
| 5.2.3 | Constrained Modulus | 105 |
| 5.3 | Experimental set-up..... | 106 |
| 5.3.1 | Dual-purpose laboratory compression cell | 106 |
| 5.3.2 | Instrumentation | 108 |
| 5.3.3 | Calibration | 109 |
| 5.4 | Description of the MSW sample tested..... | 110 |
| 5.5 | Procedure..... | 110 |
| 5.6 | Results and Discussion | 112 |
| 5.6.1 | Degree of degradation of the waste sample during the experiment | 113 |
| 5.6.2 | At-rest lateral earth pressure | 116 |
| 5.6.3 | Constrained Modulus | 119 |
| 5.6.4 | Compressibility | 120 |

| | | |
|--|--|------------|
| 5.7 | Conclusions | 128 |
| 5.8 | References | 130 |
| Chapter 6 A design chart for estimation of horizontal displacement in municipal landfills | | |
| | 134 | |
| 6.1 | Introduction | 135 |
| 6.2 | Approach | 137 |
| 6.3 | Non-linear elastic hyperbolic (NLEH) model..... | 138 |
| 6.4 | Mechanical properties of MSW | 140 |
| 6.4.1 | Estimation of Young's modulus | 141 |
| 6.4.2 | Estimation of Unit weight | 144 |
| 6.4.3 | Estimation of shear strength parameters..... | 147 |
| 6.4.4 | Range of material properties of MSW for the development of design chart..... | 154 |
| 6.5 | Parametric study | 154 |
| 6.5.1 | Methodology | 154 |
| 6.6 | Results | 155 |
| 6.6.1 | Effect of height and sideslope on lateral deformation | 155 |
| 6.6.2 | Effect of mechanical properties of MSW | 156 |
| 6.6.2.1 | Effect of K, n and R_f | 156 |
| 6.6.2.2 | Effect of c' and ϕ' | 157 |
| 6.6.2.3 | Effect of Unit weight | 157 |
| 6.7 | Design Chart..... | 160 |
| 6.7.1 | Presentation..... | 160 |
| 6.7.2 | Validation..... | 162 |
| 6.8 | Conclusions | 163 |
| 6.9 | References | 164 |
| Chapter 7 Summary and conclusions | | 169 |

| | |
|--|-----|
| 7.1 Contribution of this research to the state of Practical and Theoretical knowledge..... | 173 |
| 7.2 Recommendations for future research | 174 |
| APPENDIX A | 176 |

List of Tables

| | |
|---|-----|
| Table 1-1 Mechanisms suggested by investigating authors for major landfill failures..... | 6 |
| Table 3-1 Shear strength parameters of MSW from literature | 38 |
| Table 3-2 Details of triaxial tests on intact and recompacted MSW samples..... | 46 |
| Table 3-3 Details of Direct Shear tests on MSW samples..... | 48 |
| Table 3-4 Shear strength parameters of MSW obtained from Direct shear and triaxial tests. | 55 |
| Table 4-1 Overview of the laboratory tests used in this paper | 82 |
| Table 4-2 Summary of estimated values of initial tangent Young's modulus E_i , ultimate deviatoric stress $(\sigma'_1 - \sigma'_3)_{ult}$, and R_f | 85 |
| Table 4-3 Summary of estimated values of hyperbolic parameters K , n , and R_f | 89 |
| Table 4-4 Summary of shear strength parameters used for the validation of hyperbolic model for MSW | 92 |
| Table 5-1 Biochemical characterization of waste used in this study | 114 |
| Table 5-2 Secondary compression ratio estimated in this study..... | 125 |
| Table 5-3 Compressibility indices of MSW from published studies | 126 |
| Table 6-1 Summary of hyperbolic model parameters K , n and R_f for MSW estimated from laboratory test results (after Singh et al. 2008)..... | 145 |
| Table 6-2 Summary and statistical analysis results of shear strength parameters for MSW estimated from published literature..... | 148 |
| Table 6-3 Elastic and shear strength properties and relative proportions of MSW constituent groups used in stochastic modelling | 150 |
| Table 6-4 Summary and statistical analysis results of shear strength parameters for MSW estimated from stochastic modelling..... | 152 |
| Table 6-5 Range of hyperbolic model input parameters used in the development of the design chart..... | 154 |

| | |
|--|-----|
| Table 6-6 Range of parameters used in the parametric study for the development of the design chart..... | 155 |
| Table 6-7 Magnitudes of maximum horizontal displacement for various combinations of parameters K , n and R_f ($H = 20$ m; $\cot(\theta) = 4$)..... | 158 |

List of Figures

| | |
|---|----|
| Figure 1-1 MSW generation rate in USA (Source EPA, 2006)..... | 2 |
| Figure 1-2 Aerial View of Payatas landfill (Philippines) failure (Source: Zekkos, 2005)..... | 4 |
| Figure 1-3 Aerial View of Payatas landfill (Philippines) failure (Source: Zekkos, 2005)..... | 4 |
| Figure 1-4 View of Bandung landfill failure (http://www.dr-koelsch.de) | 5 |
| Figure 1-5 View of Bandung landfill failure (http://www.dr-koelsch.de) | 5 |
| Figure 2-1 Shear strength envelope proposed by Kavazanjian et al. (1995)..... | 17 |
| Figure 2-2 Shear strength envelope proposed by Manassero et al. (1996) | 18 |
| Figure 2-3 Shear strength envelopes proposed by Eid et al. (2000)..... | 19 |
| Figure 3-1 Triaxial apparatus used in the present study | 40 |
| Figure 3-2 Direct shear apparatus used in the present study | 41 |
| Figure 3-3 Details of Sampler and Adaptor used in the present study | 43 |
| Figure 3-4 Frozen intact sample after its extrusion from the sampler | 45 |
| Figure 3-5 Deviatoric stress vs. axial strain plots obtained from triaxial compression tests on intact and recompacted samples of MSW: (a) Intact samples; (b) Recompacted samples | 50 |
| Figure 3-6 Stress paths and failure envelopes in deviatoric stress vs. mean effective stress space from triaxial tests on MSW: (a) Recompacted samples; (b) Intact samples | 53 |
| Figure 3-7 Extrapolation of measured deviatoric stress vs. axial strain and excess pore-water pressure vs. axial strain curves using a non-linear hyperbolic model to obtain deviatoric stress at failure for intact sample U-1 | 58 |
| Figure 3-8 Measured and extrapolated shear stress vs. shear strain plots for the direct shear tests | 60 |
| Figure 3-9 Shear strength envelopes for MSW obtained from Direct shear tests results..... | 61 |
| Figure 3-10 Shear strength envelopes for MSW (a) from present study and the literature (b) upper and lower bound failure envelope from this study and from literature..... | 62 |
| Figure 4-1 Hyperbolic stress-strain curve | 73 |
| Figure 4-2 Modulus of municipal solid waste from large-scale compression tests | 75 |

| | |
|--|-----|
| Figure 4-3 A typical example of extrapolation of stress-strain and pore pressure data taken from Caicedo et al. (2002) for $\sigma'_3 = 350$ kPa..... | 78 |
| Figure 4-4 Dual-purpose landfill compression cell (LCC) used in the present study | 80 |
| Figure 4-5 Determination of E_i and $(\sigma'_1 - \sigma'_3)_{ult}$ for selected samples from the Brock West and Spadina Landfills | 83 |
| Figure 4-6 Determination of E_i and $(\sigma'_1 - \sigma'_3)_{ult}$ for selected tests from published literature | 84 |
| Figure 4-7 Determination of parameters K and n from the present study: (a) data from testing of samples from Brock West landfill; (b) data from testing of samples from Spadina landfill | 87 |
| Figure 4-8 Determination of parameters K and n from published test results..... | 88 |
| Figure 4-9 Estimation of shear strength parameters c' and ϕ' using strength envelope in $q - p'$ space | 91 |
| Figure 4-10 Proposed hyperbolic model fitted to experimental data from Spadina landfill | 93 |
| Figure 4-11 Proposed hyperbolic model fitted to experimental data from Brock West landfill | 94 |
| Figure 4-12 Proposed hyperbolic model fitted to experimental data from published studies | 94 |
| Figure 4-13 Proposed hyperbolic model fitted to experimental data from Caicedo et al. (2002) .. | 95 |
| Figure 5-1 Dual purpose landfill compression cell (LCC) used in the present study | 107 |
| Figure 5-2 Time-settlement curve for the entire duration of the experiment (present study) | 113 |
| Figure 5-3 Cumulative gas production for the entire duration of experiment | 115 |
| Figure 5-4 Biogas composition measured during the entire duration of experiment | 115 |
| Figure 5-5 Depletion of leachate COD and ammonia during degradation | 116 |
| Figure 5-6 Variation of effective stresses during the test duration..... | 117 |
| Figure 5-7 Estimation of K_0 | 118 |
| Figure 5-8 Constrained modulus measured in present study and from published literature | 120 |
| Figure 5-9 Primary compression ratio (C_{ce}) measured in this study | 121 |
| Figure 5-10 Secondary compression for $\sigma_v = 22kPa$ | 122 |

| | |
|---|-----|
| Figure 5-11 Secondary compression for $\sigma_v = 42kPa$ | 123 |
| Figure 5-12 Secondary compression for $\sigma_v = 84kPa$ | 123 |
| Figure 5-13 Secondary compression for $\sigma_v = 180kPa$ | 124 |
| Figure 6-1 Stress-strain curve for the non-linear elastic hyperbolic (NLEH) model | 139 |
| Figure 6-2 Modulus of MSW from large compression cell | 142 |
| Figure 6-3 Range of values of unit weight profiles used in the development of the design chart | 147 |
| Figure 6-4 A typical finite element ‘unit cell’ mesh used in the stochastic modelling of MSW behaviour | 151 |
| Figure 6-5 Method of estimation of t_{ult} by extrapolating numerical results using hyperbolic curves | 153 |
| Figure 6-6 Effect of (a) height of the landfill H , and (b) horizontal stretch of the side slope of the landfill $\cot(\theta)$ on maximum horizontal displacement δh_{max} | 156 |
| Figure 6-7 Effect of combinations of parameters K , n and R_f on maximum horizontal displacement δh_{max} for effective confining stress $\sigma'_3 < 100$ kPa | 158 |
| Figure 6-8 Effect of unit weight (represented by near-surface unit weight γ_i) on maximum horizontal displacement | 159 |
| Figure 6-9 Results of the parametric study plotted in $\delta h_{max} - (H / \sqrt{\cot(\theta)})$ space (all analyses with high density) | 160 |
| Figure 6-10 Design chart for the estimation of maximum horizontal displacement δh_{max} | 161 |
| Figure 6-11 A distorted gas lateral located on the south slope of the Brock West landfill, Ontario | 162 |

List of symbols

| | | | |
|---------------------------------|---|------------------|------------------------------|
| σ'_n | normal effective stress | σ'_v | vertical effective stress |
| σ'_1 | major effective principle stress | σ'_h | horizontal effective stress |
| σ'_3 | minor effective principle stress | p' | mean effective stress |
| E_i | initial tangent modulus | E_t | tangent modulus |
| γ_i | near-surface unit weight | γ | unit weight |
| $(\sigma'_1 - \sigma'_3), q$ | deviator stress | τ | shear strength |
| $(\sigma'_1 - \sigma'_3)_f$ | deviator stress at failure | τ_{ult} | ultimate shear strength |
| $(\sigma'_1 - \sigma'_3)_{ult}$ | ultimate deviator stress | ε_a | axial strain |
| E_0 | constrained modulus | ν | Poisson's ratio |
| K_0 | at-rest lateral pressure | δh_{max} | maximum lateral displacement |
| c' | apparent cohesion expressed in terms of effective stresses | | |
| ϕ' | angle of shearing resistance expressed in terms of effective stresses | | |
| C_c | primary compression index (expressed in terms of void ratio) | | |
| C_α | secondary compression index (expressed in terms of void ratio) | | |
| C_{ce} | primary compression ratio (expressed in terms of axial strain) | | |
| $C_{\alpha e}$ | secondary compression ratio (expressed in terms of axial strain) | | |
| n | exponent governing the rate of variation of E_t with σ'_3 | | |
| K | modulus number | | |

CHAPTER 1 INTRODUCTION

1.1 Background

Historically, geotechnical investigations of the stability of municipal waste landfills have been the exception rather than the norm, since landfills were generally constructed with relatively flat side-slopes (flatter than 3H: 1V) and low heights. Stability has not been, in general, a significant issue and more attention has been paid to environmental aspects of design.

Population growth coupled with economic development, rapid urbanization, and improvements in living standards have contributed to the tremendous growth in municipal solid waste (MSW) production. This trend is limited not only to industrialized countries. Developing countries also exhibit a similar trend. The USEPA reports an increase in waste production more than 200% in the USA from 1960 to 2006 (EPA 2006, Figure 1-1). The combined industrial and domestic generation of waste on a worldwide basis is rated approximately as 1.4 to 2.2 kg/capita/day (Koerner and Soong 2000). These facts coupled with escalating costs for land for handling waste, have led operators to accommodate more waste by expanding the existing facilities both horizontally and vertically by building steeper side-slopes.

As the height of landfills increases, higher shear stresses develop and consequently higher shear strengths must be mobilized within the MSW to ensure stability of the landfill. Since MSW represents the largest structural element in a sanitary landfill, its

contribution to the overall stability of the landfill is likely to be substantial. From a serviceability point of view, the compressibility characteristics of MSW are important. The high compressibility of MSW may lead to large pre- and post-closure settlements, resulting in surface accumulation of water, and the development of surface cracks and failure of the cover system. Excessive lateral deformation can also significantly affect the integrity of gas collection systems installed for gas recovery and mitigation of greenhouse gas emissions.

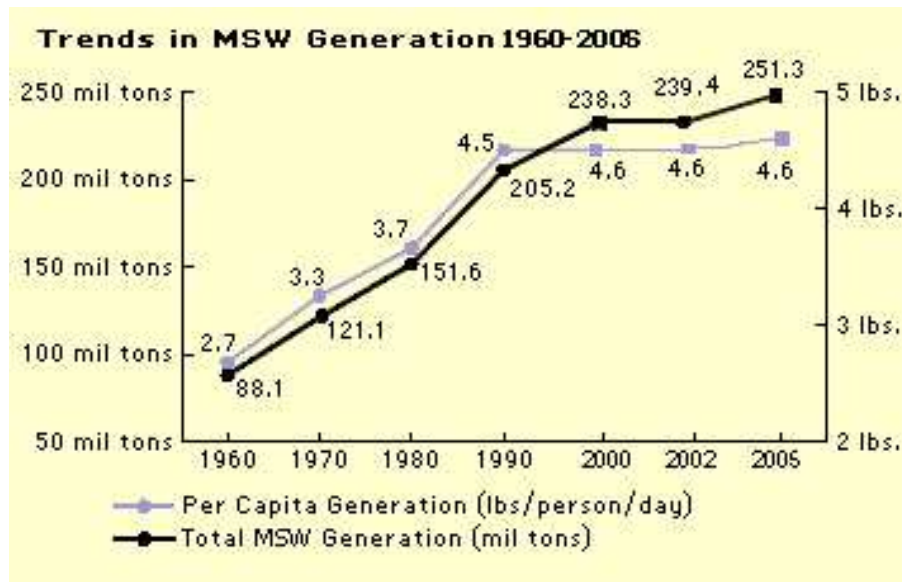


Figure 1-1 MSW generation rate in USA (Source EPA, 2006)

Over the past two decades, catastrophic failures have occurred in both engineered as well as non-engineered landfills. Apart from causing environmental damage, these failures have been responsible for causing the loss of hundreds of lives especially in developing countries. Some of these failures shown in Figure 1-2 to Figure 1-5 have been well documented (Kocasoy and Curi 1995, Brink et al. 1999, Hendron et al. 1999, Eid et al. 2000, Koerner and Soong 2000, Kolsch et al. 2005, and Merry et al. 2005) while many

remain as unpublished reports. Post-failure investigations (Table 1-1) have highlighted some common triggering factors such as high pore pressures (resulting from leachate injection or excessive infiltration due to poor surface drainage) and inadequate interface shear strength (waste- foundation soil, waste- geosynthetics or within composite liner system). It is interesting to note in Table 1-1 that the shear strength of waste has generally been found to be adequate in all these investigations. This suggests that if the landfill is correctly engineered and monitored, it is unlikely to experience catastrophic failure during its service life unless the operating conditions change significantly. However, there could still be lateral deformations which do not constitute failure in the sense of significant and rapid downslope mass movement, but may cause sufficient damage to buried infrastructure in the landfill in response to changes in the mechanical properties of the waste over time.

Satisfactory performance of these facilities from an environmental perspective requires that each installed component be designed to accommodate the anticipated deformations associated with such changes over time in the mechanical properties of the waste. However, knowledge of the evolution of the mechanical properties of waste with time is incomplete and this complicates the design and operation of these facilities. It is therefore important to be able to characterize the changes occurring in the mechanical properties of waste as it degrades. It is evident from the above discussion that safe operations of landfills will require prudent engineering analyses and such analyses will require a thorough characterization of the mechanical properties of municipal solid waste.



Figure 1-2 Aerial View of Payatas landfill (Philippines) failure (Source: Zekkos, 2005)



Figure 1-3 Aerial View of Payatas landfill (Philippines) failure (Source: Zekkos, 2005)



Figure 1-4 View of Bandung landfill failure (<http://www.dr-koelsch.de>)



Figure 1-5 View of Bandung landfill failure (<http://www.dr-koelsch.de>)

Table 1-1 Mechanisms suggested by investigating authors for major landfill failures

| Year | Landfill location | Qty involved(m ³) | Investigation and suggested triggering mechanism | Reference |
|------|---|-------------------------------|--|--|
| 1984 | North America (Unlined) | 110,000 | Single rotational failure.Heavy rainfall for 3-days, deep vertical cracks opened at the top of the waste in a section underlain by soft soil.Rise in phreatic surface from +0.0m to +3.2m within the waste mass | Reference from Koerner & Soong (2000) |
| 1988 | Kettleman Hills (Composite Liner) | 490,000 | Translational failure developed by sliding along interfaces within the multi-layer liner system, within the clay layers that form part of the liner system and along combinations of liner interfaces and through the caly. | Mitchell et al (1990) and Seed et al. (1990) |
| 1989 | North America (Unlined) | 500,000 | Multi-rotational failure. Landfill expansion activity, removal of stiff clay overburden exposing the soft clay as the remaining foundation material, approximately 120mm of rainfall for 10 days; six sequential large crevasses opened up in the waste mass | Reference from Koerner & Soong (2000) |
| 1989 | Verona, Italy (composite liner) | | Progressive failure occurring on slip surfaces located entirely in the shallower part of the upper clay layer of the composite liner system. | Mazzucato et al. (1999) |
| 1993 | Istanbul (Unlined) | 470,000 | Translational failure initiated by shear instability of uncompacted waste which was exacerbated by heavy rainfall, landfill gas liberated during movement caught fire resulting in explosion, which further accelerated the movement | Kocasoy and Curi (1995) |
| 1994 | Europe (Lined) | 60,000 | Translational failure. Failure surfaces were the geomembrane to CCL interfaces along the base and the back slope. It was reported that the geomembrane was placed during a very wet period when the CCL was already at high water content | Reference from Koerner & Soong (2000) |
| 1996 | Rumpke ,USA (Unlined) | 1,200,000 | Translational failure. Native soils on the bottom and sides of the ravine were not excavated prior to waste placement, mobilization of postpeak shear strength in the brown native soil was the suggested primary reason for failure | Eid et al. (2000) |
| 1997 | Bulbul Drive landfill, South Africa (Lined) | 300,000 | Translational failure. Piggyback expansion; failure surface was the sloping old-to-recent waste interface, along which the liquid waste saturated the edge-control wood bark berms. From here, the failure surface then transitioned to the liner system beneath the waste with the actual slip surface being the upper geotextile-to-geomembrane interface. | Blight (2004) |
| 2000 | Payatas, Phillipines (Unlined) | 15,000 | Rotational failure.The failure was preceede by large quantities of precipitation ten days prior to the incidence. Preliminary stability analyses suggest that landfill gas-pore water interaction in saturated waste may have been a significant factor in the triggering of the slope failure. | Merry et al. (2005) |
| 2005 | Bandung,Indonesia (Unlined) | 2,700,000 | Translational failure happened after 3 days of heavy rain. The stability analysis suggested that the failure was triggered by water pressure in the soft subsoil in combination with a severe damage of tensile elements due to a smouldering landfill fire | Koelsch et al (2005) |

1.2 Problem Statement

This research originates, in part, from observations of apparent instability at the Brock West Landfill site in Ontario, Canada. These deformations led to the distortion of several buried gas laterals. The Brock West site was the first landfill in Canada to implement landfill gas (LFG) fired electricity generation (Environment Canada 2007) and observations at this site might be useful for other such facilities involved with rapid stabilization and LFG extraction. Over the past several years, this facility has experienced a significant reduction in the quantity of LFG collected, despite the relatively recent placement of the waste which would tend to suggest that stable gas generation should persist for some time. It is hypothesized that this observed decline in LFG collection may not solely reflect an actual decrease in gas generation but also decreased collection efficiency due to ‘pinching off’ of gas laterals and deformation of vertical gas wells associated with on-going vertical and lateral deformations. If this hypothesis is correct, uncollected gas must be associated with uncontrolled emissions from the site with potentially significant consequences.

It is, therefore, important to examine the mechanism of MSW deformation of such facilities. The current research, in a broad sense, is aimed at examining the mechanism of deformation in MSW so that serviceability of operational structures can be maintained.

1.3 Research Objectives

Based on the shortcomings and knowledge gaps identified in the existing literature pertaining to mechanical properties of MSW and as part of investigation into the

observed movement at the Brock West landfill, the following specific objectives were identified for this research:

- (i) Develop a method for obtaining intact samples of MSW and examine the significance of using intact versus recompacted samples in characterizing the stress-deformation behaviour of MSW.
- (ii) Characterize MSW shear strength and Young's modulus of elasticity from interpretation of triaxial test results and determine the parameters of a non-linear elastic constitutive model as applied to MSW.
- (iii) Measure the evolution of compressibility behaviour of MSW with degradation and verify the mechanism of secondary compression in waste.
- (iv) Develop a simple design chart for predicting lateral deformations in landfills.

1.4 Organization of this thesis

The thesis is presented in a “manuscript style” format i.e. the various chapters of this thesis have been submitted to journals as a manuscript for possible publication as an article. Repetition of some figures and tables, therefore, might be expected amongst various chapters. An introductory chapter (the current chapter) and a chapter containing a brief review of the literature (chapter 2) are provided at the outset of this thesis which provides the context for this research work. The thesis concludes with chapter 7 which summarizes overall conclusions and contributions derived from this research work. A preface is included in the beginning of each chapter which discusses the contents covered

in that chapter and elucidates its relevance in meeting the specific research objectives. The chapters comprising this thesis are presented as follows:

Chapter 2 presents a brief review of published works regarding the important mechanical properties of waste. The purpose is to provide an overview of the findings that have been reported by various researchers and to identify the existing knowledge gaps. This chapter also presents a brief overview of the types of waste used for preparing samples and, the sampling techniques used by various researchers.

Chapter 3 describes a method for characterizing shear strength of MSW. A method for obtaining intact samples of waste from the landfill is also developed. The results of laboratory and field testing of large samples of MSW are presented and the shear strength of waste is interpreted from stress paths. The significance of using intact versus recompacted samples in determining the stress-strain behaviour of waste is also discussed.

Chapter 4 describes a non-linear elastic constitutive model of landfilled municipal solid waste and provides a method for estimating Young's modulus for MSW. The required parameters of this model are evaluated from the results of numerous triaxial tests both from this research program and from published literature.

Chapter 5 presents the results of a long-term experimental study of the effect of degradation on the compressibility behaviour of MSW. The mechanism of secondary compression in waste is also explained.

Chapter 6 describes the development of a simple design chart to estimate the maximum expected lateral displacement within a landfill. The mechanical properties of

MSW used in the development of this design chart were obtained from the results of laboratory testing data, stochastic numerical modelling and published studies, discussed in earlier chapters and the chapter itself. The design chart incorporates non-linear variations in unit weight and Young's modulus with depth.

Chapter 7 provides a brief summary of the thesis highlighting major conclusions. The contribution of this thesis to the current state of practical and theoretical knowledge and the scope for further studies and research work are presented.

Appendix A provides a list of articles originating from this research program which have been submitted to various journals and presented in conferences.

1.5 References

- Blight, G.E. 2004. A flow failure in a municipal solid waste landfill- the failure at Bulbul, South Africa. Proc. Advances in Geotechnical Engineering- The Skempton Conference, Eds. Jardin, R.J., Potts, D.M. and Higgins, K.G., Thomas Telford, 777-788.
- Brink, D., Day, P. W. and du Preez, L. 1999. Failure and remediation of Bulbul Drive landfill: Kwazulu-Natal, South Africa. Proc. 7th International Waste management and Landfill Symposium, Sardinia, Italy, 555-562.
- Eid, H.T., Stark, T.D., Evans, W.D. and Sherry, P.E. 2000. Municipal solid waste slope failure – I: Waste and foundation soil properties. Journal of Geotechnical and Geoenvironmental Engineering, ASCE, 126(5): 397-407.
- Environment Canada (2007) http://www.ec.gc.ca/wmd_dgd/default.asp?lang=En&nav=B81863DD-1 (Accessed on March 4, 2008)
- EPA, US Environmental Protection Agency. 2006. <http://www.epa.gov/epaoswer/non-hw/muncpl/facts.htm> (Accessed on March 4, 2008)

- Hendron, D.M., Fernandez, G., Prommer, P.J., Giroud, J.P. and Orozco, L.F. 1999. Investigation of the cause of the 27 September 1997 slope failure at the Dona Juana landfill. Proc. 7th International Waste management and Landfill Symposium, Sardinia, Italy, 545-567.
- Kocasoy, G. and Curi, K. 1995. The Umraniye–Hekimbasi open dump accident. Waste Management and Research, 13: 305–314.
- Koerner, R.M and Soong, T.Y. 2000. Stability assessment of ten large landfill failures. Geotechnical Special Publication, ASCE, 103:1-38.
- Koelsch, F., Fricke, K., Mahler, C. and Damanhuri, E. 2005. Stability of landfills- The Bandung dumpsite disaster. Proc. 10th International Waste management and Landfill Symposium, Sardinia, Italy (On-CD-Rom).
- Merry, S. M., Kavazanjian, E. and Fritz, W.U. 2005. Reconnaissance of the July 10, 2000, Payatas Landfill failure. Journal of Performance of Constructed Facilities, ASCE, 19(2): 100-107.
- Zekkos, D.P. 2005. Evaluation of static and dynamic properties of municipal solid waste. PhD thesis, Deptt. of Civil and Envir.Engg.Univ.of California, Berkley.

CHAPTER 2 LITERATURE REVIEW

2.1 Introduction

Waste Mechanics is a discipline that deals with the mechanical behaviour of MSW. This discipline is relatively new, and continues to evolve with time. Each new piece of information is, therefore, a valuable contribution to the development of this subject.

MSW comprises all wastes arising from human activities which are normally solid and discarded as useless or unwanted by the individuals or companies from which the waste originates. As such, the constituents of MSW have different sizes, shapes, and, physical and bio-chemical properties. The heterogeneous composition of waste makes the quantification of its engineering properties difficult and challenging. The mechanical properties of waste exhibit a wide scatter due to various reasons such as variable sample composition, use of different types of samples (age, unit weight, pre-treated, shredded, and unsorted) and lack of universally accepted procedures for testing and interpretation of test data. A good understanding and knowledge of MSW properties is required for reliably evaluating and predicting its mechanical behaviour.

Historically, the design of landfills has focused primarily on the compressibility characteristics of MSW so that post closure settlements could be predicted and minimized. The systematic study of landfill settlement issues appear to have started with the publication of the landmark paper by Sowers (1973). Since then, numerous studies have been completed on the compressibility characteristics of MSW. Studies of the shear

strength of MSW proliferated after another landmark paper by Landva et al. (1984). A brief overview of the state-of-the-art on characterization of important mechanical properties of waste such as shear strength, compressibility, Poisson's ratio and elastic modulus is provided in the following sections. A section is also included in the end which summarizes the methods and devices used for sampling and the types of samples used for characterizing MSW properties.

2.2 Shear strength of MSW

The characterization of shear strength of MSW is important for the design of slopes; interfaces with soils and geosynthetics; vertical or piggy-back expansion of landfills and seismic stability evaluations.

Direct shear tests have been the preferred method for measuring the shear strength of MSW likely because of the ease in handling the large size waste particles. Various shapes (square, rectangular, and circular) and sizes (varying from 63.5 mm diameter to 1.5 m x 1.5 m square) of direct shear apparatus have been used for characterizing shear strength of MSW. Both, in-situ tests (Houston et al. 1995, Withiam et al. 1995, Mazzucato et al. 1999, Thomas et al. 1999, Caicedo et al. 2002) and tests on recompacted samples (Landva et al. 1984, Landva and Clark 1990, Siegel et al. 1990, Howland and Landva 1992, Gabr and Valero 1995, Kavazanjian et al. 1999, Sadek et al. 1999, Pelky et al. 2001, Caicedo et al. 2002, Harris et al. 2006, Dixon and Langer 2008, Reddy et al. 2008) have been conducted for characterizing shear strength of MSW.

Some authors (Kolsh 1995, Athanasopoulos et al. 2008) have also tried to explain the analogy between MSW and reinforced earth. The study conducted by Kolsh 1995 is

much like a tensile test and was intended to measure fibrous cohesion in waste. The author defined a new parameter known as the angle of internal tensile stress (ζ). Athanasopoulos et al. (2008) studied the effect of orientation and the stiffness of fibrous material on mobilized shear stress. These authors suggested that the shear strength of waste is highly anisotropic and the mobilized shear stress depends on the fiber orientation and the stiffness of the fibrous material. Direct shear tests have also been conducted on large compacted waste bales (900 mm x 800 mm x 1600 mm, 400 mm x 500 mm x 600 mm) to evaluate shear resistance behaviour at the contact surfaces of different coupled materials found in MSW (Del Greco and Oggeri 1993, Van Impe and Bouazza 1998).

Triaxial compression tests have not been as common as direct shear tests. Some authors (Jessberger et al.1995, Gabr and Valero 1995, Grisolia et al. 1995, Caicedo et al. 2002, Vilar and Carvalho 2004, Chen et al. 2008) have measured shear strength of recompacted samples of MSW from triaxial compression tests. Samples have been prepared at different unit weights, moisture contents, and composition. However, the effect of these quantities on the observed mechanical behavior of MSW has not been systematically documented. Since the deviator stress observed in these tests showed an increase without reaching any peak strength, these authors have interpreted shear strength at different values of axial strains with 20% being the common maximum value (Grisolia 1995, Jessberger et al. 1995, Chen et al. 2008). Similar to direct shear tests both, small and large size recompacted samples (75 mm to 300 mm diameter) have been used with tests conducted under drained as well as undrained conditions with pore pressure measurements. The unit weight of sample was observed to have minor influence on the measured shear strength (Vilar and Carvalho 2004).

Little data is available in the literature on the evolution of shear strength of MSW with time. Landva et al. (1984) observed a slight decrease in the angle of shearing resistance (ϕ') in a one-year-old MSW sample, which was soaked in leachate and sheared in a direct shear apparatus. Kavazanjian (1995) has also reported a decrease in the apparent cohesion (c') and ϕ' of MSW after its accelerated degradation in the laboratory. However, Van Impe (1998) contradicts these observations and reports higher shear strength parameters for old refuse samples compared to freshly deposited refuse.

This review of the literature highlights the wide variation in shear strength parameters of MSW. These variations are primarily attributed to variations in the test methods, sample age, composition and unit weight, and the assumptions made in interpretation of test data. The results of direct shear tests do not clearly indicate, whether the measured shear strength parameters are representative of peak shear stress conditions or that they represent mobilized shear stress at some pre-defined value of shear displacement. The shear strength interpreted from small size direct shear apparatus and shredded/screened waste (Gabr and Valero 1995, Caicedo et al. 2002), and their use in design and stability analyses is still being debated. In-situ direct shear tests on undisturbed samples undoubtedly can provide more realistic shear strength over that measured from recompacted samples since a larger sample can be tested under actual conditions (composition, matrix structure and unit weight). However, such tests are difficult to perform at great depths and might not be suitable (in terms of time and cost) for conducting a large number of tests to obtain representative shear strength of MSW.

This review also suggests that some authors, while quoting the strength parameters estimated from their respective studies, have seldom given any reference to test drainage

conditions and the measurement of pore water pressure. The use of terms “cohesion” and “angle of friction” to describe c' and ϕ' also appears to have little physical basis. Vertical cuts in MSW have been observed to be stable at depths of up to 6 m or more (e.g. Kavazanjian et al. 1995), pointing to the existence of shear strength at zero effective normal stress. However, the physical basis for this mobilization of shear strength is not properly understood. Without this understanding, it is probably more appropriate to use terms such as “apparent cohesion” or “cohesive intercept” for describing c' . Similarly, in the light of the uncertainty in establishing the normal effective stress within MSW, there is some doubt as to whether ϕ' represents inter-component frictional resistance or not. There exists a need for a critical review of the practice of interpreting MSW shear strength test results using the principle of effective stress and the Mohr-Coulomb failure criterion.

The published literature on shear strength does not systematically document the effect of degradation. However, based on mechanical response to degradation in organic soils (Andersland and Al-Khafaji 1980, Wardwell and Nelson 1981, Al-Khafaji and Andersland 1981), it is likely that MSW containing high percentage of organic matter might show a decrease in shear strength with time. These changes in shear strength may affect the stability of the landfill significantly. Given the limited data on MSW shear strength and the wide scatter in these values, researchers (e.g. Kavazanjian et al. 1995; Manassero et al. 1996; Van Impe 1998 and Eid et al. 2000) relied on field performance, and observed slope failures to back calculate shear strength of failed waste mass. Kavazanjian et al. (1995) proposed lower bound drained shear strength envelop (Figure

2-1) based on back analysis of existing landfill slopes and published laboratory data for recompacted samples which can be stated as:

- (i) for an applied normal effective stress (σ'_n) less than 30 kPa, MSW behaves like a purely cohesive material with an apparent cohesion (c') of 24 kPa and,
- (ii) for σ'_n more than 30 kPa, MSW behaves like a purely frictional material with an angle of shearing resistance (ϕ') of 33° .

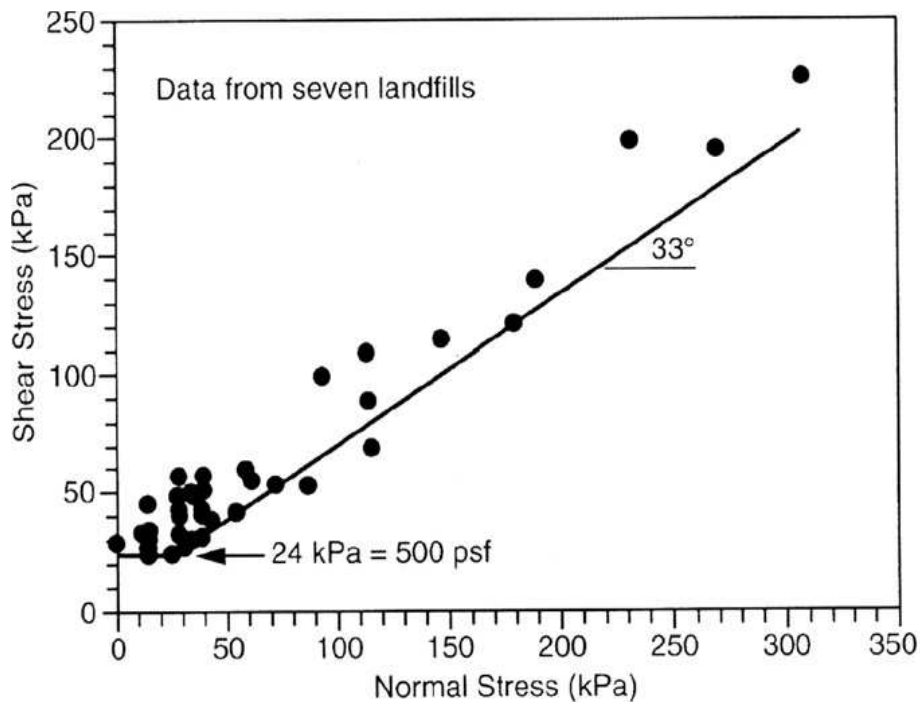


Figure 2-1 Shear strength envelope proposed by Kavazanjian et al. (1995)

A similar shear strength envelope proposed by Manassero et al. (1996), shown in Figure 2-2, suggests that:

- (i) for σ'_n less than 26 kPa, MSW behaves like a purely cohesive material, with c' of 20 kPa;

- (ii) for σ'_n between 26 kPa to 60 kPa, MSW is considered to be a purely frictional material with ϕ' of 38° and;
- (iii) for σ'_n greater than 60 kPa, MSW can be characterized by c' of 20 kPa and ϕ' of 24° .

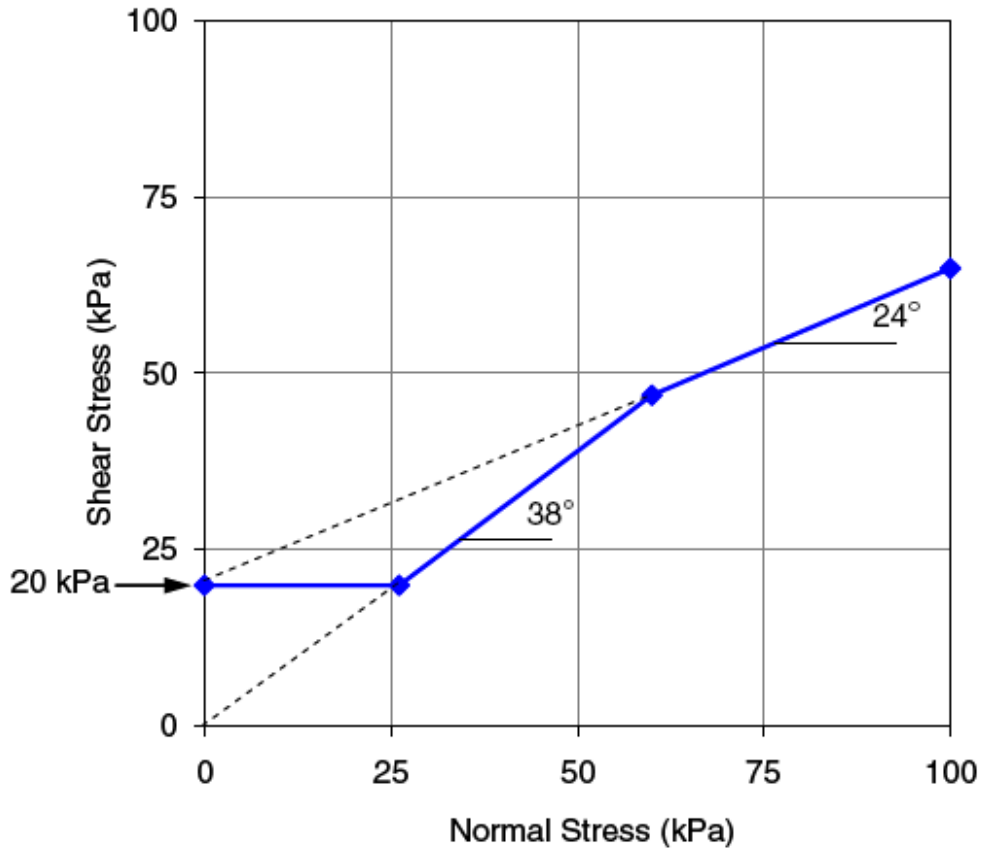


Figure 2-2 Shear strength envelope proposed by Manassero et al. (1996)

Eid et al. (2000), proposed a simple linear failure envelop (Figure 2-3) based on the results of large scale direct shear tests and back analysis of failed slopes, which is given by c' of 40 kPa and ϕ' of 35° .

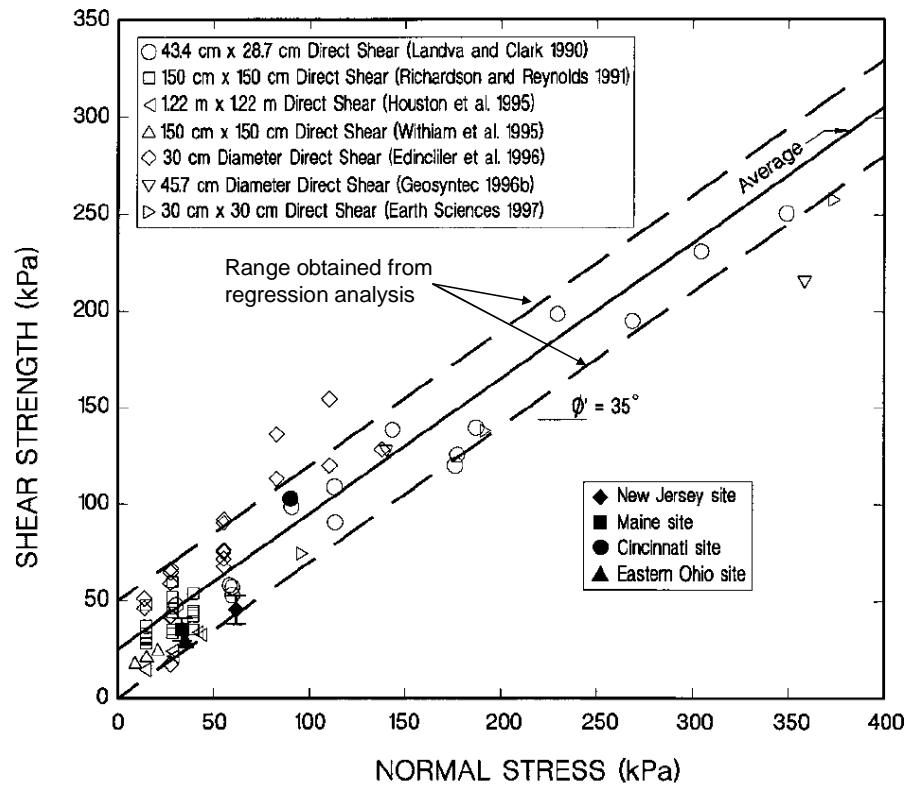


Figure 2-3 Shear strength envelopes proposed by Eid et al. (2000)

2.3 Compressibility characteristics of MSW

The compressibility characteristics of waste are of special concern when designing interim and final closure covers for landfills. The mechanism of compression in waste has been described by various authors (Van Impe and Bouazza 1996, Gasparini et al. 1995, Wall and Zeiss 1995, Coduto and Huitric 1990, Morris and Woods 1990, Sowers 1973). The rate of landfill settlement depends primarily on waste composition, operational practices and factors affecting biodegradation (Wall and Zeiss 1995, Edil et al. 1990). The total compression in MSW can be assumed to be a result of primary compression and secondary compression (Dixon and Jones 2005). Primary compression can be expected to occur during first few days of waste placement. However, secondary compression which

primarily occurs due to degradation can continue indefinitely (Coduto and Huitric 1990). Due to the primary settlements occurring over a short period, the primary compression is of limited interest to engineers except when considering piggy-back expansion (Kavazanjian 2006).

MSW compressibility has been characterized from one-dimensional laboratory consolidation tests (Gabr and Valero 1995, Landva et al. 2000, Vilar and Carvalho 2004, Reddy et al. 2008, Chen et al. 2008) as well as real- time monitoring of settlements at landfills (Coumoulous 1999, El-Fadel and Al-Rashed 1998, Gasparini et al. 1995, Grisolia et al. 1993, Sharma 1990). Various sizes of consolidometer have been used (63 mm to 600 mm in diameter) and the results of these tests expressed in terms of primary and secondary compression indices.

Similar to shear strength, wide variability is observed in the values of the primary compression index (0.16 to 0.92) and the secondary compression index (0.009 to 0.1) likely reflecting variations in samples (fresh/ degraded/ shredded/ sorted etc.), moisture contents, and time considered for secondary compression. The unit weight of the sample may also influence the secondary compression index. Although no relationship has been observed between secondary compression index (C_α) and void ratio, lower density specimens yielded larger values of C_α (Vilar and Carvalho 2004). It can be understood that depending on the extent of degradation and the test duration, the coefficients of secondary compression reported in the literature encompass components of creep and biological effects.

Biodegradation processes in anaerobic systems are influenced most by moisture contents as it provides an aqueous environment that facilitates the transport of nutrients and microbes within the landfill (El-Fadel and Al-Rashed 1998). Landfills operated as 'bioreactors', can therefore, be expected to exhibit greater secondary compression than traditional dry-tomb landfills. However, there is a general lack of experimental data depicting the effect of MSW degradation on compressibility characteristics. Case histories given by Gasparini et al. (1995), Hilde and Reginster (1995) and Kostantinos et al. (1997) show data on anticipated ultimate settlements in landfills taking into consideration degradation effects. Few authors (Wall and Zeiss 1995 and Hossain et al. 2003) have performed settlement experiments to investigate the effect of MSW degradation on compressibility characteristics. With many communities planning post-closure use of landfills as biogas production facilities and as a recreational facility, it is important to understand the mechanism for change in the compressibility characteristics of MSW with time.

2.4 Elastic Modulus

Elastic modulus is an important mechanical property of waste which governs the deformation behaviour. The low elastic modulus of MSW can result in movement of barrier into the waste until limit equilibrium conditions are established (Dixon and Jones, 1998). Two forms of elastic modulus have generally been reported in the literature; a dynamic modulus (small strain shear modulus) required for seismic response analysis and a static modulus, required for settlement analyses. Both, field measurements (intrusive and non-intrusive) and laboratory methods have been used to estimate elastic modulus.

Non-intrusive methods make use of geophysical measurements, generally made at the surface and comprises two types of body waves: primary waves referred to as P-waves or longitudinal or compression waves; and secondary waves referred to as S-waves or transverse or shear waves. The depth of penetration of these waves depends upon the input energy level generated at the surface. For estimation of small-strain stiffness of the waste, a shear wave velocity profile is obtained from the measurements of shear wave velocity using the equation:

$$G_{\max} = \rho V_s^2$$

where G_{\max} is the small-strain shear modulus, ρ is the mass density of the material, and V_s is the shear wave velocity of the material. However, it is worth pointing out that shear modulus estimated in this way is subjective and is based upon the assumption of unit weight and Poisson's ratio.

Shear wave velocity measured from downhole tests have generally been in the range of 125 m/s near surface to 230 m/s at 15 m depth (Sharma et al. 1990, Houston et al. 1995, Kavazanjian et al. 1995, Matasovic and Kavazanjian 1998). Based on surface wave measurements at six southern California landfills, Kavazanjian et al. (1996) proposed a shear wave velocity profile which can be used in seismic analysis of MSW landfills. Some authors (e.g. Rix et al. 1998 and Pereira et al. 2002) have used the SASW (Spectral Analysis of Surface Wave) method to estimate shear wave velocity. In this method, a source and typically two accelerometers are placed at a known distance along a line on the surface. The source generates Rayleigh (surface) waves. By spectral analysis of the signals, the Rayleigh wave velocity at different frequencies is measured to generate

the dispersion curve. The Rayleigh wave velocity is then converted to shear wave velocity using an assumed value of the Poisson's ratio. Pereira et al. (2002) estimated the shear wave velocity to range from 100 m/s to 210 m/s near the surface.

Data on the static modulus of waste is sparse. Large one-dimensional compression cells 0.60 m to 2.0 m in diameters have been used (Beaven and Powrie 1995, Castelli and Maugeri 2008) for the estimation of the constrained modulus (E'_0) of waste. Based upon results from a number of compression tests on non-degraded waste, Beaven and Powrie (1995) measured constrained modulus from their 'Pitsea' compression cell, which varied from 138 kPa to 2418 kPa for vertical stresses up to 600 kPa. For the same level of vertical stresses, Castelli and Maugeri (2008) observed an increase in the value of E'_0 from 68 kPa to 7231 kPa. These authors however, did not investigate the effect of degradation on constrained modulus.

Intrusive methods have also been used to measure the shear modulus of waste. These methods involve geophysical measurements made in boreholes using instruments such as a pressuremeter and cone penetrometer. Dixon and Jones (1998) used a pressuremeter to obtain a relationship between the applied pressure and waste deformation. From this relationship, and using simple mathematical expressions, an estimate of shear strength, shear modulus and in-situ lateral stresses was obtained. The results from such testing are based on the assumption that minimal disturbance is caused during the insertion of the instrument to the desired depth. This method has merits as it allows measurement of large strain behaviour which is pertinent to waste.

In general, literature on the elastic modulus of MSW is limited and the available published data suggests, as expected, low values of elastic modulus. The progressive change in waste elastic modulus with degradation has not been explored in detail.

2.5 Lateral stress and Poisson's ratio

Knowledge of the lateral stresses that develop in waste over time is required in order to estimate lateral deformations. This data is necessary especially for the side slopes as these deformations can potentially impair the functioning of gas collection systems. Lateral stresses are also an important consideration in the design of vaults and conduits, retaining walls, and deep foundations installed for post-closure development (Kavazanjian, 2006). Determination of lateral stresses requires an estimate of K_0 , the ratio of the lateral to the vertical effective stresses under the conditions of no lateral deformation. From the theory of elasticity, the at-rest lateral earth pressure (K_0) and Poisson's ratio (ν) are related as follows:

$$K_0 = \frac{\nu}{1 - \nu}$$

Published literature reveals that various techniques, both field (intrusive and non-intrusive methods) and laboratory methods, have been used to measure K_0 and ν . Non-intrusive methods make use of measurements of S- and P-wave velocity from downhole or cross-hole testing (Sharma et al. 1990, Houston et al. 1995, Carvalho and Vilar 1998, Kavazanjian 1998). The ν value interpreted from shear wave velocity measurement is observed to range from 0.11 to 0.49 with ν decreasing from 0.30 to 0.11 from 1.52 m to

10.0 m depths (Houston et al. 1995). Intrusive methods have made use of self-boring pressuremeter and pairs of vertical and horizontal cells for measurements of K_0 . The values of K_0 interpreted from measurements of pressure and radial displacement using self-boring pressuremeter (Dixon and Jones 1998) showed considerable scatter (0.2 to 1.0) with no clear relationship between K_0 and depth (although a generally higher K_0 is evident at shallow depths). The authors comment on high values of K_0 being due to disturbance caused by self-boring pressuremeter resulting in the formation of large diameter cavity, and due to heterogeneous nature of waste. The authors further suggests that higher values than that obtained by Landva et al. (2000) might be applicable for in-situ waste. Direct measurement of K_0 from vertical and horizontal stress cells (Dixon et al. 2004) also exhibit some scatter (0.4 to 0.8). The authors suggest that high values of K_0 observed at greater depths could be a result of rotation of stress cells within the waste mass

Laboratory measurement of K_0 have been achieved by split ring consolidometer (Landva et al. 2000), ultra-thin tactile pressure sensors (Kavazanjian 2006) and triaxial compression tests (Towhata et al. 2004). The values of K_0 measured using laboratory methods are generally consistent and vary in a narrow range (0.2 to 0.4). The influence of waste degradation on K_0 with time has not been documented.

2.6 Types of sample and sampling techniques

Samples have been obtained either directly from fresh waste or from various depths within the landfill. Artificial samples of waste, prepared by mixing different constituents typically found in MSW, have also been used by a few authors such as Dixon and Langer (2008), Landva et al. (2000), Pelkey et al. (2001) and Grisolia et al. (1995).

2.6.1 Laboratory vs. On-site testing and Intact vs. Recompacted samples

On-site testing of disturbed and undisturbed samples of MSW has not been popular. A few researchers such as Cowland et al. (1993) and Houston et al. (1995) have conducted on-site testing of undisturbed samples of MSW. These tests were conducted using a large direct shear apparatus and by loading a large block of MSW to cause a shear failure. The main advantage of on-site testing is that a large sample can be tested which is more representative of the waste material. However, such tests are limited to very shallow depths (e.g. 1.0 m to 2.0 m) and are difficult to conduct at greater depths. The literature review revealed that laboratory testing has generally been carried out on recompacted samples. However, no account of any attempt made to obtain intact samples from great depths (e.g. greater than 5.0 m) could be found in the literature.

2.6.2 Sampling Devices

In the absence of a fixed protocol for sampling, researchers have used different methods for procuring MSW sample. Landva and Clark (1990) and Landva et al. (1984) have tried to collect samples with the help of a “Becker” type of drill. However, these authors encountered difficulties while trying to sample waste by this technique because the drive

shoe often became clogged with large sized MSW components, requiring the drill hole to be relocated frequently.

Sampling using split spoon samplers (Landva and Clark, 1990; Gabr and Valero, 1995 and Siegel et al., 1990) has also not been met with much success due to bridging of the sampler opening by large and resilient waste fragments. In such cases, the sampler was usually withdrawn and re-driven after cleaning either in the same borehole or in a new borehole. Attempts to recover samples using thin walled Shelby tubes (Gabr and Valero 1995) were also not very successful because of crushing of the tube during driving. Auger drilling has proved to be the most efficient and preferred method for recovering disturbed samples of MSW from great depths (e.g. 5.0 m) Landva and Clark (1990), Vilar and Carvalho (2004) have used continuous augers with diameters varying between 100 mm to 400 mm for obtaining samples representative of different depths and different stages of degradation.

It seems possible that the use of different types of samples and sampling techniques as discussed above is also one of the reasons for the large variability in the measured values of the mechanical properties of MSW. Due to difficulties in obtaining intact samples, more reliance has been placed on the use of recompacted samples. The applicability of test results from recompacted samples in the design of landfills and its components needs further investigation. It has been noted from the review of the literature that often the authors do not document information of the method used for sampling. The samples were often processed before testing to reduce the size of constituents. The recorded data often lacks information about the extent of degradation, unit weight and the moisture content of the sample used.

2.7 References

- Al-Khafaji, A. W. N., and Andersland, O. B. 1981. Compressibility and strength of decomposing fibre-clay soils. *Geotechnique*, 31(4): 497-508.
- Andersland, O. B. and Al-Khafaji, A. W. N. 1980. Organic material and soil compressibility. *Journal of Geotechnical Engineering, ASCE*, 106(GT7): 749-758.
- Beaven, R.P. and Powrie, W. 1995. Hydrogeological and Geotechnical properties of refuse using a large scale compression cell. *Proc. 5th International Waste Management and Landfill Symposium, Sardinia*, 745-760.
- Caicedo, B., Yamin, L., Giraldo, E. and Coronado, O. 2002. Geomechanical properties of municipal solid waste in Dona Juana sanitary landfill. *Proc. 4th International Congress on Environmental Geotechnics, Brazil*, 1: 177-182.
- Carvalho, M.de F., Vilar, O.M. 1998. In situ tests in urban waste sanitary landfill. *Environmental Geotechnics*, Editor Seco e Pinto, 1998, Balkema, Rotterdam, 121-126.
- Castelli, F. and Maugeri, M. 2008. Experimental analysis of waste compressibility. *Geotechnical Special Publication, ASCE*, 177: 208-215.
- Chen, Y., Zhan, T.L.T. and Ling, W. 2008. Mechanical properties of municipal solid waste from Suzhou landfill in China. *Geotechnical Special Publication, ASCE*, 177: 160-167.
- Coduto, D. P., and Huitric, R. 1990. Monitoring landfill movements using precise instruments. *Geotechniques of Waste Fills – Theory and Practice*, ASTM STP 1070, A. Landva and G.D. Knowles, Editors, ASTM, Philadelphia, P.A., 358-369.
- Coumoulous, D.G., and Koryalos, T.P. 1999. Prediction of long-term settlement behaviour of landfill covers after closure. *Proc. 7th International Waste Management and Landfill Symposium, Sardinia*.
- Del Greco, O. and Oggeri, C. 1993. Geotechnical parameters of sanitary wastes. *Proc. 4th International Waste Management and Landfill Symposium, Sardinia*.

- Dixon, N. and Jones, D.R.V. 2005. Engineering properties of municipal solid waste. *Geotextiles and Geomembranes*, 23: 205-233.
- Dixon, N., Ng'ambi, S., Jones, D.R.V. 2004. Structural performance of a steep slope landfill lining system. *Proc. Institution of Civil Engineers, Geotechnical Engineering*, 157: 115-125.
- Dixon, N., Jones, D.R.V. and Whittle, R.W. 1999. Mechanical properties of household waste: In-situ assessment using pressuremeter. *Proc. 7th International Waste Management and Landfill Symposium, Sardinia*, 453-460.
- Dixon, N. and Jones, D.R.V. 1998. Stress states in, and stiffness of, landfill waste. *Geotechnical Engineering of landfills*. Editors: Dixon, N., Murray, E. J and Jones, D. R .V. Thomas Telford, UK, 19-34.
- Edinçiler, A. Benson, C. H. and Edil, T. B. 1996. Shear strength of municipal solid waste. Interim Report - Year 1, Environmental Geotechnics Report 96-2, Department of Civil and Environmental Engineering, University of Wisconsin, Madison.
- Edil, T.B., Ranguette, V.J. and Wuellner, W.W. 1990. Settlement of municipal refuse. *Geotechniques of Waste Fills – Theory and Practice*, ASTM STP 1070, A. Landva and G.D. Knowles, Editors, ASTM, Philadelphia, P.A., 225-239.
- El-Fadel, M. and Al-Rashed, H. 1998. Settlement in municipal solid waste landfills II. Mathematical modelling. *Journal of Solid Waste Technology and Management*, 25.
- Gabr, M.A. and Valero, S.N. 1995. Geotechnical Properties of Municipal Solid Waste. *Geotechnical Testing Journal*, ASTM, 18(2): 241-251.
- Gasparini, P.A., Saetti, G.F. and Marastoni, M. 1995. Experimental research on MSW compaction degree and its change with time. *Proc. 5th International Waste Management and Landfill Symposium, Sardinia*, 833-842.
- GeoSyntec Consultants. 1996. Preliminary assessment of the potential causes of 9 March 1996 North Slope landslide and evaluation of proposed intermediate cover

reconstruction. Consulting Report-Prepared for Rumpke Waste, Inc., Proj. No. CHE8014, March, GeoSyntec Consultants, Atlanta, Ga.

- Grisolia, M., Napoleoni, Q. and Tancredi, G. 1995. The use of triaxial test for the mechanical characterization of MSW. Proc. 5th International Waste Management and Landfill Symposium, Sardinia, 761-768.
- Hilde, J.L. and Reginster, J. 1995. Three year study of vertical and horizontal movements in a MSW landfill. Proc. 5th International Waste Management and Landfill Symposium, Sardinia, 855-860.
- Hossain, M.S., Gabr, M.A. and Barlaz, M.A. 2003. Relationship of compressibility parameters to municipal solid waste decomposition. Journal of Geotechnical and Geoenvironmental Engineering, 129(12):1151-1158.
- Howland, J.D., Landva, A.O. 1992. Stability analysis of a municipal solid waste landfill. Geotechnical special publication, ASCE, 31: 1216-1231.
- Houston, W.N., Houston, S.L., Liu, J.W., Elsayed, A. and Sanders, C.O. 1995. In-situ testing methods for dynamic properties of MSW landfills. Geotechnical Special Publication, ASCE, 54: 73-82.
- Jessberger, H.L., Syllwasschy, O. and Kockel, R. 1995. Investigation of waste body behaviour and waste structure interaction. Proc. 5th International Waste Management and Landfill Symposium, Sardinia, 731-743.
- Kavazanjian, E, Jr. (2006). Waste mechanics: Recent findings and unanswered questions. Geotechnical Special Publication, ASCE, 148: 34-54.
- Kavazanjian, E.Jr. 1999. Seismic design of Solid Waste Containment Facilities. Proc. 8th Canadian Conference on Earthquake Engineering, Vancouver, BC, 51- 89.
- Kavazanjian, E., Jr., matasovic, N., Stokoe, K. and Bray, J.D. 1996. In-situ shear wave velocity of solid waste from surface wave measurements. Proc. 2nd International Congress on Environmental Geotechnics, Osaka, Japan, Balkema, 1: 97-104.

- Kavazanjian, E. Jr., Matasovic, N., Bonaparte, R. and Schmertmann, G.R. 1995. "Evaluation of MSW properties for Seismic Analysis. Geotechnical Special Publication, ASCE, 46: 1126-1141.
- Konstantinos, A., Papachristou, E. and Georgios, D. 1997. Settlement measurements at the MSW landfill of Thessaloniki, Greece. Proc. 6th International Waste Management and Landfill Symposium, Sardinia, 545-549.
- Landva, A.O., Valsangkar, A.J. and Pelkey, S.G. 2000. Lateral earth pressure at rest and compressibility of municipal solid waste. Canadian Geotechnical Journal, 37: 1157-1165.
- Landva, A. O., and Clark, J. I. 1990. Geotechnics of waste fills. Geotechniques of Waste Fills – Theory and Practice, ASTM STP 1070, A. Landva and G.D. Knowles, Editors, American Society for Testing and Materials, Philadelphia, P.A., 86-103.
- Landva, A.O., Weisner, W.R. and Burwash, W.J. 1984. Geotechnical engineering and refuse landfills. 6th International Conference on Waste management, Canada.
- Mahler, C. F., De Lamare Netto, A. 2003. Shear resistance of mechanical biological pre-treated domestic urban waste. Proc.9th International Waste Management and Landfill Symposium, Sardinia, Italy. (on CD-Rom).
- Manassero, M., Van Impe, W. F., and Bouazza, A. 1996. Waste Disposal and Containment. Proc. 2nd International Congress on Environmental Geotechniques, Osaka, Japan, A.A. Balkema, 3: 1425-1474.
- Matasovic, N., Kavazanjian, E. Jr. 1998. Cyclic characterization of OII landfill solid waste. Journal of Geotechnical and Geoenvironmental Engineering, 124(3): 197-210.
- Mazzucato, A., Simonini, P. and Colombo, S. 1999. Analysis of block slide in a MSW landfill. Proc. 7th International Waste Management and Landfill Symposium, Sardinia.
- McDougall, J. R., and Pyrah, I. C. 2004. Phase relations for decomposable soils. Geotechnique, 54(7): 487-493.

- Pelkey, S.A., Valsangkar, A.J. and Landva, A. 2001. Shear displacement dependent strength of municipal solid waste and its major constituents. *Geotechnical Testing Journal*, ASTM, 24(4): 381-390.
- Pereira, A.G.H., Sopena, L., Mateos, T.G. 2002. Compressibility of a municipal solid waste landfill. *Proc. 4th International Congress on Environmental Geotechnics*, Brazil, 201-206.
- Reddy, K.R., Gangathulasi, J., Hettiarachchi, H. and Bogner, J. 2008. Geotechnical properties of Municipal Solid Waste subjected to leachate recirculation. *Geotechnical Special Publication*, ASCE, 177: 144-151.
- Richardson, G.N. and Reynolds, R.D. 1991. Geosynthetic considerations in a landfill on compressible clays. *Proc. Geosynthetics '91*, Industrial Fabrics Association International, St. Paul, Minn., 2.
- Rix, G.J., Lai, C.G., Foti, S., Zywicki, D. 1998. Surface wave tests in landfills and embankments. *Geotechnical Special Publication*, ASCE, 75(2): 1008-1019.
- Sadek, S., El-Fadel, M., Manasseh, C. and Abou-Ibrahim, A. 1999. Geotechnical properties of decomposed solid waste materials. *Proc. International Conference on Solid Waste Technology and Management*, 350-357.
- Sharma, H.D., Dukes, M.T. and Olsen, D.M. 1990. Field measurements of dynamic moduli and Poisson's ratio of refuse and underlying soils at a landfill site. *Geotechniques of Waste fills – Theory and Practice*. Editors Landva, A. and Knowles, D.K. ASTM STP 1070, 57-70.
- Siegel, R.A., Robertson, R.J. and Anderson, D.G. 1990. Slope stability investigation at a landfill in Southern California. *Geotechniques of Waste Fills – Theory and Practice*, ASTM STP 1070, A. Landva and G.D. Knowles, Editors, American Society for Testing and Materials, Philadelphia, P.A., 259-284.
- Sowers, G. F. 1973. Settlement of waste disposal fills. *Proc. 8th International Conference on Soil Mechanics and Foundation Engineering*, Moscow, 2, A. A. Balkema, 207-210.

- Thomas, S., Aboura, A.A., Gourc, J.P., Gotteland, P., Billard, H., Delineau, T., Gisbert, T., Ouvry, J.F. and Vuillemin, M. 1999. An in-situ waste mechanical experimentation on a French landfill. Proc. 7th International Waste Management and Landfill Symposium, Sardinia.
- Towhata, I., Kawano, Y., Yonai, Y., and Koelsch, F. 2004. Laboratory tests on dynamic properties of municipal wastes. Proc. 11th Conference in Soil Dynamics and Earthquake Engineering and 3rd International Conference on Earthquake Geotechnical Engineering, 1: 688-693.
- Van Impe, W.F. 1998. Environmental Geotechnics: ITC 5 Activities, State of Art. Proc. 3rd International Congress on Environmental Geotechnics, Lisbon, Portugal, 4: 1163-1187.
- Vilar, O.M. and Carvalho, M.F. 2004. Mechanical properties of municipal solid waste. Journal of Testing and Evaluation, ASTM, 32(6):1-12.
- Wall, D.K. and Zeiss, C. 1995. Municipal landfill biodegradation and settlement. Journal of Environmental Engineering, ASCE, 121(3): 214-224.
- Wardwell, R. E., and Nelson, J. D. 1981. Settlement of sludge landfills and fibre decomposition. Proc. 10th International Conference on Soil Mechanics and Foundation Engineering, Stockholm, Sweden, 2: 397-401.
- Withiam, J.L., Tarvin, P.A., Bushell, T.D., Snow, R.E. and German, H.W. 1995. Prediction and Performance of municipal landfill slope. Geotechnical Special Publication, ASCE, 46: 1005-1019

CHAPTER 3 SHEAR STRENGTH TESTING OF INTACT AND RECOMPACTED SAMPLES OF MUNICIPAL SOLID WASTE

Preface[†]

Considerable research has been done on methods to measure the shear strength of MSW. One of the issues in this regard has been the use of recompacted versus intact samples and the interpretation of test data for determining shear strength parameters. This paper presents the results of shear strength testing of intact and recompacted samples of MSW using a large triaxial compression apparatus. A method for obtaining intact samples of MSW has been developed and used to obtain intact samples from a large Canadian landfill. Shear strength testing of MSW was carried out using a large triaxial compression apparatus as well as using a large direct shear apparatus. Shear behavior of MSW observed from testing of intact and recompacted samples is discussed. The use of stress paths observed during shearing in a triaxial compression test is examined for characterizing shear strength of MSW. The observations from this study address the first and partly the second objective of this research: (i) to develop a method for obtaining intact samples of waste and to examine the significance of using intact versus recompacted samples in characterizing the stress-deformation behaviour of MSW and, (ii) to characterize MSW shear strength from the interpretation of triaxial test results.

[†]A similar version of this chapter is under review for possible publication as a research paper in *Canadian Geotechnical Journal*.

Citation: M. K. Singh, J. S. Sharma and I. R. Fleming “Shear Strength Testing of Intact and Recompacted samples of Municipal Solid Waste”.

Abstract

This paper presents preliminary results of shear strength testing of intact and recompacted samples of municipal solid waste (MSW). A method for in-situ sampling of MSW from landfills using a push-in sampler was developed and used to obtain intact samples of MSW from a large municipal landfill. Shear strength testing of MSW was carried out using a large triaxial compression apparatus as well as using a large direct shear apparatus. The results are presented in terms of cohesion intercept (c') and angle of shearing resistance (ϕ'), and compared with those available in the literature. Based on these results and their favorable comparison with the published literature, it can be concluded that meaningful shear strength parameters for MSW can be obtained using consolidated undrained triaxial tests on large-diameter intact and recompacted samples. A fairly consistent picture of shear behaviour of MSW obtained from effective stress paths in triaxial tests appears to suggest that shear behaviour of MSW can be explained using the principle of effective stress. It is suggested that recompacted samples could be used for obtaining reasonable estimates of c' and ϕ' for MSW; however, it may be necessary to use intact samples to determine pre-failure deformation behaviour of MSW.

3.1 Introduction

Over the past decade, the stability of landfill slopes has received considerable attention because of a number of high-profile failures of large municipal landfills. Notable recent examples of landfill failure include: the 1997 Doña Juana landfill failure in Bogotá, Colombia (Hendron et al. 1999), the 2000 Payatas landfill failure in Manilla, Philippines

(Merry et al. 2005) and the Bandung landfill failure in Indonesia (Kölsch et al. 2005). The apparent increase in the number of landfill failures likely reflects the fact that present-day landfills have been constructed to greater heights in response to economic, social, and regulatory considerations. Landfills extending 70 to 90 m above the ground surface are becoming increasingly a common sight as municipalities worldwide are under pressure to constrain the footprints of their landfills by accepting more municipal solid waste (MSW) per unit base area of the landfill. This reduction in footprint is being achieved by designing new higher landfills or extending the heights of older landfills using “piggyback” expansions. A higher landfill puts greater demand on the shear strength of MSW for its stability because MSW is the largest structural element of a municipal landfill.

Many communities, as a part of their sustainable development initiatives, are also considering the collection of landfill gas (LFG) generated from decomposing MSW inside closed landfills. The condition of MSW inside a closed landfill changes over time because of degradation, decomposition or creep. It is, therefore, logical to expect a change in the shear strength of MSW with time, which may affect the long-term stability of a closed landfill. To ensure the stability of both the open and the closed landfills, it is vital to understand how MSW mobilizes its shear strength and to obtain accurate estimates of the shear strength of MSW.

Like soils, the shear strength of MSW has been evaluated using triaxial compression test or direct shear tests, or by conducting limit equilibrium back analysis of failed landfill slopes. The shear strength of MSW is commonly described using the Mohr-Coulomb failure criterion

$$\tau = c' + \sigma'_n \tan(\phi') \quad [1]$$

where τ is the shear strength of MSW, σ'_n is the normal effective stress and the cohesion intercept c' and angle of friction ϕ' are collectively termed the shear strength parameters of MSW.

Satisfactory design of an engineered municipal landfill facility requires meaningful values of c' and ϕ' for MSW. Considerable research has been done to date on the estimation of c' and ϕ' values for MSW using small and large direct shear tests, large triaxial tests as well as in-situ tests. Consequently, an extensive database of c' and ϕ' values of MSW (Table 3-1) is available to practitioners. It is, however, difficult to interpret and use this database in practice because of the inherently heterogeneous nature of MSW, the use of non-representative MSW samples, and the absence of a universally-accepted method for the estimation of MSW shear strength parameters. This has prompted some researchers (e.g. Kavazanjian 2003) to suggest that back-analysis of case studies involving failure of landfill slopes or the use of field trials involving controlled failure by excavation are the only appropriate ways of obtaining representative c' and ϕ' values for MSW. Such field trials, however, are generally quite expensive and time consuming to conduct. It is often more practical to obtain shear strength parameters through laboratory or in-situ shear testing of MSW samples.

From the point-of-view of shear strength testing of MSW, one question is whether to test samples that have been recompacted under laboratory conditions or to obtain and test samples in their intact state. Testing of intact MSW samples, which usually involves in situ shearing of MSW using a transportable direct shear apparatus (e.g. Houston et al.

1995; Mazzucato et al. 1999), is far more demanding compared with testing of recompacted MSW samples.

Table 3-1 Shear strength parameters of MSW from literature

| Reference | Shear Strength Parameter | | Details |
|------------------------------|--------------------------|-------------|--|
| | c' (kPa) | ϕ' (°) | |
| Cowland et al. (1993) | 10 | 25 | Back analysis of deep trench cut in waste |
| Caicedo et al. (2002) | 67 | 23 | Large DS, pressure phicometer |
| Eid et al. (2000) | 25 | 35 | Large DS and also back calculation from four failed slopes |
| Gabr & Valero (1995) | 17 | 34 | Small CU triaxial (values at 20% axial strain |
| Grisolia et al. (1995) | 2-3 | 15-20 | Large Triaxial (at 10-15% axial strain) |
| | 10 | 30-40 | Large Triaxial (at 10-15% axial strain) |
| Houston et al. (1995) | 5 | 33-35 | Large DS on undisturbed samples |
| Jessberger and Kockel (1995) | 0 | 31-49 | Both large and small Triaxial |
| Kavazanjian et al. (1995) | 24 | 0 | For normal stress upto 30 kPa |
| | 0 | 30 | For normal stress more than 30 kPa |
| Landva & Clark (1990) | 0-23 | 24-41 | DS |
| Landva & Clark (1986) | 10-23 | 24-42 | DS on waste from various canadian landfills |
| Mazzucato et al. (1999) | 43 | 31 | Large DS |
| Pelkey et al. (2001) | 0 | 26-29 | Large DS |
| Siegel et al. (1990) | 0 | 39-53 | DS. At 10 % shear displacement, and cohesion assumed zero |
| Vilar & Carvalho (2002) | 39.2 | 29 | At natural water content (20% strain) |
| | 60.7 | 23 | Saturated sample(20% strain) |
| Whitian et al. (1995) | 10 | 30 | Large DS |

[Legend: c' - cohesion; ϕ' - angle of friction; DS - Direct shear test, CU- Consolidated Undrained test]

It is, therefore, not surprising that shear strength parameters for MSW have traditionally been obtained using the more easily obtainable recompacted samples (e.g. Landva et al. 1984; Landva and Clark 1990; Grisolia et al. 1995; Kavazanjian et al. 1999). It is also worth noting that recompacted or artificial MSW samples have been used in almost all published cases of the use of large triaxial tests to obtain c' and ϕ' values for MSW (e.g. Gabr and Valero 1995; Grisolia et al. 1995; Jessberger et al. 1995; Caicedo et al. 2002; Vilar and Carvalho 2002).

In this paper, the results of a program of shear strength testing of intact and recompacted samples of MSW are presented. A method for in situ sampling of MSW was developed and used to obtain intact samples of MSW from a large municipal landfill in Ontario, Canada. Shear strength testing of MSW was carried out using a large triaxial compression apparatus as well as using a large direct shear apparatus. The shear strength parameters of MSW obtained from triaxial and direct shear tests are compared with those available in the literature and the relative importance of using intact or recompacted samples is discussed.

3.2 Equipment

3.2.1 Large Triaxial compression apparatus

Figure 3-1 shows the large triaxial compression apparatus used in the present study for the testing of intact and recompacted MSW samples. The plexiglass triaxial cell, which is reinforced using stainless steel straps, is capable of accommodating cylindrical samples of MSW up to 210 mm in diameter and up to 450 mm in height. The triaxial cell is connected to conventional systems for the application of cell pressure and back pressure

and is equipped with a pore-water pressure transducer to record changes in pore-water pressure during shearing. The apparatus is strain-controlled, in that it is possible to achieve a user-specified rate of axial displacement of the pedestal on which the sample sits. Axial load is mobilized using a reaction frame and is recorded using a load cell. The axial displacement of the sample is recorded using a linear variable differential transformer (LVDT) as well as a mechanical dial gauge. The pore-water pressure transducer, the load cell, and the LVDT are connected to a data logger and a stabilized DC power supply unit. The data logger is connected to a personal computer for automated acquisition of instrument readings.



Figure 3-1 Triaxial apparatus used in the present study

3.2.2 Large scale Direct shear apparatus

A large (1.0 m x 1.0 m x 1.0 m) transportable direct shear apparatus (Figure 3-2) with ancillary hydraulics and computer control/data acquisition was used at the Brock West landfill to obtain shear strength parameters of recompacted MSW. In this direct shear

apparatus, a rigid steel loading plate connected to a hydraulic actuator was used to apply a constant vertical stress to the MSW sample. The shearing of the sample was achieved by applying a horizontal load to the lower shear box, which is seated on a set of rollers, while restraining the upper shear box in the horizontal direction. The surfaces of the steel plates sliding against each other at the interface between the top and bottom boxes are treated with a specially formulated industrial coating to minimize friction and abrasion. The apparatus is instrumented to record displacements of the vertical loading plate and horizontal (shear) displacement of the lower box. Vertical and horizontal loads are recorded using load cells mounted at the ends of the hydraulic actuators.



Figure 3-2 Direct shear apparatus used in the present study

3.3 Methodology

3.3.1 Collection of Intact MSW samples

The MSW samples for the present study were obtained from the Brock West Landfill site, located on the edge of a rural/residential area in the town of Pickering, Ontario

approximately 40 km northeast of Toronto. This 64 hectare landfill, which is owned by the City of Toronto, began accepting waste in 1975 and was closed in 1997 after accepting approximately 18 million metric tonnes of waste. It was the first landfill in Canada to be converted into a landfill gas (LFG) electricity generation facility after its closure (Environment Canada 2007).

A typical cross-section of the samplers used for the collection of intact MSW samples is shown in Figure 3-3. An adaptor is also shown in Figure 3-3 which was designed and fabricated to obtain samples from greater depth in bore holes. Two different samplers (internal diameters 150 mm and 200 mm), each 750 mm long were used. These samplers were similar to a Shelby tube except that each sampler had ribs machined on its inside over a length of 300 mm from the cutting edge in order to prevent the MSW sample from slipping out of the sampler during its retraction.

Sampling of MSW was carried out at the bottom of a pit that was excavated on the south slope of the landfill. Samplers were pushed approximately 450 mm into the waste using a hydraulic-powered excavator bucket. Samplers with MSW inside them were retrieved by pulling the steel cables attached to the top each sampler. In cases where pulling of samplers proved difficult, they were retrieved by excavating around the sampler. The ends of the retrieved samplers were packed with soil and sealed. The sealed samplers were then shipped to the University of Saskatchewan's geotechnical laboratory. A total of six intact samples were collected from the Brock West site.

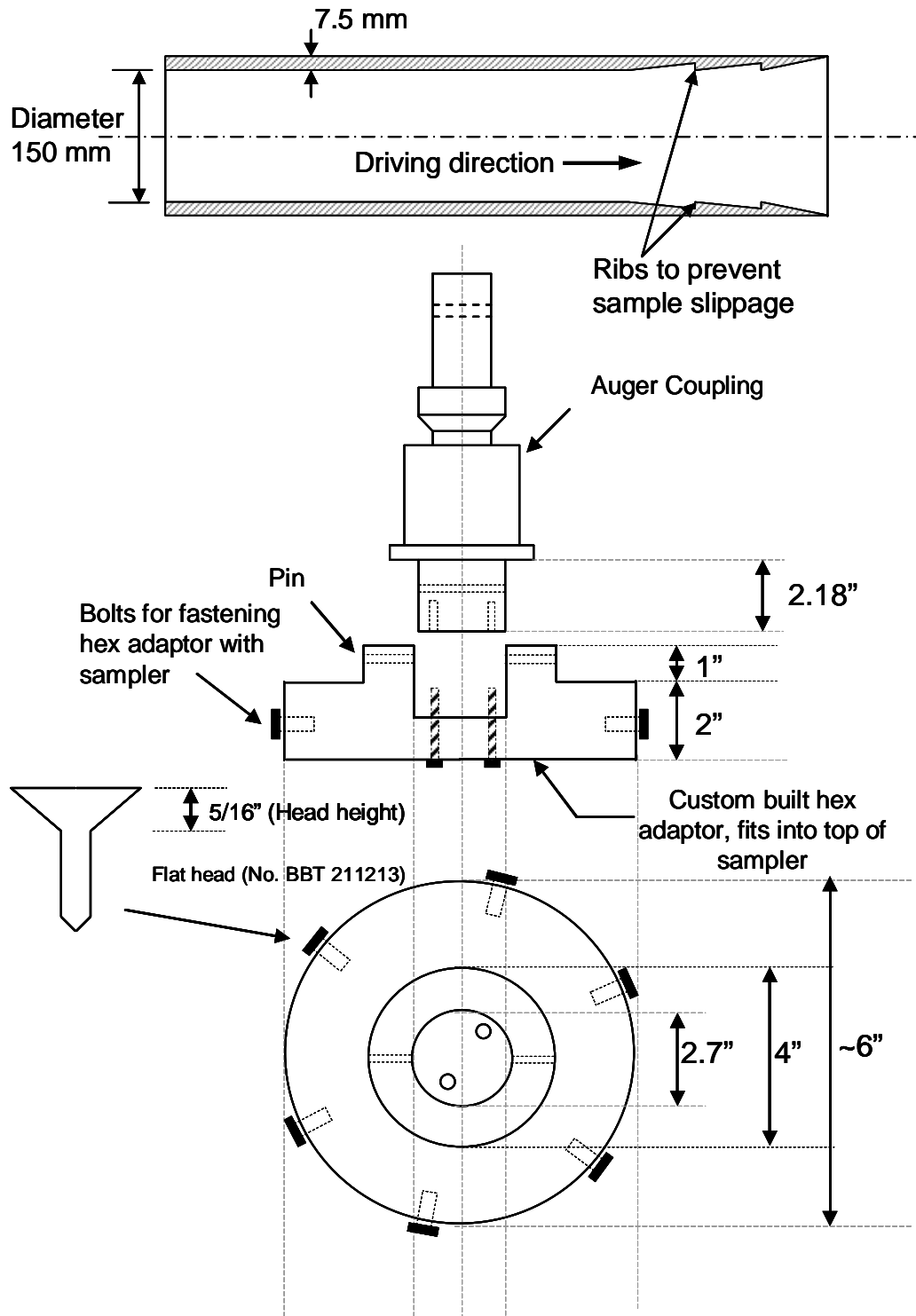


Figure 3-3 Details of Sampler and Adaptor used in the present study

3.3.2 Preparation of MSW samples for Triaxial testing

3.3.2.1 *Intact samples*

The gravimetric moisture content and the average unit weight of each of the six intact samples were determined prior to extrusion and preparation for triaxial testing. Approximately 250 g of MSW was removed from the top end of each sample for moisture content determination using the oven drying method. The average bulk unit weight was determined by recording the gross weight and the dimensions of the sample.

After determining the gravimetric moisture content and the average unit weight, the MSW sample within each sampler was saturated and the volume of water needed for full saturation was recorded. Each sampler containing saturated MSW was then frozen. Such freezing of MSW was necessary to preserve its in-situ 'structure' during extrusion and preparation of samples for triaxial testing.

A sampler containing frozen MSW was removed from the freezer a few minutes before a triaxial test and extruded using a specially-fabricated hydraulic extruder. A freshly-extruded frozen MSW sample is shown in Figure 3-4. The ends of the frozen MSW sample were trimmed so that these ends were flat and orthogonal to the vertical axis of the sample. Any big pieces of MSW sticking out of the ends were removed and the void left by their removal was filled with moist silty soil.

3.3.2.2 *Recompacted samples*

Recompacted samples were prepared in the laboratory using the material from the intact samples after their triaxial testing. In this way, the same material was used for both an intact and a recompacted sample in order that the results could be compared. For

recompaction, the waste was placed inside a steel sampler and compacted in four lifts to achieve the desired bulk unit weight. Fragments of MSW that were too large to fit inside the sampler were either discarded or, where possible, were broken by hand to make them fit inside the sampler. Recompacted samples were saturated and frozen in the same manner as the intact samples. Extrusion and preparation of the recompacted samples was also done in the same way as the intact samples.



Figure 3-4 Frozen intact sample after its extrusion from the sampler

3.3.2.3 Consolidated undrained Triaxial tests on MSW

Consolidated undrained triaxial tests were conducted on intact and recompacted MSW samples using the large triaxial compression apparatus as described above. Five tests were conducted using intact samples and nine tests were conducted using recompacted samples. One intact sample disintegrated upon extrusion because of the presence of a large piece of wood in it; therefore, it was not possible to conduct a triaxial test on this sample. Details of these tests are given in Table 3-2. The procedure for conducting these

tests was very similar to that prescribed by ASTM D-4767 (ASTM 2004) for conducting consolidated undrained triaxial tests on fine-grained soils.

Table 3-2 Details of triaxial tests on intact and recompacted MSW samples

| Sample ID | Type | D (mm) | w (%) | γ (kN/m ³) | σ'_3 (kPa) | Composition |
|-----------|-------------|-------------|------------|----------------------------------|----------------------|--|
| U-1 | Intact | 150 | 25 | 13.7 | 150 | Plastics, paper, textile, wood, soil and humus |
| U-2 | Intact | 150 | 17 | 11.3 | 0 | |
| U-3 | Intact | 150 | 21 | 13.2 | 35 | |
| U-4 | Intact | 200 | 19 | 13.0 | 60 | |
| U-6 | Intact | 200 | 27 | 11.5 | 60 | |
| R-1 | Recompacted | 150 | - | 14.8 | 50 | Plastics, paper, textile, wood, soil and humus |
| R-2 | Recompacted | 150 | - | 15.3 | 60 | |
| R-3 | Recompacted | 150 | - | 14.6 | 120 | |
| R-4 | Recompacted | 150 | - | 15.8 | 140 | |
| R-5 | Recompacted | 150 | - | 15.7 | 125 | |
| R-6 | Recompacted | 150 | - | 15.9 | 100 | |
| R-7 | Recompacted | 150 | - | 12.6 | 100 | |
| R-8 | Recompacted | 150 | - | 13.0 | 30 | |
| R-9 | Recompacted | 150 | - | 13.7 | 60 | |

[Legend: D – diameter of the sample; w – in-situ moisture content of the sample; γ – bulk unit weight of the sample; σ'_3 – effective confining pressure at the start of the triaxial test.]

As mentioned above, the MSW samples were in a frozen state at the time of extrusion and trimming. A trimmed, frozen sample of MSW was placed on the pedestal of the triaxial cell and an end cap was placed over its top end. After ensuring that the axis of the sample was vertical and coinciding with the axis of the loading ram, a rubber membrane was stretched over the sample and its ends were sealed using O-rings. The triaxial cell was then assembled and gradually filled with water while allowing the air to escape from the top. The frozen sample was then allowed to thaw completely. The thawed sample was then allowed to ‘consolidate’ for 24 hours under a chosen value of effective confining pressure. Back pressure was applied during consolidation to ensure

full saturation of the sample. The sample was sheared at an axial displacement rate of 0.4 mm/min. Shearing was stopped when: (a) the axial load did not increase appreciably with increasing axial displacement; (b) the axial load decreased with increasing axial displacement; (c) excessive deformation of the sample (e.g. bulging or buckling) was observed; or (d) when the maximum permissible axial displacement of the sample pedestal was reached. At the end of each test, the sample was dismantled from the triaxial cell and was examined for the presence of large chunks (bigger than about 80 mm) of rigid materials such as wood, stone, metal, etc. The results from a sample containing one or more of such large chunks were discarded. The data for each test were downloaded from the data logging computer for subsequent processing and analysis.

3.3.2.4 *Direct shear test on MSW*

Four direct shear tests were conducted on MSW at the Brock West landfill site using the large direct shear apparatus described above. The details of these four tests are given in Table 3-3. Two pits were excavated with a backhoe at different locations in the Brock West landfill site and the MSW was transported to the direct shear box using a front-end loader. Before its placement inside the direct shear box, the MSW was inspected and large rocks and pieces of concrete and timber were removed. Test samples were prepared by depositing MSW inside the shear box in several lifts. Each lift was compressed statically under the desired effective normal pressure. This process was repeated until the shear box was completely filled to the top.

The horizontal displacement rate for each direct shear test was 5 mm/min. In order to maintain a constant effective normal stress on the test specimen, the normal load on the test specimen was reduced in proportion to the reduction in the area of the shear plane

with increasing horizontal displacement. Real-time recording of the horizontal load, the vertical load, the horizontal displacement of the lower shear box, and the vertical displacement of the top loading plate was done using a data acquisition system. The recorded horizontal load data were corrected to account for the small frictional resistance generated by the rollers supporting the lower shear box.

Table 3-3 Details of Direct Shear tests on MSW samples

| Sample ID | w (%) | γ (kN/m ³) | σ'_n (kPa) | Composition |
|-----------|------------|----------------------------------|----------------------|---------------------------------------|
| D-1 | 9.7 | 9.5 | 150 | Plastics, paper, metal, wood and soil |
| D-2 | 14.8 | 10.1 | 100 | |
| D-3 | 11.2 | 8.9 | 60 | |
| D-4 | 8.5 | 8.8 | 135 | |

[Legend: w – in-situ moisture content of the sample; γ – bulk unit weight of the sample; σ'_n – normal effective stress during the direct shear test.]

3.4 Results and Discussions

3.4.1 Composition of MSW

Post-test visual examination of the intact samples revealed that the MSW was slightly degraded, blackish brown and slightly odorous, which indicated a relatively low level of organic matter decomposition. It contained cardboard, paper, wood, textiles, and thin plastic sheets along with small fractions of inorganic/inert materials like metals, glass, ceramic, and gravel, which is typical of domestic waste. A horizontally-layered structure associated with paper and cardboard was also visible. Pieces of textile could be torn easily.

3.4.2 Stress-strain response of MSW in Triaxial tests

The stress-strain response of MSW is presented in terms of cumulative axial strain $\varepsilon_a = \Delta L/L_0$ (where ΔL is the change in the length of the sample and L_0 is the length of the sample prior to shearing) and deviatoric stress $q = \Delta\sigma_1 = \sigma_1 - \sigma_3$ (where σ_3 is the total cell pressure, and $\sigma_1 = \sigma_3 + \Delta\sigma_1$, i.e. σ_1 the total axial stress applied to the sample).

Figure 3-5 shows q vs. ε_a plots for intact as well as recompacted MSW samples. Nonlinear stress-strain behaviour was exhibited by both the intact and the recompacted samples. Several recompacted samples (e.g. R-5, R-6, R-7 and R-9) showed a distinct peak in their stress-strain response - no distinct peak was observed in the stress-strain responses of the intact samples. The occurrence of distinct peaks in stress-strain response of recompacted samples is rather unusual and has not been reported by other researchers (e.g. Grisolia et al. 1995; Machado et al. 2002) who have conducted triaxial tests on large-diameter MSW samples.

An interesting feature of the stress-strain response of recompacted samples is the post-peak linear increase in deviatoric stress with increasing axial strain (indicated by the arrows in Figure 3-5 (b)) as exhibited by all but two recompacted samples. Several intact samples also exhibited this behaviour (Figure 3-5 (a)). It is shown in the next section that such a linear increase in deviatoric stress is indicative of the development of a shear band (or a failure plane) within the sample.

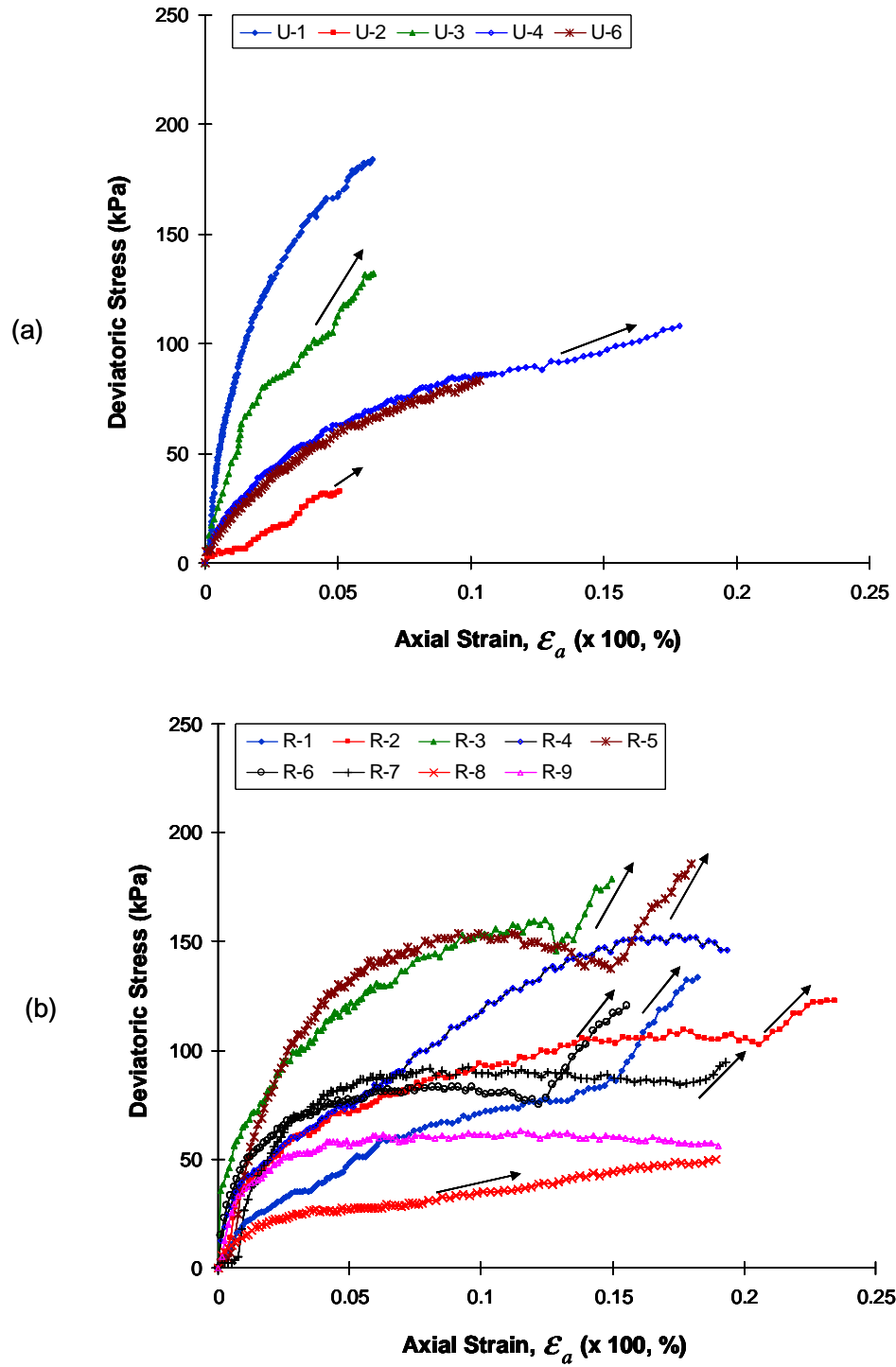


Figure 3-5 Deviatoric stress vs. axial strain plots obtained from triaxial compression tests on intact and recompacted samples of MSW: (a) Intact samples; (b) Recompacted samples

3.4.3 Shear strength of MSW from Triaxial tests

For the purpose of obtaining shear strength parameters of MSW, the results of the triaxial tests are presented in terms of stress paths of deviatoric stress q vs. mean effective stress p' (where $p' = (\sigma'_1 + 2\sigma'_3)/3$, σ'_3 is effective confining stress, and σ'_1 is the effective axial stress) stress paths. This approach has also been used by Caicedo et al. (2002) for the presentation of results from consolidated undrained triaxial tests on recompacted MSW samples. The effective confining pressure and effective axial stress were obtained by subtracting the pore-water pressure u from the total cell pressure σ_3 and total axial stress σ_1 , respectively. At the beginning of undrained shearing, the mean effective stress p' was equal to effective confining pressure σ'_3 (equal to total cell pressure minus the back pressure) and the deviatoric stress q was equal to zero. The effective confining pressure value at the beginning of undrained shearing for each of the 14 triaxial tests is given in Table 3-2.

3.4.3.1 Shear strength of Recompacted MSW

Figure 3-6(a) shows the stress paths in $q - p'$ stress space for the nine recompacted MSW samples. There is striking similarity between these stress paths and those typically experienced by a horizontally layered or cross-anisotropic soil sample (e.g. Graham and Houlsby 1983; Wood 1990). As mentioned above, all the recompacted samples were prepared by compacting MSW in four horizontal lifts. Such 'one-dimensional' deposition and stress history has imparted cross-anisotropy in recompacted MSW samples.

During the initial stage of undrained shearing, each stress path appeared to have followed a straight line with a slope of +3 (i.e. incremental stress ratio $\Delta q / \Delta p' = +3$)

with respect to the p' -axis. Since the total stress paths for a conventional (constant cell pressure) triaxial test are also inclined at a slope of +3 with respect to the p' -axis, it can be inferred that there was hardly any excess pore-water pressure induced in the sample during the initial stage of undrained shearing. This could be attributed to the compressible structure of MSW. It is hypothesized that during this stage of the test, the application of axial stress resulted in compression of various components of MSW, but not the compression of the inter-component voids.

As the undrained shearing continued, the stress path began to curve towards the q -axis, signifying a reduction in p' due to increase in pore-water pressures inside the sample. During this stage of undrained shearing, the incremental stress ratio $\Delta q / \Delta p'$ was negative. The stress paths for several samples (e.g. sample R-3 in Figure 3-6(a)) appeared to have reversed their trend of negative $\Delta q / \Delta p'$ after achieving a certain critical value of q / p' . From this point onwards, the stress paths had positive $\Delta q / \Delta p'$ and appeared to be heading along a straight line irrespective of their initial p' values.

Stress paths for samples R-1, R-2, R-3, R-5 and R-8 all end up on a straight line with a slope of 1.95 and a q -intercept of 15 kPa (solid line in Figure 3-6(a)) while the stress paths for samples R-4, R-6 and R-7 end up on another straight line with a slope of 1.43 and a q -intercept of zero (dashed line in Figure 3-6(a)). Stress path for sample R-9 terminates in a zone bound by the two straight lines; however, it is likely that this stress path would have ended up on the upper straight line if the sample could be sheared further.

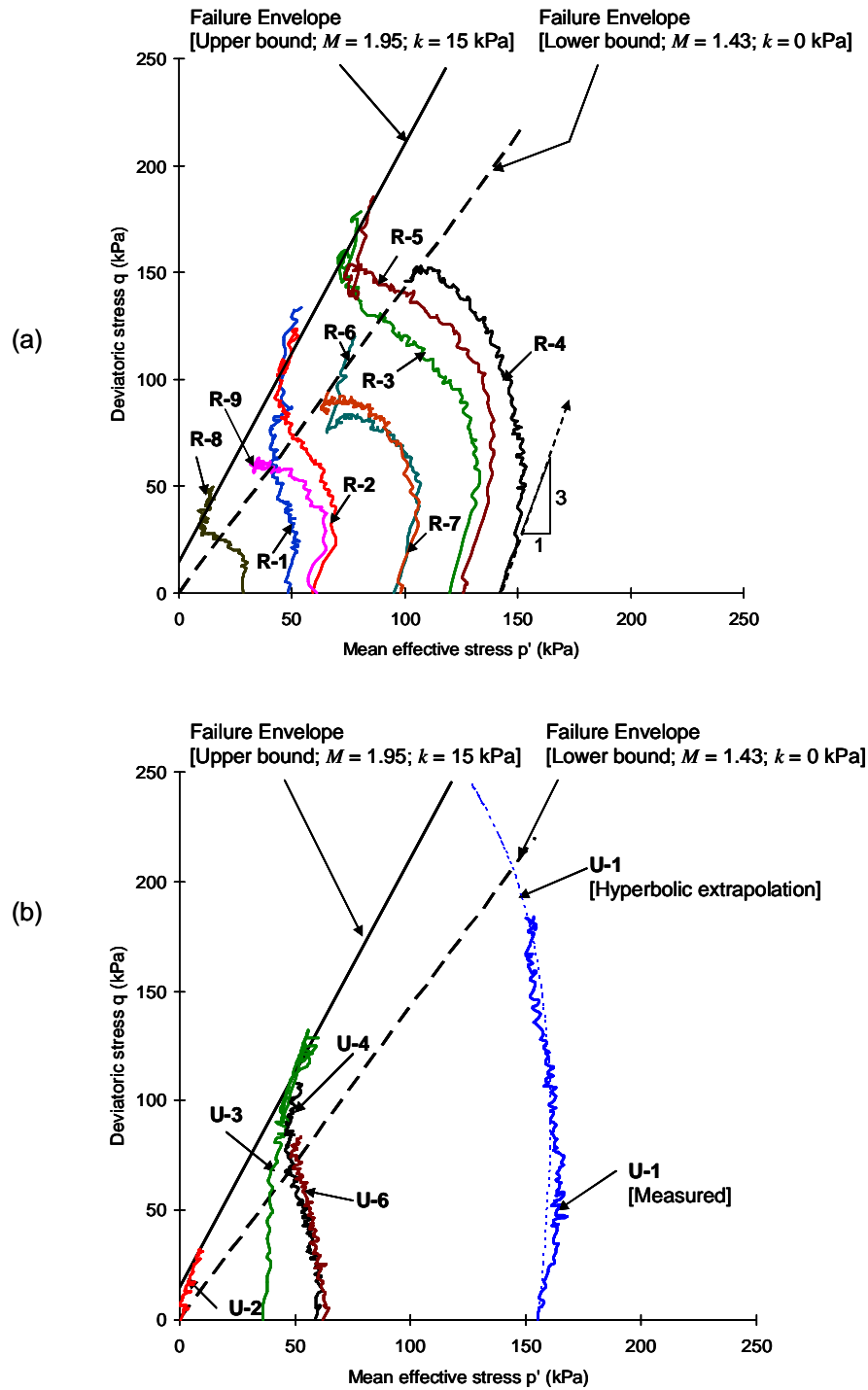


Figure 3-6 Stress paths and failure envelopes in deviatoric stress vs. mean effective stress space from triaxial tests on MSW: (a) Recompacted samples; (b) Intact samples

As mentioned in the previous section, the linear increase in q and p' along a failure envelope is likely associated with the development of a shear band (or a failure plane) inside a sample soon after the sample achieves a critical value of q/p' . Once the shear band forms, the mechanism of shearing changes from undrained to drained shearing because of dilation and localized draining of pore-water along the failure plane. Shearing on the failure plane now continues at a constant positive incremental stress ratio, i.e. the stress path moves along a straight line. The upper solid black and the lower dashed black straight lines (Figure 3-6(a)) on which the stress paths for all recompacted samples end up, therefore, represent the upper bound and the lower bound failure envelopes for the recompacted MSW. Whether a sample would end up on the upper bound failure envelope or the lower bound failure envelope probably depends on the extent of dilation occurring at the failure plane. It is hypothesized that a sample that has better interlocking between its constituent elements would experience greater dilation at the failure plane, and therefore, it would mobilize higher shear strength and end up on the upper bound failure envelope.

The Mohr-Coulomb shear strength parameters – cohesion intercept c' and the angle of friction ϕ' – associated with these two failure envelopes can be obtained using the following two equations:

$$\phi' = \sin^{-1} \left(\frac{3M}{6+M} \right) \quad [2]$$

$$c' = k \left[\frac{3 - \sin(\phi')}{6 \cos(\phi')} \right] \quad [3]$$

where M is the slope of failure envelope and k is the q -intercept of the failure envelope in $q - p'$ stress space. The upper bound and the lower bound values of c' and ϕ' associated with these two failure envelopes are given in Table 3-4.

Table 3-4 Shear strength parameters of MSW obtained from Direct shear and triaxial tests.

| Parameter | From Triaxial Tests | | From Direct Shear Tests | |
|-------------|---------------------|-------------|-------------------------|--------------|
| | Lower Bound | Upper Bound | Measured | Extrapolated |
| c' (kPa) | 0 | 8.4 | 14 to 26 | 0 to 19 |
| ϕ' (°) | 35 | 47 | 30 to 36 | 41 to 47 |

The development of the shear band in recompacted samples (Figure 3-5(b)) occurred at 8 to 21% axial strains. These axial strain levels are lower than typical ‘at failure’ strain levels of 20 to 40% reported in the literature (e.g. Oweis and Khera 1990; Siegel et al. 1990; Gabr and Valero 1995). Formation of shear bands at low strain levels could be the result of strain incompatibility leading to slippage at the interfaces between stiffer reinforcing elements (e.g. plastic and metal sheets) and the surrounding softer waste mass. Shear bands are unlikely to form within a waste mass if most of the reinforcing elements are ‘stretchy’, and therefore, deform conformably with the surrounding waste. It has been noted by several researchers (e.g. Landva et al. 1984; Cowland et al. 1993; Jessberger et al. 1995) that samples of waste that do not exhibit peaks in their stress-strain response, typically undergo bulging failure at large strain levels, and often contain a combination of ‘weak’ spots occupied by highly compressible materials and stretchable reinforcing materials. Post-test visual examination of samples R-4 and R-9, which exhibited such bulging failure, confirmed the presence of such materials in these samples.

At this point, a brief discussion on the possibility of the formation of shear bands in a landfill would be appropriate. It can be argued that shear bands could potentially develop in landfills under conditions suited to their formation. For instance, strain incompatibility leading to the formation of shear bands could occur within a landfill if the reinforcing elements remain largely intact but the surrounding waste softens, either because of rapid decomposition or because of elevated pore-water pressures caused, for example, by a clogged leachate collection system. This scenario is more likely to occur in closed landfills (such as the Brock West landfill) given the time required for most leachate collection systems to clog (Rowe and Fleming 1998). Formation of shear bands in such landfills could potentially result in the onset and rapid progression of failure within the waste mass. Excellent examples of this type of failure are the 1993 Umraniye-Hekimbasi landfill failure in Istanbul, Turkey (Kocasoy and Curi 1995), the 1997 Bulbul landfill failure in Durban, South Africa (Brink et al. 1999), the 1997 Doña Juana landfill failure in Bogotá, Colombia (Hendron et al. 1999; Caicedo et al. 2002), and the 2000 Payatas landfill failure in Manila, Philippines (Merry et al. 2005).

3.4.3.2 Shear strength of Intact MSW

Figure 3-6(b) shows the stress paths in $q - p'$ stress space for the five intact MSW samples. Comparing Figure 3-6(b) with Figure 3-6(a), it is evident that the stress paths followed by the intact MSW samples are not as curved as those followed by the recompacted MSW samples. This suggests that the structure of the intact samples is less anisotropic than that of the recompacted samples. The intact samples for the present study were obtained from a relatively shallow depth. It is possible that intact samples of MSW taken from greater depths would be cross-anisotropic to a greater extent by virtue of

having experienced predominantly one-dimensional compression under overburden stress.

The upper bound and the lower bound failure envelopes obtained for the recompacted samples are shown superimposed on the stress paths for intact samples in Figure 3-6(b). The stress paths for three intact samples (U-2, U-3 and U-4) end up either on or close to the upper bound failure envelope while the stress path for sample U-6 ends up close to the lower bound failure envelope. The stress path for sample U-1 terminates below the lower bound failure envelope. The triaxial test on sample U-1 was terminated prematurely because the sample buckled excessively and came in contact with the inner wall of the triaxial cell. As such, sample U-1 could not be tested to failure. An attempt was made to extend the stress path of sample U-1 by extrapolating the deviatoric stress vs. axial strain and excess pore-water pressure vs. axial strain curves. Such extrapolation was achieved by fitting hyperbolic curves through the measured data points as shown in Figure 3-7. The fitted hyperbolic curves were then used to extend the stress path for sample U-1 in $q - p'$ stress space as indicated by the dotted curve in Figure 3-6(b). It is likely that if further shearing of sample U-1 could be achieved, the stress path for sample U-1 would have ended up close to the upper bound failure envelope.

The stress path for intact sample U-2, which was tested at zero effective confining pressure, is along a straight line with a slope of +3 with respect to the p' -axis. It is suggested that failure was achieved in sample U-2 along a ‘tension cut-off’ line, which for triaxial tests has a slope of +3 with respect to the p' -axis. Admittedly, the existence of a tension cut-off line for saturated MSW can not be confirmed on the basis of just one

triaxial test; more tests on saturated MSW samples at low values of effective confining pressure would be needed.

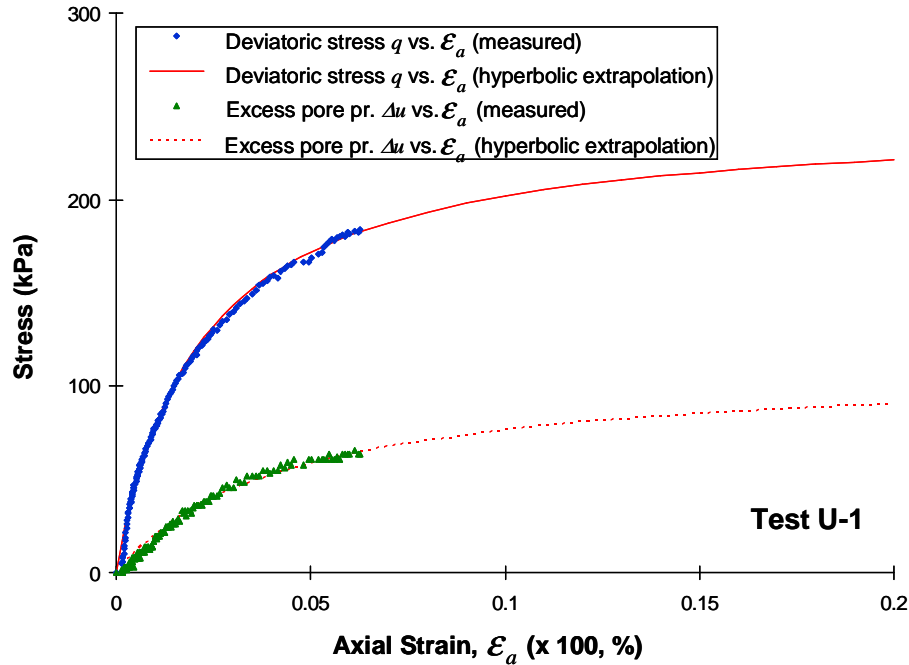


Figure 3-7 Extrapolation of measured deviatoric stress vs. axial strain and excess pore-water pressure vs. axial strain curves using a non-linear hyperbolic model to obtain deviatoric stress at failure for intact sample U-1

Only a limited number of triaxial tests could be conducted on intact MSW samples; however, it is evident from the results of these tests that although the pre-failure deformation behaviour of the intact samples is different from that of the recompacted samples, they both appear to be mobilizing fairly similar shear strength values. The authors have initiated a testing program involving triaxial testing of a larger number of intact and recompacted MSW samples to confirm this observation.

3.4.4 Stress-strain behaviour of MSW from Direct shear test

Figure 3-8 shows the measured shear stress vs. shear strain curves of the four direct shear tests. The shear stress vs. shear strain response of MSW in direct shear tests is nonlinear and very similar to the deviatoric stress vs. axial strain response of MSW in triaxial tests (Figure 3-5). The value of initial tangent shear modulus of MSW appears to increase with increasing effective normal stress. It can also be seen from Figure 3-8 that no distinct peak in shear stress could be achieved within the maximum permissible horizontal displacement of the shear box. This is consistent with the experience of other researchers (e.g. Kölsch 1995; Kavazanjian et al. 1999) who have conducted large direct shear tests on recompacted MSW samples. It was, therefore, decided to ‘extrapolate’ the shear stress vs. shear strain curve for each test by fitting hyperbolic curves through measured data points and values of ‘ultimate’ shear stress were obtained as asymptotes to the fitted hyperbolic curves.

3.4.5 Shear strength of MSW from Direct shear tests

Plots of shear stress at failure vs. effective normal stress for the four direct shear tests are shown in Figure 3-9. The shear stress at the end of the test was taken as shear stress at failure for the measured results. The asymptotic ‘ultimate’ shear stress value (as explained in the previous section) was taken as the shear stress at failure for the hyperbolic extrapolations. Mohr-Coulomb (M-C) failure envelopes were fitted through the measured and the extrapolated results (Figure 3-9) and shear strength parameters (c' and ϕ') were obtained using the slopes and the y-intercepts of these failure envelopes. The M-C failure envelope denoted by the solid line was fitted using all four measured data points whereas the M-C failure envelope denoted by the dashed line was fitted by

ignoring the results for test D-1 (conducted at 150 kPa effective normal stress). Similarly, the M-C failure envelopes for the extrapolated results were obtained by considering all four tests or by ignoring the results for test D-1.

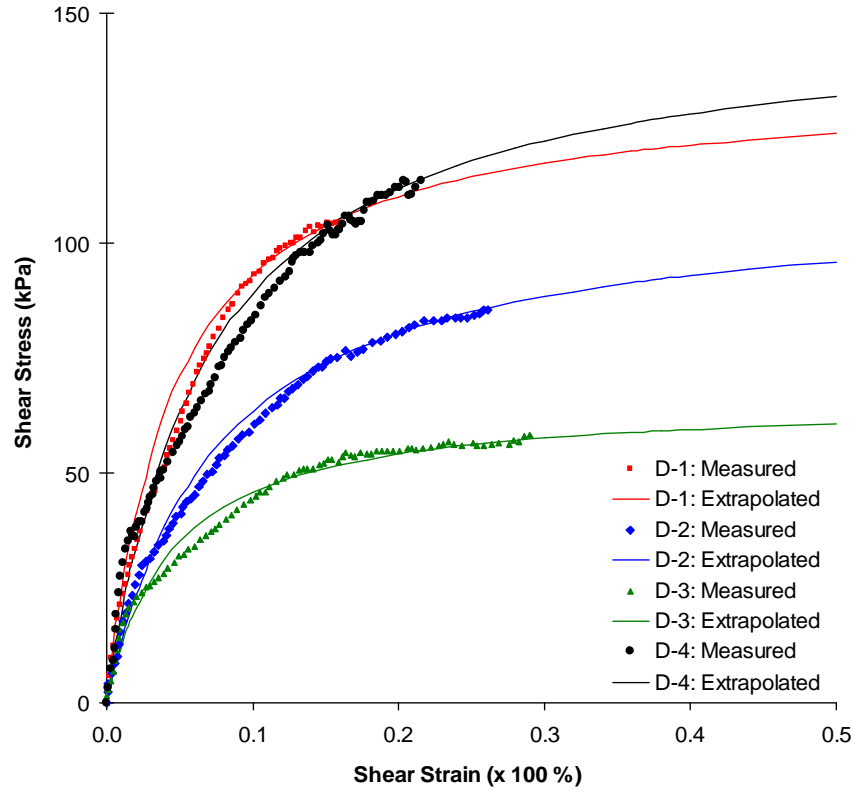


Figure 3-8 Measured and extrapolated shear stress vs. shear strain plots for the direct shear tests

The range of values of c' and ϕ' corresponding to these four M-C failure envelopes are given in Table 3-4. It is interesting to note that the estimates of c' and ϕ' obtained using the hyperbolic extrapolation of direct shear test results are very similar to the upper bound estimates of c' and ϕ' obtained from the triaxial test results.

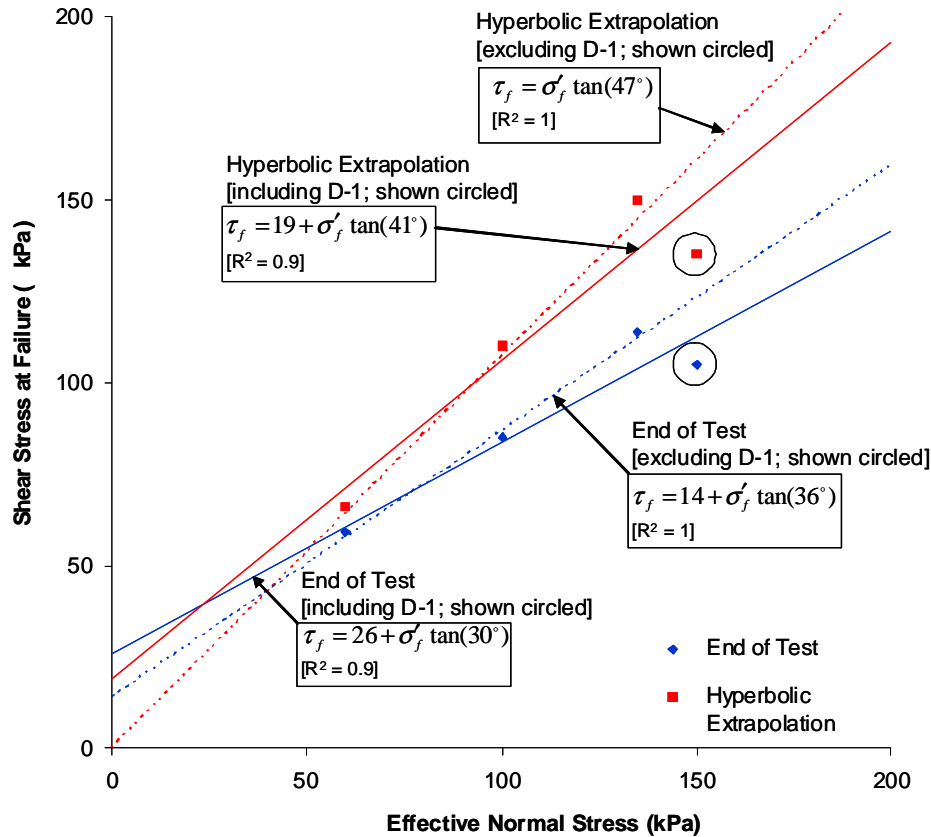


Figure 3-9 Shear strength envelopes for MSW obtained from Direct shear tests results

3.4.6 Measured shear strength of MSW – Comparison with published literature

The MSW failure envelopes obtained from the present study, i.e. upper bound and lower bound failure envelopes obtained from triaxial tests (Figure 3-6) and the four failure envelopes obtained from direct shear tests (Figure 3-9) are plotted together in Figure 3-10(a). Also included in Figure 3-10(a) are the upper bound and lower bound failure envelopes for MSW inferred from the values of c' and ϕ' for MSW obtained from the literature (Table 3-1). It can be seen from Figure 3-10(a) that the MSW failure envelopes obtained from the present study lie in between the upper bound and the lower bound MSW failure envelopes obtained from the literature.

It is interesting to note from Figure 3-10(a) that the MSW failure envelopes obtained from the direct shear tests on the basis of hyperbolic extrapolation of measured shear stress vs. shear strain response plot very close to the upper bound failure envelope obtained from triaxial tests on recompacted MSW samples, which was established using the results of recompacted samples that had reached failure condition in triaxial tests. This observation appears to provide some justification to the use of hyperbolic extrapolation of stress-strain curves from direct shear tests to obtain the values of shear stress at failure.

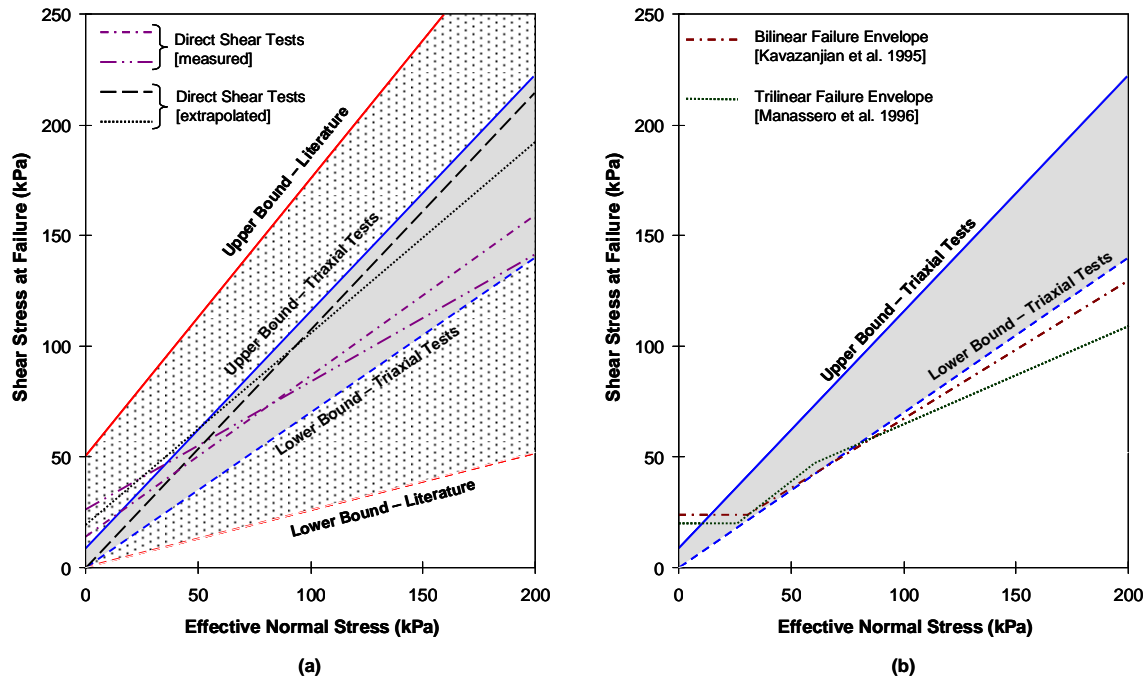


Figure 3-10 Shear strength envelopes for MSW (a) from present study and the literature (b) upper and lower bound failure envelope from this study and from literature.

Figure 3-10(b) shows a comparison between the upper bound and lower bound failure envelopes obtained from the triaxial tests with the bilinear failure envelope proposed by Kavazanjian et al. (1995) and the trilinear failure envelope proposed by

Manassero et al. (1996), which are widely used in practice for the assessment of stability of landfill slopes. The lower bound failure envelope obtained from the triaxial tests plots fairly close to the ‘frictional’ portion of the bilinear failure envelope. It also plots fairly close to the middle portion of the tri-linear failure envelope; however, at higher effective normal stresses, it plots higher than the tri-linear failure envelope.

At effective normal stresses less than 30 kPa, the bilinear failure envelope becomes ‘cohesive’ whereas the lower bound failure envelope continues to be ‘frictional’. This difference in the two failure envelopes may be caused by the fact that the bilinear failure envelope is based on the back-analyses of landfill failures (Kavazanjian et al. 1995) where MSW was only partially saturated. The lower bound failure envelope, on the other hand, is based on the results of fully saturated MSW samples. It is, therefore, likely that the ‘cohesive’ portion of the bilinear failure envelope includes some effect of apparent cohesion associated with negative pore-water pressures in the MSW under conditions of partial saturation.

3.5 Conclusions

Preliminary results from a program of shear strength testing of intact and recompacted samples of municipal solid waste (MSW) have been presented in this paper. A method of taking intact samples from landfill sites using a push-in sampler was developed and used successfully to obtain intact samples of MSW from the Brock West landfill site near Toronto, Ontario. Consolidated undrained tests were conducted on saturated MSW samples using a large triaxial compression apparatus. A large transportable direct shear apparatus was also used for shear strength testing of MSW samples. The results of shear

strength testing were presented in terms of Mohr-Coulomb shear strength parameters, i.e. cohesion intercept (c') and angle of friction (ϕ'), and compared with those available in the literature.

Based on these results and their favorable comparison with the published literature, it can be concluded that it is feasible to obtain meaningful shear strength parameters for MSW using consolidated undrained triaxial tests on large-diameter intact and recompacted MSW samples. Values c' and ϕ' for MSW obtained from these triaxial tests were comparable with those obtained from direct shear tests.

Using a triaxial compression apparatus, it is possible to shear saturated samples of MSW and to measure their pore-water pressure response during shearing. It is difficult, if not impossible, to achieve this in a direct shear apparatus. Consequently, the results of a triaxial test can be analyzed in terms of effective stresses and the effective stress paths followed by the MSW samples during shearing can be plotted. On the basis of the fairly coherent picture of shear behaviour of MSW presented by these effective stress paths (Figure 3-6), it is reasonable to conclude that the mechanical behaviour of saturated MSW samples can be explained using the principle of effective stress.

It was found that the intact and recompacted saturated samples of MSW mobilize fairly similar values of shear strength when sheared in a triaxial compression test (Figure 3-6). It can, therefore, be suggested that reasonable values of c' and ϕ' for MSW can be obtained using recompacted samples. It should, however, be noted that this suggestion is based on the results of only five intact samples. More triaxial tests on intact as well as recompacted samples are required to support this conclusion.

Although the intact and the recompacted saturated samples mobilized similar values of shear strength, their pre-failure response was quite different. As shown in Figure 3-6, recompacted samples behaved in a fairly ductile manner and generated higher excess pore-water pressures whereas intact samples showed a stiffer response and generated lower pore-water pressures. This observation is important from the viewpoint of evaluating deformation and serviceability conditions within a landfill. It appears to support the use of intact samples for establishing deformation characteristics of MSW. More triaxial tests on intact as well as recompacted samples are required to confirm this observation.

3.6 References

- ASTM. 2004. Standard Test Method for Consolidated Undrained Triaxial Compression Test for Cohesive Soils. American Society for Testing of Materials (ASTM), West Conshohocken, Penn. ASTM D4767.
- Brink, D., Day, P.W. and du Preez, L. 1999. Failure and remediation of Bulbul Drive landfill: Kwazulu-Natal, South Africa. Proc. 7th International Waste Management and Landfill Symposium, Sardinia, 555-562.
- Caicedo, B., Giraldo, E. and Yamin, L. 2002. The landslide of Dona Juana landfill in Bogota. A case study. Proc. 4th International Conference on Environmental Geotechnics. Edited by L.G. de Mello and M. Almeida, AA Balkema, Lisse, The Netherlands, 171-175.
- Cowland, J.W., Tang, K.Y. and Gabay, J. 1993. Density and strength properties of Hong Kong refuse. Proc. 4th International Waste Management and Landfill Symposium, Sardinia, 1433-1446.

- Eid, H.T., Stark, T.D., Evans, W.D. and Sherry, P.E. 2000. Municipal solid waste slope failure – I: Waste and foundation soil properties. *Journal of Geotechnical and Geoenvironmental Engineering*, ASCE, 126(5): 397-407.
- Environment Canada. 2007. The Brock West Project. Article available on-line at <http://www.ec.gc.ca/wmd-dgd/default.asp?lang=En&nav=B81863DD-1> (accessed May 12, 2007).
- Gabr, M.A. and Valero, S.N. 1995. Geotechnical Properties of Municipal Solid Waste. *Geotechnical Testing Journal*, ASTM, 18(2), 241-251.
- Graham, J. and Houlsby, G.T. 1983. Elastic anisotropy of a natural clay. *Géotechnique*, 33(2): 165-180.
- Grisolia, M., Napoleoni, Q. and Tancredi, G. 1995. The use of triaxial test for the mechanical characterization of MSW. *Proc.5th International Waste Management and Landfill Symposium*, Sardinia, 761-768.
- Hendron, D.M., Fernandez, G., Prommer, P.J., Giroud, J.P. and Orozco, L.F. 1999. Investigation of the cause of the 27 September 1997 slope failure at the Doña Juana landfill. *Proc. 7th International Waste Management and Landfill Symposium*, Sardinia, 545-554.
- Houston, W.N., Houston, S.L., Liu, J.W., Elsayed, A. and Sanders, C.O. 1995. In-situ testing methods for dynamic properties of MSW landfills. *Geotechnical Special Publication*, ASCE, 54: 73-82.
- Jessberger, H.L., Syllwasschy, O. and Kockel, R. 1995. Investigation of waste body behaviour and waste structure interaction. *Proc. 5th International Waste Management and Landfill Symposium*, Sardinia, 731-743.
- Kavazanjian, Jr. E., Matasovic, N. and Bachus, R.C. 1999. Large diameter static and cyclic laboratory testing of municipal solid waste. *Proc.7th International Waste management and Landfill Symposium*, Sardinia, 437-444.

- Kavazanjian, Jr. E. 2003. Evaluation of MSW properties using field measurements. Proc.17th Geosynthetic Research Institute Conference: Hot Topics in Geosynthetics – IV, Las Vegas, Nevada, 74 113.
- Kocasoy, G. and Curi, K. 1995. The Ümraniye-Hekimbasi open dump accident. Waste Management and Research, 13: 305-314.
- Kölsch, F. 1995. Material values for some mechanical properties of domestic waste. Proc. 5th International Waste management and Landfill Symposium, Sardinia, 711-729.
- Kölsch, F., Fricke, K., Mahler, C. and Damanhuri, E. 2005. Stability of landfills – The Bandung dumpsite disaster. Proc.10th International Waste Management and Landfill Symposium, Sardinia (on CD-ROM).
- Landva, A.O., and Clark, J.I. 1986. Geotechnical testing of wastefill. Proc. 39th Canadian Geotechnical Conference, Ottawa, 371-385.
- Landva, A. O. and Clark, J. I. 1990. Geotechnics of waste fills. Geotechnics of Waste Fills – Theory and Practice. Edited by A.O. Landva and G.E. Knowles. ASTM Special Technical Publication, 1070, 86-103.
- Landva, A.O., Clark, J.I., Weisner, W.R. and Burwash, W.J. 1984. Geotechnical engineering and refuse landfills. Proc. 6th National Conference on Waste Management, Vancouver, Canada, 1–37.
- Machado, S.L., Carvalho, M.F. and Vilar, O.M. 2002. Constitutive Model for Municipal Solid Waste. Journal of Geotechnical and Geoenvironmental Engineering, ASCE, 128(11): 940-951.
- Manassero, M., Van Impe, W. F. and Bouazza, A. 1996. Waste disposal and containment. Proc. 2nd International Congress on Environmental Geotechnics, Osaka, Japan, 3: 1425-1474.
- Mazzucato, A., Simonini, P. and Colombo, S. 1999. Analysis of block slide in a MSW landfill. Proc. 7th International Waste management and Landfill Symposium, Sardinia, 537-544.

- Merry, S.M., Kavazanjian Jr. E. and Fritz, W.U. 2005. Reconnaissance of the July 10, 2000 Payatas landfill failure. *Journal of Performance of Constructed Facilities*, ASCE, 19(2): 100-107.
- Oweis, I.S. and Khera, R.P. 1990. *Geotechnology of Waste Management*, PWS Publishing Company, Boston.
- Pelkey, S.A., Valsangkar, A.J., and Landva, A. 2001. Shear displacement dependent strength of municipal solid waste and its major constituents. *Geotechnical Testing Journal*, ASTM, 24(4): 381-390.
- Rowe, R.K. and Fleming, I.R. 1998. Estimating the time for clogging of leachate collection systems. *Proc. 3rd International Congress on Environmental Geotechnics*, Lisbon, Portugal, 23-38.
- Siegel, R.A., Robertson, R.J. and Anderson, D.G. 1990. Slope stability investigation at a landfill in Southern California. *Geotechnics of Waste Fills – Theory and Practice*. Edited by A.O. Landva and G.E. Knowles. ASTM Special Technical Publication, 1070, 259-284.
- Vilar, O.M. and Carvalho, M.F. 2002. Shear strength properties of municipal solid waste. *Proc. 4th International Conference on Environmental Geotechnics*. Edited by L.G. de Mello and M. Almeida, AA Balkema, Lisse, The Netherlands, 59-64.
- Withiam, J.L., Tarvin, P.A., Bushell, T.D., Snow, R.E. and German, H.W. 1995. Prediction and Performance of municipal landfill slope. *Geotechnical Special Publication*, ASCE, 46: 1005-1019.
- Wood, D.M. 1990. *Soil Behaviour and Critical State Soil Mechanics*. Cambridge University Press, Cambridge, UK.

CHAPTER 4 APPLICATION OF A NON-LINEAR STRESS-STRAIN MODEL TO MUNICIPAL SOLID WASTE

Preface[†]

A non-linear elastic hyperbolic model is proposed for describing the stress-deformation behaviour of MSW. The parameters of this model are specific to the material and can be determined experimentally. The following paper describes the estimation of parameters required for this model from evaluation of the results of numerous triaxial tests including the results obtained in this research program and from published literature. Based on statistical analysis of test results, lower and upper bound values for model parameters are determined. It is proposed that the hyperbolic model when used with the lower and upper bounds of the model parameters can be used for predicting the lower and upper bounds of stress-deformation behaviour of the MSW. The prediction is based on the assumption that the allowable axial strain does not exceed 20%. A method for characterizing modulus of elasticity of MSW from interpretation of triaxial test results is also described. The work presented in this paper addresses in part, the second objective: to characterize Young's modulus of elasticity of MSW from interpretation of triaxial test results and determine the parameters of a non-linear constitutive model as applied to MSW.

[†]A similar version of this chapter is under review for possible publication as a research paper in *Geotechnique*.

Citation: M. K. Singh, I. R. Fleming and J. S. Sharma "Application of a non-linear stress-strain model to Municipal Solid Waste".

Abstract

The stress-strain behaviour of municipal solid waste is nonlinear, that is, it exhibits a fairly rapid drop in stiffness as the stress state approaches failure, which is typically assumed at 20% strain. A hyperbolic elastic model has been used for soils as it incorporates both the non-linearity of the stress-strain relationship and the stress dependency of stiffness. It is hypothesized that a hyperbolic elastic model may also be appropriate for describing the stress-strain response of MSW. The parameters of this model are specific to the material tested and need to be determined experimentally. This paper presents the application of a hyperbolic elastic model to landfilled MSW. The model parameters were determined using data from six published studies as well as the results from laboratory testing carried out by the authors on large samples of MSW from two different landfills in Canada. Based on a statistical analysis of the testing results, three of the five parameters were replaced by constants with upper and lower bounds for a desired degree of confidence. It is proposed that the resulting hyperbolic curves may be used to predict the stress-strain behaviour of municipal solid waste up to 20% strain.

4.1 Introduction

MSW is a complex material and its stress-strain response depends on various factors such as its composition, density, fabric structure, state of degradation, and drainage conditions. The purpose of this paper is to propose a constitutive model for the pre-failure stress-deformation behaviour of MSW. Based upon triaxial test results, both those previously published and those presented in this paper, it has been observed that the mechanical

behaviour of MSW might be approximated by a non-linear elastic constitutive model. Such an argument is supported by the fact that MSW shows large pre-failure deformations (Jessberger and Kockel 1993; Grisolia et al. 1995; Manassero et al. 1997).

The hyperbolic elastic model proposed by Kondner (1963) for soils and modified by Duncan and Chang (1970) has been used to describe pre-failure deformation. The hyperbolic elastic model incorporates both the non-linearity of the stress-strain relationship and the stress dependency of stiffness (Duncan and Chang 1970). These two important aspects of stress-strain behaviour may also be pertinent to MSW and the evaluation of a hyperbolic elastic model to describe the stress-strain behaviour of MSW, therefore, seems to be appropriate.

The stress-strain behaviour of MSW has been simulated using constitutive models of soil such as elastic-perfectly plastic (Singh et al. 2007), and the Cam-Clay model (Machado et al. 2002). The hyperbolic elastic model has been used only rarely to describe the stress-strain behaviour of MSW. Filz et al. (2001) simulated the Kettleman Hills landfill failure using a modified elastic-plastic model described by Morrison (1995). This modified model simulates pre-failure deformation using the hyperbolic model developed by Duncan and Chang (1970) and post-failure behaviour with a Mohr-Coulomb plasticity model. Filz et al. (2001) selected values for the hyperbolic elastic model parameters to simulate the Kettleman Hills landfill failure; however, they provided little or no guidance as to how these values were estimated or the basis on which these values were assumed.

The present study aims to provide a simplified hyperbolic elastic model for MSW. Stress-strain data from triaxial compression testing of large samples of MSW have been

used to estimate the parameters for this model. The model parameters were determined from the results of laboratory testing carried out by the authors on large samples of MSW from two different landfills in Canada, as well as triaxial testing data from six published studies. Based on these 50 different triaxial compression tests (both drained and undrained) on large samples of MSW, lower and upper bound values for model constants are proposed for the hyperbolic non-linear elastic model. The prediction of stress-strain behaviour based on the assumption that the allowable axial strain does not exceed 20% is in accordance with several other researchers such as Jessberger and Kockel (1993), Gabr and Valero (1995), Grisolia et al. (1995), and Kavazanjian (1995).

4.2 Review of hyperbolic stress-strain model

The application of an hyperbolic stress-strain relationship was first proposed for soils by Kondner (1963), who suggested that the stress-strain curves obtained from triaxial compression tests of both clay and sand may be approximated by a two-parameter hyperbolic model (later modified by Duncan and Chang 1970 to a five-parameter model). In terms of the deviatoric stress, the hyperbolic stress-strain relationship proposed by Kondner (1963) is expressed as:

$$(\sigma'_1 - \sigma'_3) = \frac{\varepsilon_a}{\frac{1}{E_i} + \frac{\varepsilon_a}{(\sigma'_1 - \sigma'_3)_{ult}}} \quad [1]$$

where $(\sigma'_1 - \sigma'_3)$ is the deviatoric stress, ε_a is the axial strain, E_i is the initial tangent Young's modulus and $(\sigma'_1 - \sigma'_3)_{ult}$ is the ultimate (asymptotic) deviatoric stress (Figure 4-1). Equation (1) can be rearranged as:

$$\frac{\varepsilon_a}{(\sigma'_1 - \sigma'_3)} = a + b\varepsilon_a \quad [2]$$

Equation (2) represents a straight line of slope b and intercept a in a $\varepsilon_a/(\sigma'_1 - \sigma'_3)$ - ε_a Cartesian space. Using a linear best-fit, stress-strain data from triaxial tests may be used with these transformed axes to determine the values of b and a .

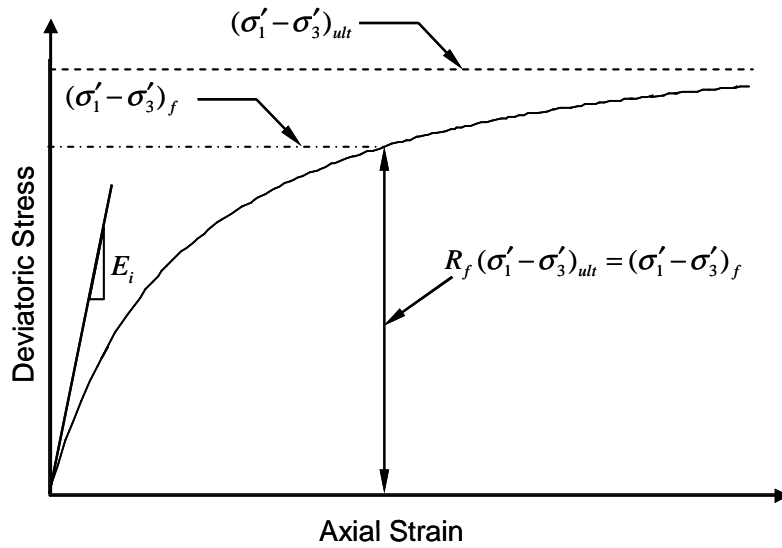


Figure 4-1 Hyperbolic stress-strain curve

Kondner (1963) pointed out that the ultimate value of deviatoric stress $(\sigma'_1 - \sigma'_3)_{ult}$ for the hyperbolic representation is greater than the failure strength of the soil, as the hyperbola will always be below the asymptote representing the ultimate deviatoric stress for all finite values of strain. The failure strength will thus be some factor of the ultimate strength. To account for this difference, Duncan and Chang (1970) introduced a reduction factor R_f (Figure 4-1) expressed as:

$$R_f = \frac{(\sigma'_1 - \sigma'_3)_f}{(\sigma'_1 - \sigma'_3)_{ult}} \quad [3]$$

where $(\sigma'_1 - \sigma'_3)_f$ is the deviatoric stress at failure (or at a value of axial strain deemed to be 'failure'). $(\sigma'_1 - \sigma'_3)_f$ can be expressed using the Mohr-Coulomb failure criterion:

$$(\sigma'_1 - \sigma'_3)_f = \frac{2c' \cos \phi' + 2\sigma'_3 \sin \phi'}{1 - \sin \phi'} \quad [4]$$

where c' is the cohesion intercept and ϕ' is the angle of shearing resistance.

Using large-scale tests on MSW, the Young's modulus of MSW has been found to increase with depth and increasing confining stress (Beaven and Powrie 1995; Singh and Fleming 2008a). Accordingly, a power function first proposed by Janbu (1963) for clayey soils and given by Equation (5) is used to capture the stress dependence of Young's modulus of MSW:

$$E_i = KP_a \left(\frac{\sigma'_3}{P_a} \right)^n \quad [5]$$

where E_i is the initial tangent modulus, σ'_3 is the effective confining stress, P_a is the atmospheric pressure (=101.33 kPa), and K and n are dimensionless parameters, which govern the magnitude and the rate of variation of E_i with σ'_3 . While municipal waste is clearly not a clayey soil, a practical advantage in using a formulation of this form is that it is coded into some stress-deformation finite element software such as SIGMA/W (GSI, 2007). Equation (5) implies that as σ'_3 approaches 0, E_i should also approach 0; this is consistent with the authors' laboratory compression cell testing data (Singh and Fleming 2008a) and data from a large-scale compression cell in the UK (Beaven and Powrie 1995) as shown in Figure 4-2.

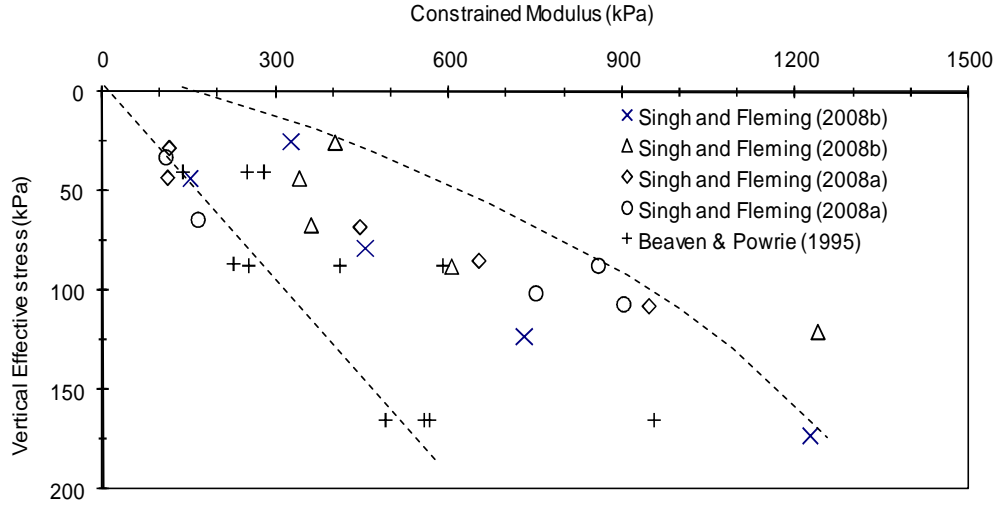


Figure 4-2 Modulus of municipal solid waste from large-scale compression tests

Incorporating R_f from Equation (3), $(\sigma'_1 - \sigma'_3)_f$ from Equation (4) and E_i from Equation (5) into Equation (1) yields:

$$(\sigma'_1 - \sigma'_3) = \frac{\epsilon_a}{\frac{1}{KP_a \left(\frac{\sigma'_3}{P_a} \right)^n} + \frac{\epsilon_a R_f (1 - \sin \phi')}{2c' \cos \phi' + 2\sigma'_3 \sin \phi'}} \quad [6]$$

Equation (6) is a five-parameter (K , n , R_f , c' and ϕ') constitutive model representing stress-strain behaviour in terms of shear strength. This model is used in this study to represent the non-linear stress-strain behaviour of MSW. In this study, however, it is further proposed that for municipal waste; K , n , and R_f may be considered to have near-constant values and Equation (6) thus effectively reduces to a two-parameter (c' , ϕ') model for effective stress analysis. To employ this approach in total stress analysis, appropriate values for K , n , and R_f are obtained using constant value of σ_3 ; however, effective stress analysis is employed in this study for interpretation of all test results.

4.3 Methodology

The methodology involves estimation of parameters K , n , and R_f of the hyperbolic model, which can be obtained experimentally from triaxial testing of MSW samples. As discussed earlier, the data used in this study were obtained from laboratory testing of samples from two different landfills in Canada as well as test data from six different published studies.

A series of consolidated undrained triaxial compression tests with pore pressure measurements were carried out on three different types of samples of MSW obtained from two Canadian landfills. The samples were sheared at an axial displacement rate of 0.4 mm/min. Shearing was discontinued when (a) the axial load did not increase appreciably with increasing axial displacement, (b) the axial load decreased with increasing axial displacement, (c) excessive deformation of the sample (e.g. bulging or buckling) was observed, or (d) when the maximum permissible axial displacement of the sample pedestal was reached. For a few cases in which tests were terminated at axial strains less than 20% due to excessive buckling, the stress-strain and pore pressure data were extrapolated to reach 20% axial strain similar to the extrapolation of stress-strain and pore pressure data from the published literature.

Experimental stress-strain curves were reproduced from published sources (Vilar and Carvalho 2004; Caicedo et al. 2002; Machado et al. 2000; Grisolia et al. 1995; Kockel 1995; Jessberger and Kockel 1993) by digitization. Similarly, experimental pore pressure curves from consolidated undrained tests by Vilar and Carvalho (2004) and Caicedo et al. (2002) were also reproduced. The experimental plot of stress-strain by

Kockel (1995) was not directly available and was taken from Krase and Dinkler (2005). Every effort was made to digitize the original plots accurately; however, minor deviation of digitized data from original data cannot be ruled out. With the exception of data from Caicedo et al. (2002), the published stress-strain data extended beyond 20% axial strain. Accordingly, both the stress-strain and pore pressure data from Caicedo et al. (2002) were extrapolated to 20% axial strain using a hyperbolic function as shown in Figure 4-3. In order to maintain uniformity in interpretation of the various stress-strain data, this method was followed for all such test results where the sample could not be sheared up to 20% axial strain.

4.4 MSW samples and Test equipment used in this study

Samples of MSW (both intact and recompacted) for laboratory testing were collected from two Canadian landfills: the Brock West Landfill near Toronto, Ontario and the Spadina Landfill in Saskatoon, Saskatchewan.

4.4.1 Samples from Brock West landfill

The Brock West landfill served the City of Toronto from 1973 to 1999, receiving 18 million tonnes of MSW. Intact samples (150 and 200 mm in diameter) were obtained from the bottom of an 8-m deep excavation on the south slope of the landfill. Specially designed samplers were pushed approximately 450 mm into the waste using the bucket of a hydraulic excavator. The samplers with an intact MSW sample inside were then retrieved by excavating around the sampler. The ends of the retrieved samplers were packed with soil and sealed to avoid disturbance of the intact sample during shipping.

Samples were then shipped to the University of Saskatchewan's geotechnical laboratory. A total of six intact samples (300-450 mm high) were collected from this site. All samples (except one) were tested in a large triaxial compression apparatus. The details of sample preparation, testing methodology and equipments used can be found in Singh et al. (2008). Recompacted samples were prepared in the laboratory using MSW from the intact samples after their initial testing. For these recompact samples, the MSW was placed inside the steel sampler and compacted in four lifts to achieve the desired bulk unit weight.

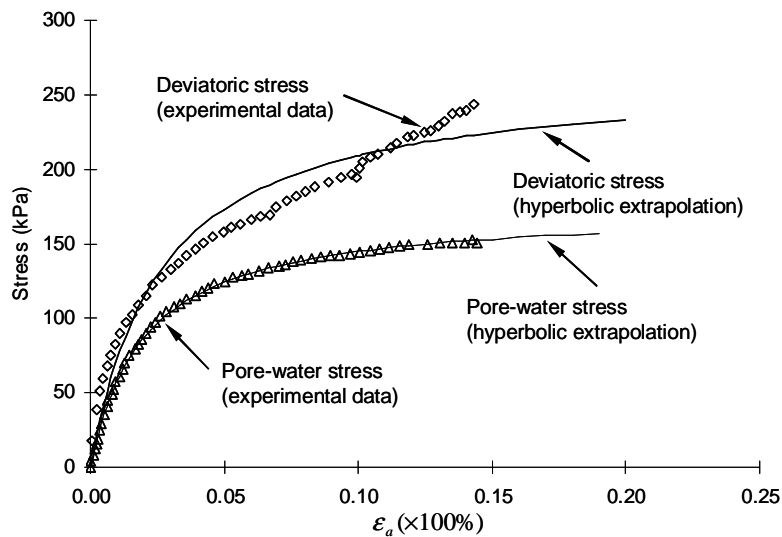


Figure 4-3 A typical example of extrapolation of stress-strain and pore pressure data taken from Caicedo et al. (2002) for $\sigma'_3 = 350$ kPa

4.4.2 Samples from Spadina Landfill

The Spadina landfill serves the City of Saskatoon and received its first waste in 1956. Filling continues and the site currently holds an estimated 6 million tonnes of MSW. Experimental data from three different types of samples from this landfill were used in

this paper. These were intact (I), recompacted (R) and statically compacted samples (LC). The samples were all 150 mm in diameter and 300-350 mm high.

Six intact samples were collected from boreholes, four from a depth of approximately 8 to 9 m and two from a depth of approximately 3 m. All samples were tested in the large triaxial compression apparatus. Recompacted samples were prepared from auger cuttings obtained from 10 to 15 m depth. In total, five recompacted samples were prepared and tested in the triaxial compression apparatus.

The statically compacted samples (LC) were obtained from a large MSW sample 400 mm diameter and 325 mm high (initially 600 mm high). This large sample of MSW was subjected to one dimensional consolidation and simultaneous accelerated degradation for several months under controlled conditions in the dual-purpose laboratory compression cell (LCC) shown in Figure 4-4. The waste placed in the LCC was a mixture of auger cuttings from 10-15 m depth and unsorted waste from 2-3 m depth. After three months of accelerated degradation, four samples, each 150 mm in diameter, were obtained by pushing a group of four sharp-edged samplers into the compacted and degraded waste using the air jack employed for the application of vertical stress to the sample in the LCC. Further details regarding the LCC can be found in Singh and Fleming (2008a).

4.4.3 Method of estimating parameters for hyperbolic model from stress-strain data

As discussed above, the parameters of the hyperbolic model can be easily obtained from triaxial stress-strain data. The first step involves estimation of E_i and R_f . A best-fit straight line can be drawn to the stress-strain data plotted on transformed axes as per

Equation (2). The slope of this straight line b is equal to $1/(\sigma'_1 - \sigma'_3)_{ult}$ and the intercept is equal to $1/E_i$. Knowing the value of $(\sigma'_1 - \sigma'_3)_{ult}$ and the value of deviatoric stress at ‘failure’ (assumed in this study to correspond to 20% axial strain), R_f can be estimated from Equation (3). In this way, for each test, values for E_i and R_f can be obtained.

The second step is the estimation of parameters K and n for each family of triaxial tests. Equation (5) can be rewritten as:

$$\log\left(\frac{E_i}{P_a}\right) = \log(K) + n \log\left(\frac{\sigma'_3}{P_a}\right) \quad [7]$$

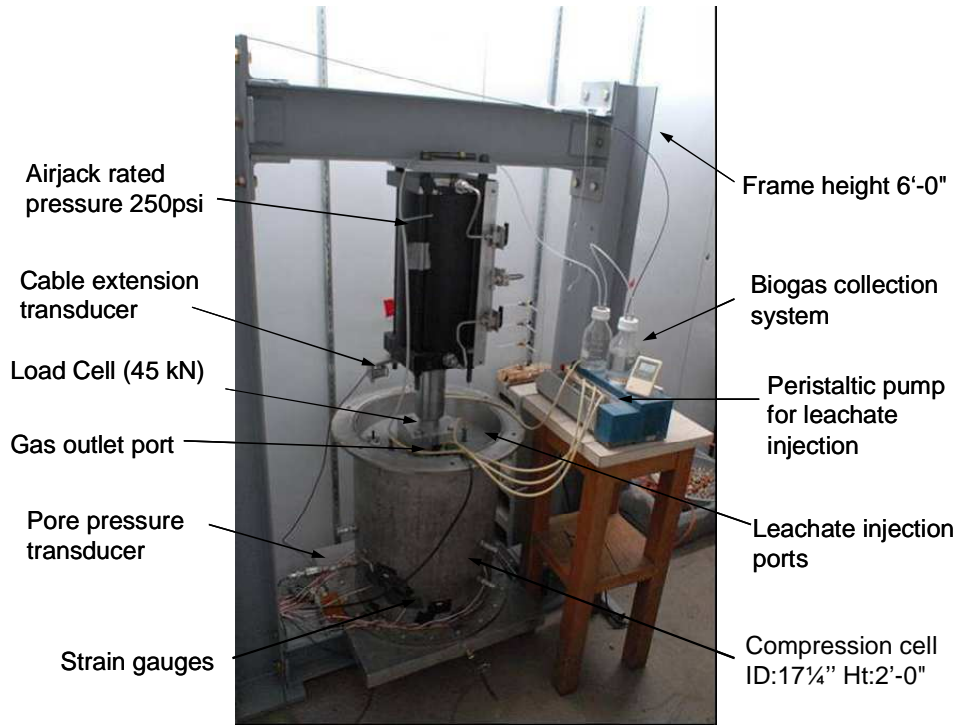


Figure 4-4 Dual-purpose landfill compression cell (LCC) used in the present study

Equation (7) represents a straight line with $\log(E_i/P_a)$ plotted against $\log(\sigma'_3/P_a)$. The slope of this line is equal to n and the y-intercept is $\log(K)$. By

plotting the values of $\log(E_i / P_a)$ against $\log(\sigma'_3 / P_a)$ for a family of tests carried out at various confining pressures and fitting a straight line to the data, values of the parameters K and n can be obtained.

The third step is to estimate the shear strength parameters (c' , ϕ') for each series of triaxial tests. Because of large deformation and lack of well-defined 'failure' for many of the tests, the authors propose that an arbitrary failure strain of 20% be used to determine the shear strength parameters. Given that the purpose of this study is to propose a constitutive model for the pre-failure stress-deformation behaviour of municipal waste, this simplification, in the opinion of the authors, is justified.

4.5 Results and Discussion

For each triaxial test, the stress-strain data were plotted in $\varepsilon_a / (\sigma'_1 - \sigma'_3) - \varepsilon_a$ Cartesian space as discussed earlier. A line of best fit to these data provides values for E_i and $(\sigma'_1 - \sigma'_3)_{ult}$. It is worth emphasizing here that the best fit line was not intended to be an 'exact' fit of the experimental data over the entire range of the stress-strain response, but it was intended to be a reasonable representation over a maximum axial strain of 20%. For all the tests, a best fit line could be drawn with $R^2 > 0.9$ for data up to an axial strain of 20% with the exception of Jessberger and Kockel (1993) for which the best fit line could only be drawn to an axial strain of between 8 and 12% with R^2 of 0.7 to 0.9. Effective confining pressures varied from 25 to 408 kPa. As discussed earlier, $(\sigma'_1 - \sigma'_3)_f$ is required to obtain the value of R_f . $(\sigma'_1 - \sigma'_3)_f$ was arbitrarily defined as the deviatoric stress at an axial strain of 20%.

A brief description of the laboratory tests conducted by various researchers and the authors are tabulated in Table 4-1. The experimental data from both drained and undrained tests have been considered here for the estimation of parameters for the hyperbolic model.

Table 4-1 Overview of the laboratory tests used in this paper

| Reference Study | Description of sample | Confining pressure (kPa) | Number and type of test results referenced in this paper |
|--|--|--------------------------|--|
| Vilar and Carvalho (2004) | Recompacted, 150mm diameter | 100 - 400 | 3- CD; 3- CU |
| Machado et al. (2002) | Recompacted, 200 mm diameter | 100 - 400 | 3 - CD |
| Caicedo et al. (2002) | Recompacted, 300 mm diameter | 50 - 350 | 3 - CU |
| Jessberger and Kockel (1993) | Recompacted, 300 mm diameter | 100 - 400 | 4 - CD |
| Kockel (1995) | Recompacted(seived waste < 120mm size) | 25 - 400 | 4 - CD |
| Grisolia et al. (1995) | Reconstructed from artificial waste, 250mm diameter | 50 - 300 | 3 - CD |
| Authors' study using samples from Spadina Landfill, Saskatoon, Canada | (a) Recompacted, 150mm diameter | 100 - 200 | 5 - CU |
| | (b) Intact, 150mm diameter | 75 - 200 | 6 - CU |
| | (c)Statically compacted and degraded waste, 150mm in diameter obtained from dual purpose laboratory compression cell | 100- 200 | 4 - CU |
| Authors' study using samples from Brock West Landfill, Ontario, Canada | (a) Recompacted, 150mm diameter | 50 - 175 | 8 - CU |
| | (b) Intact, 150 and 200 mm diameter | 50 - 350 | 4 - CU |

Note : CD- Consolidated drained test; CU - Consolidated undrained test

Figure 4-5 and Figure 4-6 illustrate the estimation of initial tangent Young's modulus and ultimate deviatoric stress for typical triaxial tests from the present study and from studies published in the literature. It may be noted from Figure 4-5 and Figure 4-6 that the stress-strain data plotted on the transformed axes diverge somewhat from the ideal linear relationship, indicating that the stress-strain behaviour of MSW is not perfectly hyperbolic. For small axial strains of the order of 10-15%, however, the stress-

strain data obtained from most of the laboratory tests conducted by the authors can be approximated by a hyperbola. This is also true for the stress-strain data from the literature where the curve is concave downward. Figure 4-5 and Figure 4-6 show the slope and the intercept of the best fit lines for selected tests, fitted to data plotted on transformed axes along with the estimated values of E_i and $(\sigma'_1 - \sigma'_3)_{ult}$.

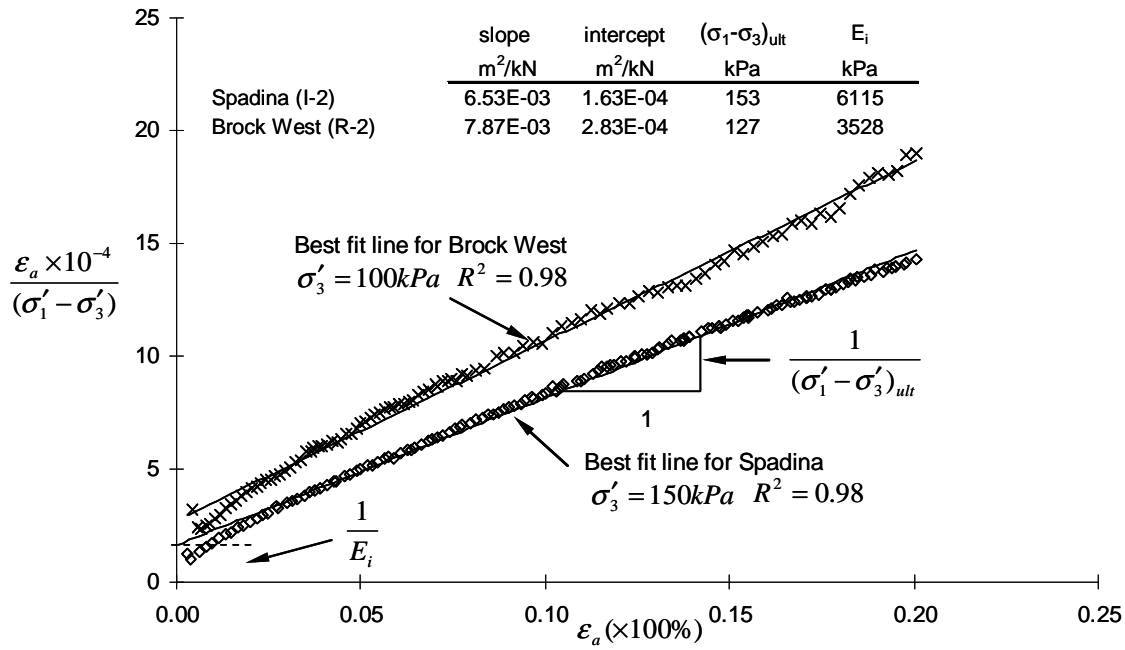


Figure 4-5 Determination of E_i and $(\sigma'_1 - \sigma'_3)_{ult}$ for selected samples from the Brock West and Spadina Landfills

A summary of the values estimated for the parameters E_i , R_f and $(\sigma'_1 - \sigma'_3)_{ult}$ are presented in Table 4-2. For each family of laboratory tests, the estimated values for the initial tangent modulus were plotted against the effective confining pressures on a log-log scale to obtain values for the parameters K and n using a best fit line through the data points. Figure 4-7 presents the test data used to estimate the parameters K and n

for each family of tests from the authors' own study. Similarly, the parameters for the published tests are shown in Figure 4-8 .

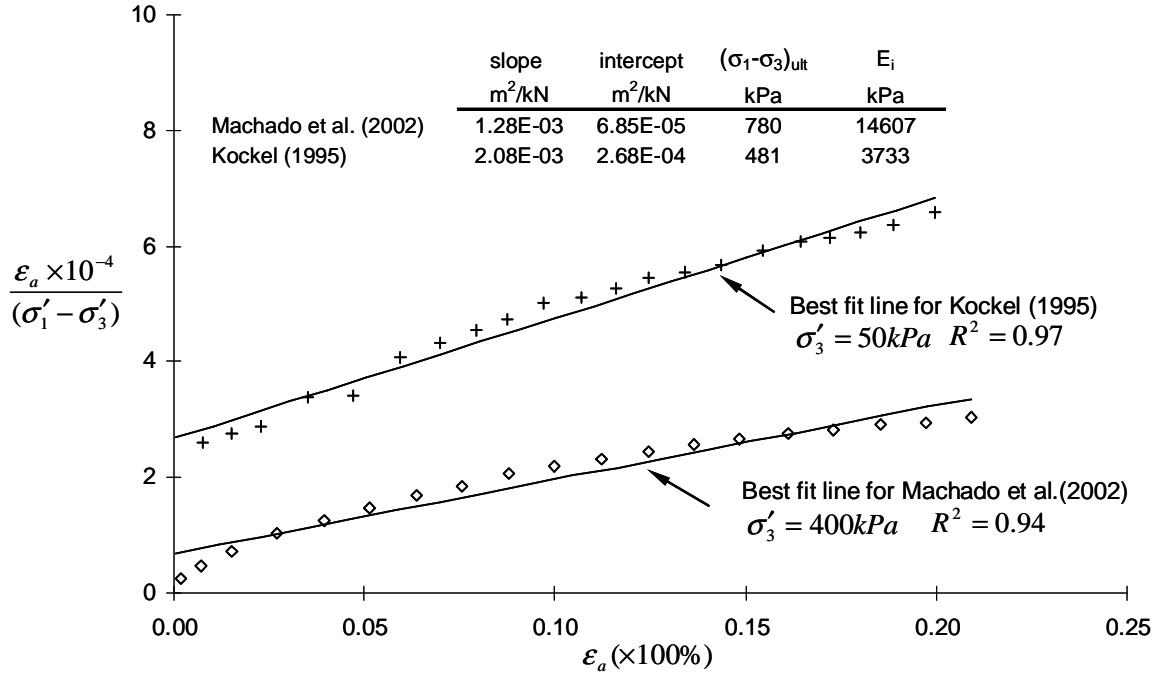


Figure 4-6 Determination of E_i and $(\sigma'_1 - \sigma'_3)_{ult}$ for selected tests from published literature

Table 4-2 Summary of estimated values of initial tangent Young's modulus E_i , ultimate deviatoric stress $(\sigma'_1 - \sigma'_3)_{ult}$, and R_f }

| Tests from Published Literature | | | | | | | Tests by Authors | | | | | | | |
|---------------------------------|-----------------|-------------|---------------------------|-------------------------------|-------|-------|------------------------|-----------------|--------------|-------------|---------------------------|-------------------------------|-------|-------|
| | Type of test | σ'_3 | $(\sigma_1 - \sigma_3)_f$ | Estimated | | R_f | | Type of test | Sample ID | σ'_3 | $(\sigma_1 - \sigma_3)_f$ | Estimated | | R_f |
| | | | | $(\sigma_1 - \sigma_3)_{ult}$ | E_i | | | | | | | $(\sigma_1 - \sigma_3)_{ult}$ | E_i | |
| | | | | | | | | | | | | | | |
| | | (kPa) | (kPa) | (kPa) | (kPa) | | | | | (kPa) | (kPa) | (kPa) | (kPa) | |
| Vilar and Carvalho (2004) | CD | 400 | 798 | 1166 | 9018 | 0.68 | Spadina Landfill | CU | I-1 | 50 | 280 | 400 | 4687 | 0.70 |
| | CD | 200 | 509 | 794 | 5153 | 0.64 | | CU | I-2 | 100 | 141 | 153 | 6115 | 0.92 |
| | CD | 100 | 267 | 396 | 2772 | 0.67 | | CU | I-3 | 150 | 358 | 432 | 10388 | 0.83 |
| | | | | | | | | CU | I-4 | 200 | 400 | 465 | 14344 | 0.86 |
| | CU | 108 | 183 | 198 | 2953 | 0.92 | | CU | I-5 | 25 | 41 | 42 | 4897 | 0.96 |
| | CU | 208 | 350 | 390 | 6551 | 0.90 | | CU | I-6 | 75 | 127 | 137 | 4390 | 0.93 |
| | CU | 408 | 546 | 607 | 11913 | 0.90 | | CU | R-1 | 100 | 197 | 253 | 4424 | 0.78 |
| Machado et al. (2002) | | | | | | | CU | R-2 | 125 | 265 | 364 | 4907 | 0.73 | |
| | CD | 400 | 671 | 780 | 14607 | 0.86 | CU | R-3 | 50 | 189 | 397 | 1813 | 0.48 | |
| | CD | 200 | 413 | 588 | 5426 | 0.70 | CU | R-4 | 200 | 281 | 416 | 4431 | 0.67 | |
| | CD | 100 | 281 | 468 | 2547 | 0.60 | CU | R-5 | 150 | 235 | 308 | 4063 | 0.76 | |
| | | | | | | | CU | LC-1 | 50 | 94 | 112 | 2906 | 0.84 | |
| Caicedo etal. (2002) | CU | 50 | 103 | 113 | 5525 | 0.91 | CU | LC-2 | 75 | 84 | 94 | 3886 | 0.89 | |
| | CU | 200 | 159 | 175 | 8446 | 0.91 | CU | LC-3 | 100 | 123 | 142 | 4556 | 0.87 | |
| | CU | 350 | 233 | 263 | 10153 | 0.89 | CU | LC-4 | 150 | 156 | 182 | 5365 | 0.85 | |
| | | | | | | | | | | | | | | |
| Jessberger and Kockel (1993) | CD | 100 | 558 | 1004 | 4700 | 0.56 | Brock West Landfill | CU | I-1 | 150 | 227 | 255 | 10587 | 0.89 |
| | CD | 200 | 845 | 3204 | 4889 | 0.26 | | CU | I-2 | 35 | 119 | 161 | 2306 | 0.74 |
| | CD | 300 | 1129 | 7572 | 5801 | 0.15 | | CU | I-3 | 60 | 101 | 124 | 2818 | 0.82 |
| | CD | 400 | 1392 | 3810 | 8696 | 0.36 | | CU | I-4 | 60 | 94 | 116 | 2497 | 0.81 |
| Kockel (1995) | CD | 400 | 1707 | 3154 | 17317 | 0.54 | CU | R-1 | 50 | 140 | 156 | 6995 | 0.90 | |
| | CD | 200 | 938 | 1712 | 9018 | 0.55 | CU | R-2 | 60 | 106 | 127 | 3528 | 0.83 | |
| | CD | 100 | 507 | 1053 | 4646 | 0.48 | CU | R-3 | 120 | 167 | 187 | 7898 | 0.89 | |
| | CD | 50 | 304 | 481 | 3733 | 0.63 | CU | R-5 | 125 | 154 | 166 | 11053 | 0.93 | |
| Grisolia et al. (1995) | | | | | | | CU | R-6 | 100 | 87 | 91 | 10265 | 0.96 | |
| | CD | 300 | 238 | 371 | 2250 | 0.64 | CU | R-7 | 100 | 90 | 94 | 10475 | 0.96 | |
| | CD | 100 | 170 | 348 | 1195 | 0.49 | CU | R-8 | 30 | 34 | 37 | 2349 | 0.93 | |
| | CD | 50 | 103 | 218 | 752 | 0.47 | CU | R-9 | 60 | 62 | 64 | 9528 | 0.97 | |

Note : $(\sigma_1 - \sigma_3)_f$ is the value of deviatoric stress at 20% axial strain; CD- Consolidated drained test; CU- Consolidated undrained test

Table 4-3 presents a summary of the parameters K and n estimated for each of the 12 families of tests (comprising 50 individual triaxial tests). The value of R_f for each family of tests shown in Table 4-3 is the average of the individual test values from Table 4-2. As seen from Table 4-3, the values of R_f and n lie in a narrow distribution, suggesting that these parameters may be considered as constants. K varies somewhat more, and on closer examination of patterns in the data it appears quite possible that there may be a site-specific variability in the value of K . For example, the data of Grisolia et al. (1995) exhibit a slope (n) similar to most of the other test data but with generally lower values of E_i . It is reasonable to expect that K might vary with density and composition of the waste. Within broad limits, however, the data suggests that a constant value of K may be assumed. This further simplifies the five-parameter constitutive model of Equation (6) to a two-parameter (c' , ϕ') model. It may be anticipated that through further research, it would be possible to determine whether or not there is systematic variation of the parameters of Table 4-3, particularly K , with specific material properties of MSW such as unit weight, age, organic content, etc. However, until such time as additional research can address this possibility, the authors suggest that the simplified two-parameter model is reasonable and supportable.

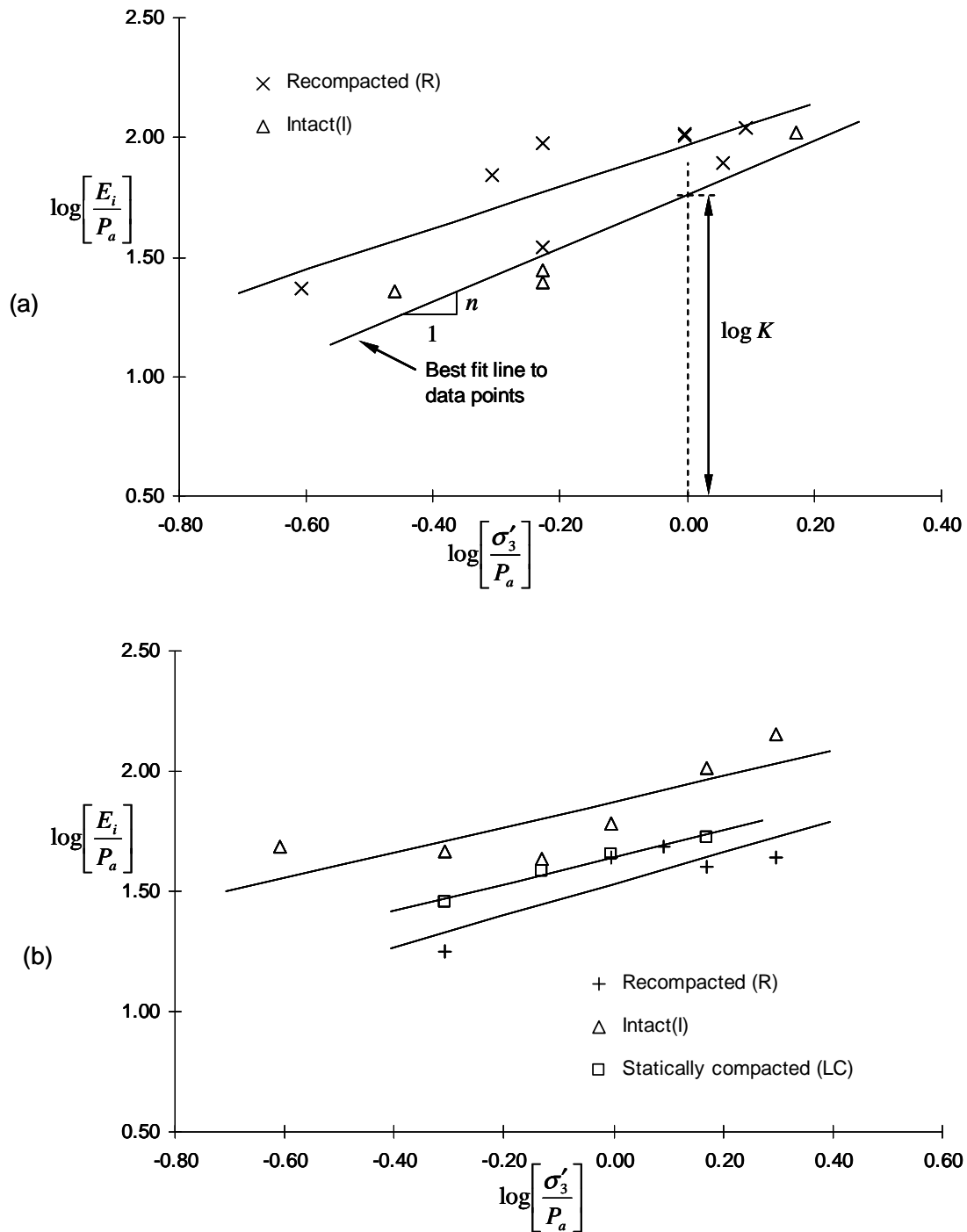


Figure 4-7 Determination of parameters K and n from the present study: (a) data from testing of samples from Brock West landfill; (b) data from testing of samples from Spadina landfill

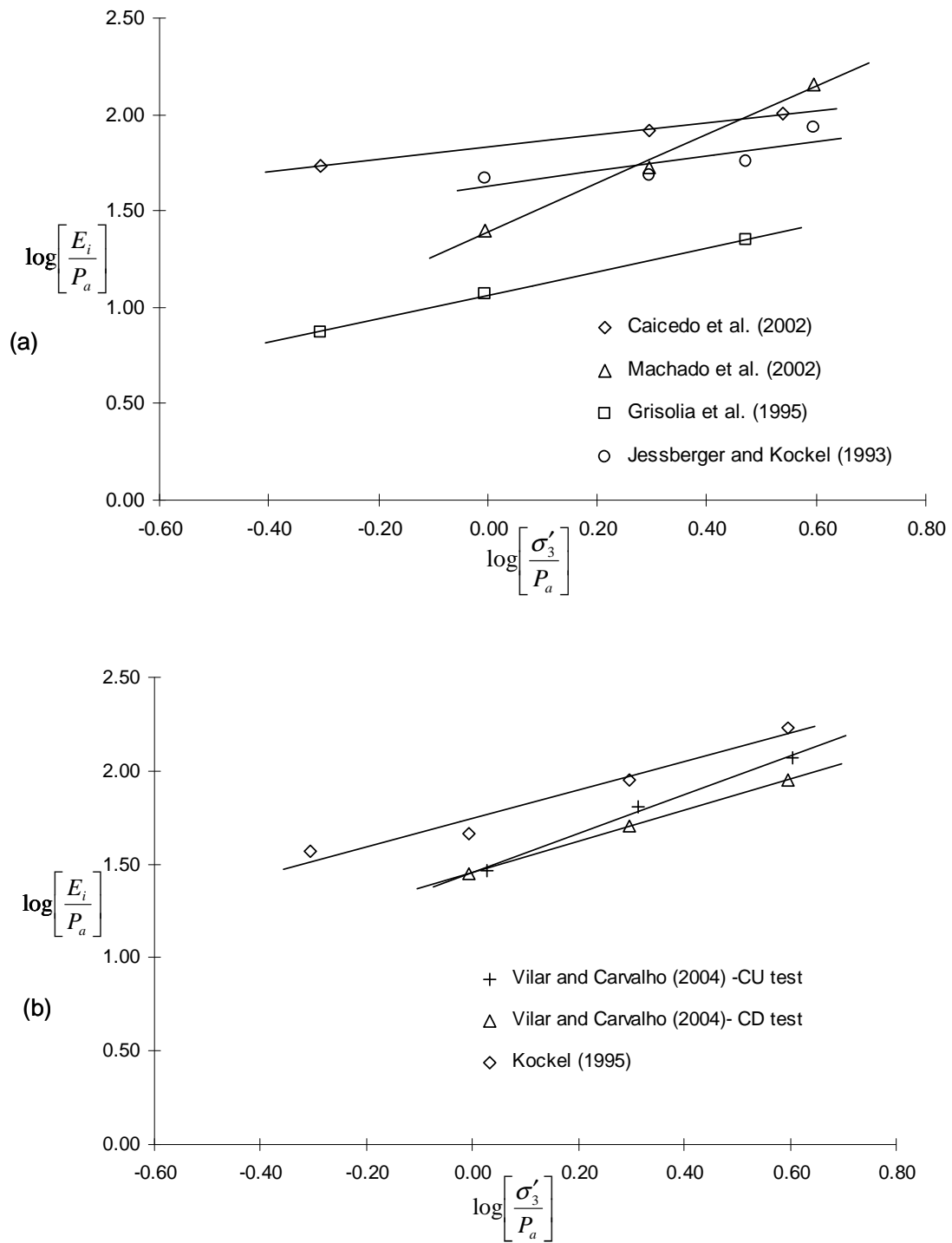


Figure 4-8 Determination of parameters K and n from published test results

Table 4-3 Summary of estimated values of hyperbolic parameters K , n , and R_f

| Reference Study | | Estimated hyperbolic parameters | | |
|---|----|---------------------------------|-----------|-------------|
| | | n | K | $*R_f$ |
| Vilar and Carvalho (2004) | CD | 0.83 | 29 | 0.70 |
| | CU | 1.05 | 28 | 0.91 |
| Machado et al. (2002) | | 1.26 | 25 | 0.72 |
| Caicedo et al. (2002) | | 0.31 | 68 | 0.90 |
| Jessberger and Kockel (1993) | | 0.39 | 42 | 0.33 |
| Kockel (1995) | | 0.76 | 55 | 0.55 |
| Grisolia et al. (1995) | | 0.61 | 12 | 0.53 |
| Authors study using samples from Spadina landfill, Saskatoon, Canada | R | 0.65 | 34 | 0.68 |
| | I | 0.53 | 75 | 0.87 |
| | LC | 0.56 | 44 | 0.86 |
| Authors study using samples from Brockwest landfill, Ontario, Canada | R | 0.87 | 93 | 0.92 |
| | I | 1.12 | 58 | 0.82 |
| Mean | | 0.75 | 47 | 0.73 |
| Standard deviation | | 0.29 | 24 | 0.18 |
| Standard error of mean | | 0.08 | 7 | 0.05 |
| using confidence level of 90% for the mean of the hyperbolic parameters | | | | |
| Upper confidence limit | | 0.88 | 58 | 0.82 |
| Lower confidence limit | | 0.61 | 36 | 0.64 |

Note: R - Recompacted, I - Intact, LC - statically compacted in compression cell

* Average value from a series of tests for each study

4.5.1 Statistical analysis of estimated hyperbolic model parameters

Statistical techniques are appropriately applied to problems of variability and prediction in engineering in cases where test data vary widely with no apparent correlation internally

or with other observations. In waste mechanics, the available data for MSW properties exhibits substantial variability, presumably reflecting heterogeneity and spatial variability of MSW from landfill to landfill and country to country. This situation is exacerbated by the various physico-chemical and biological processes that occur within the waste mass. Additional test data are required in order to determine whether these data might exhibit a systematic relationship with other measurable properties of waste.

Confidence limits were calculated for upper and lower bounds of n , K and R_f at a confidence level of 90% as shown in Table 4-3. For a particular value of effective confining stress and given known (or assumed) shear strength parameters, it is possible, therefore, to draw lower and upper bounds of the stress-strain curve using the hyperbolic model given by Equation (6). The estimated values of K given in Table 4-3 are consistent with two of the three values of K (35, 90 and 200) considered by Filz et al. (2001) for analyzing the Kettleman Hills landfill failure. However, the values of parameter n estimated in this study are somewhat higher than the values of n (0.4, 0.6 and 0.4) used by Filz et al. (2001). Here, it is worth reiterating that Filz et al. (2001) have provided no reference as to how the value of the parameters K and n were chosen. The general agreement with the parameters proposed by Filz et al. (2001) provides some additional support for the values proposed in this paper.

4.5.2 Validation of proposed hyperbolic model parameters

As described above, five parameters (K , n , R_f , c' and ϕ') are required for defining the stress-strain response using Equation (6). Using the lower and upper confidence limits for the hyperbolic parameters for MSW estimated in this study and shown in Table 4-3, it

is possible to simplify this five-parameter hyperbolic model to a two-parameter (c' , ϕ') hyperbolic model for MSW.

4.5.2.1 Estimation of shear strength parameters

To estimate the shear strength parameters for each set of MSW samples, the results of each family of triaxial tests were plotted as deviatoric stress (q) at 'failure' (at 20% axial strain as discussed above) vs. mean effective stress (p') and a best fit line was drawn in q - p' space (Figure 4-9). Table 4-4 summarizes the shear strength parameters suggested by various authors from their respective test results along with the shear strength parameters estimated using this approach.

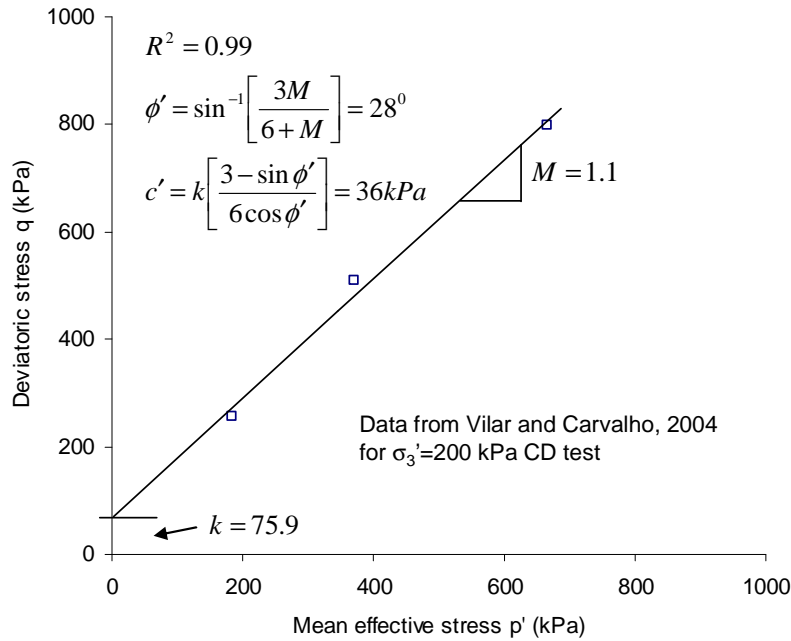


Figure 4-9 Estimation of shear strength parameters c' and ϕ' using strength envelope in q - p' space

4.5.2.2 Fitting hyperbolic model to stress-strain data from triaxial tests

The lower and upper bound values for the assumed constants (K , n , and R_f) from Table 4-3 were used with the site-specific shear strength parameters summarized in Table 4-4 to examine the validity of the proposed two-parameter hyperbolic model.

Table 4-4 Summary of shear strength parameters used for the validation of hyperbolic model for MSW

| | Suggested by respective authors | | Estimated in this study assuming ($\sigma_1 - \sigma_3$) _f at 20% axial strain | |
|------------------------------|------------------------------------|-------------|--|----------------------|
| | c' (kPa) | ϕ' (°) | c' (kPa) | ϕ' (°) |
| Vilar and Carvalho (2004) | 49 | 26 | 36 | 28 |
| | 0* | 43* | 0* | 46* |
| Machado et al. (2002) | | | 50 | 23 |
| Caicedo et al. (2002) | 45* | 14* | 40* | 9* |
| Jessberger and Kockel (1993) | | | 73 | 36 |
| Kockel (1995) | | | 25 | 42 |
| Grisolia et al. (1995) | 11 | 30 | 32 | 14 |
| Spadina Landfill | R | - | 36* | 41* |
| | I | - | 16* | 39* |
| | LC | - | 27* | 21* |
| Brock West Landfill | - | - | 0 - 8.4 ^a | 35 - 47 ^a |

* parameters obtained from CU test with pore pressure measurement

^a results from Singh et al. (2008)

The experimental data in Figure 4-10 to Figure 4-13 have been shown bounded by shaded regions representing the lower and upper bounds for the predicted stress-strain values determined using the minimum and maximum values for the ‘constants’. It is evident that for axial strains up to 20% the experimental data is confined to the shaded region although in some cases, experimental data may deviate from the shaded region at larger strains. The assumed maximum allowable strain of 20% seems logical for MSW given

the consideration that at large strain the integrity of the components installed within the landfills cannot be assured. It is, therefore, proposed that predictions of stress-strain behaviour for MSW which are guided using this method may be appropriate for providing safe design estimates.

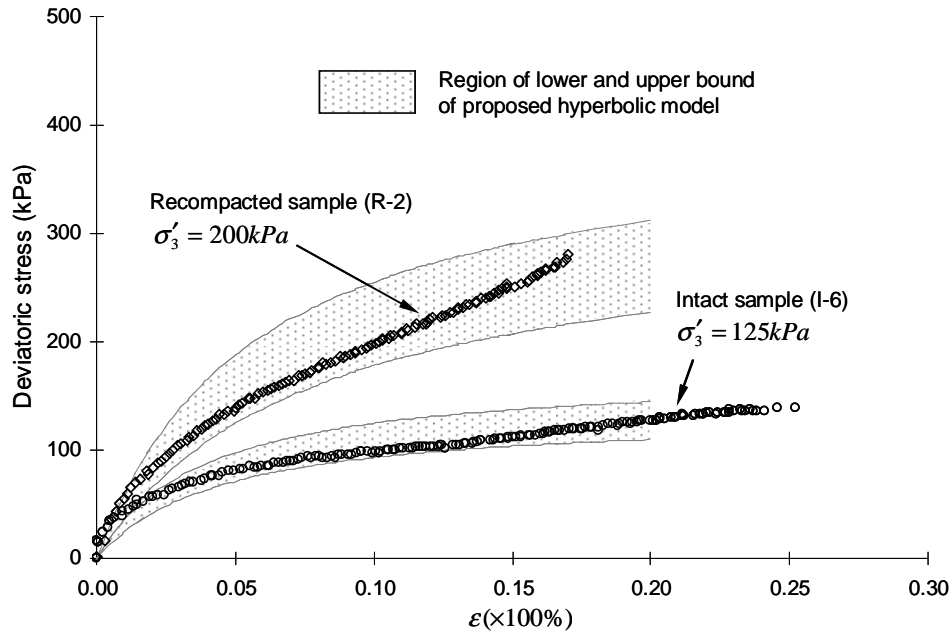


Figure 4-10 Proposed hyperbolic model fitted to experimental data from Spadina landfill

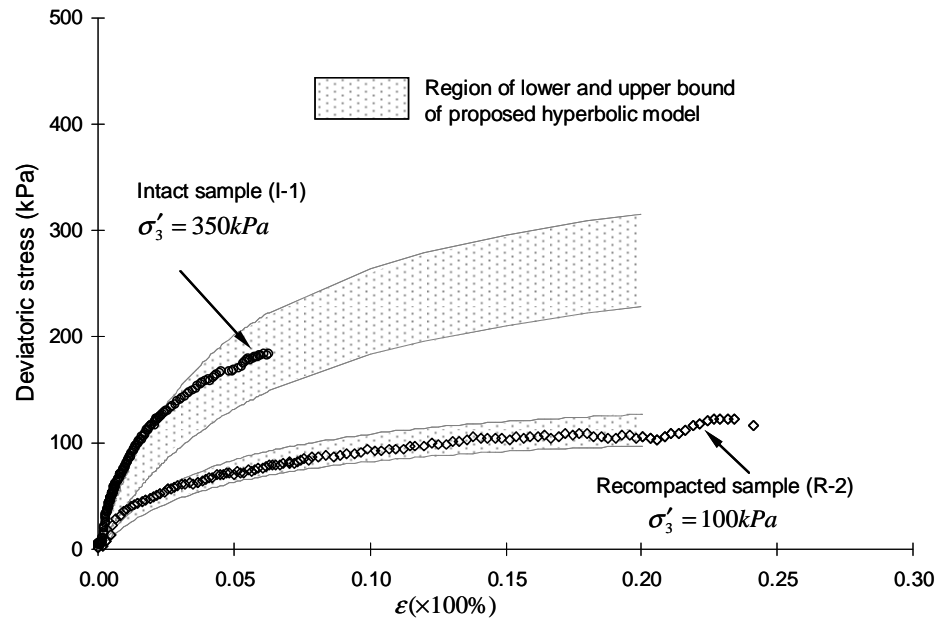


Figure 4-11 Proposed hyperbolic model fitted to experimental data from Brock West landfill

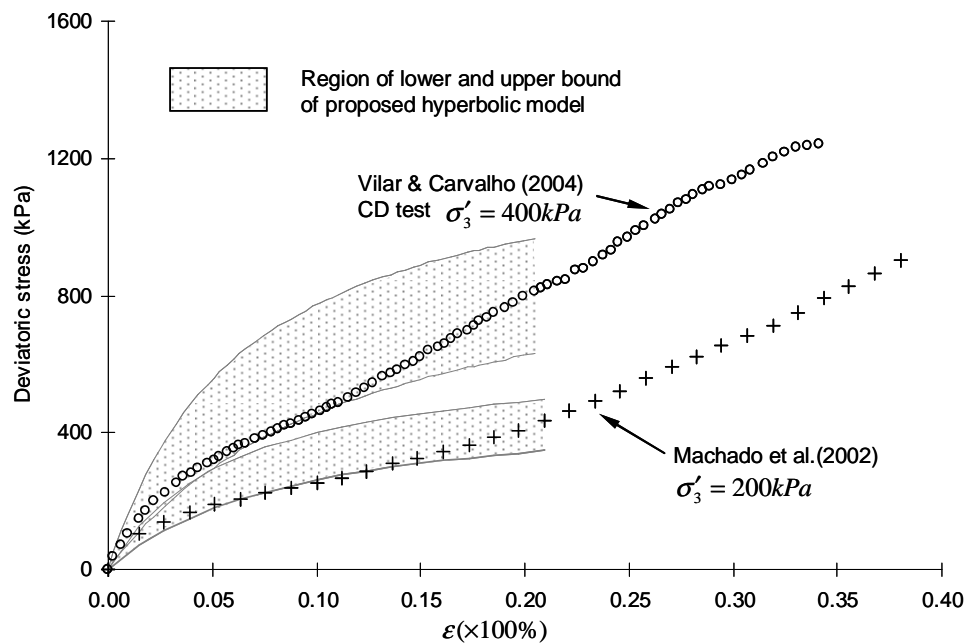


Figure 4-12 Proposed hyperbolic model fitted to experimental data from published studies

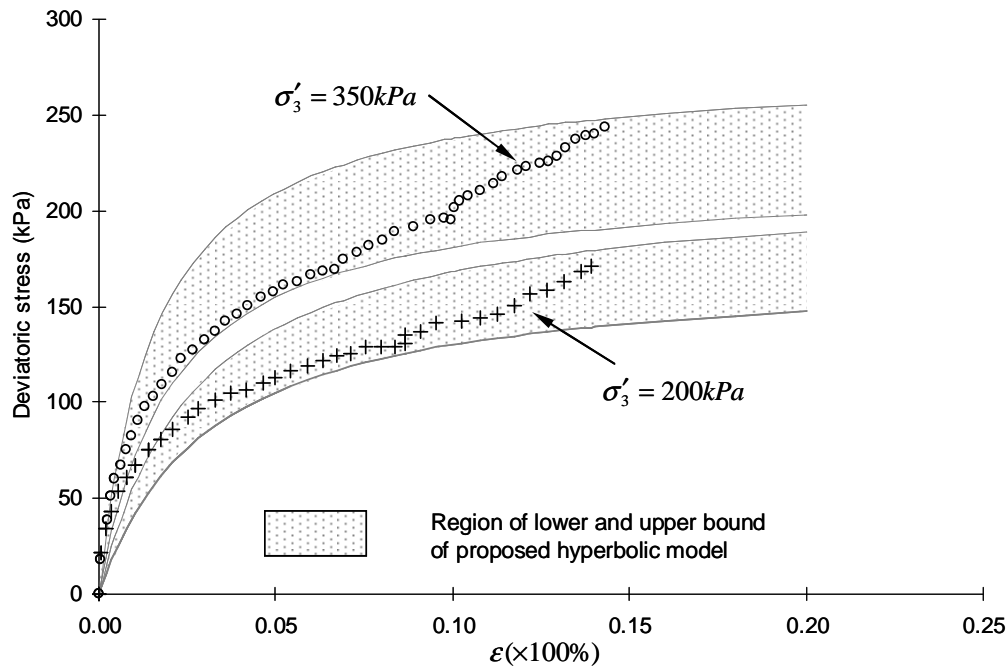


Figure 4-13 Proposed hyperbolic model fitted to experimental data from Caicedo et al. (2002)

4.6 Conclusions

Experimental results obtained from triaxial compression testing of large samples of MSW by the authors as well as several tests reported in published literature indicate that the stress-strain response of MSW can be approximated by a hyperbolic curve. The hyperbolic stress-strain curve when used with the lower and upper bound of hyperbolic parameters proposed in this study can be used for predicting the lower and upper bound of stress-strain behaviour of the MSW. A maximum allowable strain of 20% is assumed for MSW since the integrity of the components installed within the landfills can not be maintained at large strains. It is proposed that the stress-strain behaviour of MSW may be estimated using this method to provide reasonable conservative estimates of displacements for evaluation and design of engineered components of landfills.

4.7 References

- Beaven, R.P. and Powrie, W. 1995. Hydrogeological and geotechnical properties of refuse using a large scale compression cell. Proc. 5th Int. Waste Management and Landfill Symposium, Sardinia, 745-760.
- Caicedo, B., Yamin, L., Giraldo, E. and Coronado, O. 2002. Geomechanical properties of municipal solid waste in Dona Juana sanitary landfill. Proc. 4th Int. Congress on Environmental Geotechnics, Brazil, 1, 177-182.
- Duncan, J.M. and Chang, C.Y. 1970. Nonlinear analysis of stress and strain in soils. Journal of Soil Mechanics and Foundation Engineering, ASCE, 96(SM5): 1629-1653.
- Filz, G.M., Esterhuizen, J.B. and Duncan, J.M. 2001. Progressive failure of lined waste impoundments. Journal of Geotechnical and Geoenvironmental Engineering, ASCE, 127(10): 841-848.
- Gabr, M.A. and Valero, S.N. 1995. Geotechnical Properties of Municipal Solid Waste. Geotechnical Testing Journal, ASTM, 18(2): 241-251.
- Grisolia, M., Napoleoni, Q. and Tancredi, G. 1995. The use of triaxial test for the mechanical characterization of MSW. Proc. 5th International Waste Management and Landfill Symposium, Sardinia, 761-768.
- GSI. 2007. SIGMA/W 2007 Stress-deformation analysis software. Geo-Slope International (GSI). See <http://www.geo-slope.com/products/sigmaw2007.aspx> [accessed on April 4, 2008].
- Janbu, N. 1963. Soil compressibility as determined by oedometer and triaxial tests. Proc. 3rd European Conference on Soil Mechanics, Wiesbaden, 1: 19-25.
- Jessberger, H.L. and Kockel, R. 1993. Determination and assessment of the mechanical properties of waste materials. Proc. 4th International Waste Management and Landfill Symposium, Sardinia, 1383-1392.

- Kavazanjian, E. 1995. Evaluation of MSW properties for seismic analysis. Geotechnical Special Publication, ASCE, 46: 1126-1141.
- Kockel, R. 1995. Scherfestigkeit von Mischabfall im Hinblick auf die Standsicherheit von Deponien. PhD thesis, Mitteilungen Heft 133, Leichtweiß-Institut für Wasserbau, Technische Universität Braunschweig.
- Kondner, R. L. 1963. Hyperbolic stress-strain response: cohesive soils. Journal of Soil Mechanics and Foundation Engineering, ASCE, 89(SM1): 115-141.
- Krase, V. and Dinkler, D. 2005. Constitutive modelling of mechanical behaviour of municipal solid waste. Proc. 10th International Waste Management and Landfill Symposium, Sardinia. (on CD-Rom).
- Machado, S.L., Carvalho, M.F. and Vilar, O.M. 2002. Constitutive model for municipal solid waste. Journal of Geotechnical and Geoenvironmental Engineering, ASCE, 128(11): 940-951.
- Manassero, M., Van Impe, W. F. and Bouazza, A. 1997. Waste Disposal and Containment. Proc. 2nd International Congress on Environmental Geotechnics, Osaka, 3: 1425-1474.
- Morrison, C.S. 1995. The development of a modular finite element program for analysis of soil-structure interaction. PhD thesis, Virginia Polytechnic Institute and State University, Blacksburg, Virginia, USA.
- Singh, M.K. and Fleming, I.R. 2008a. Estimation of the mechanical properties of MSW during degradation in a laboratory compression cell. Geotechnical Special Publication, ASCE, 177: 200-207.
- Singh, M.K. and Fleming, I.R. 2008b. Evolution of compressibility behaviour of municipal solid waste during degradation. Manuscript submitted to Journal of Geotechnical and Geoenvironmental Engineering, ASCE.
- Singh, M.K., Sharma, J.S. and Fleming, I.R. 2008. Shear strength testing of Intact and recompacted samples of municipal solid waste. Manuscript submitted to Canadian Geotechnical Journal.

- Singh, M.K., Fleming, I.R. and Sharma, J.S. 2007. Estimation of mechanical properties of municipal solid waste using stochastic modelling. Proc. 11th International Waste Management and Landfill Symposium, Sardinia. (on CD-Rom).
- Vilar, O.M. and Carvalho, M.F. 2004. Mechanical properties of municipal solid waste. Journal of Testing and Evaluation, ASTM, 32(6): 1-12.

CHAPTER 5 EVOLUTION OF COMPRESSIBILITY BEHAVIOUR OF MUNICIPAL WASTE DURING DEGRADATION

Preface[†]

The model parameters proposed in a previous chapter to describe the pre-failure stress-deformation behaviour of MSW were observed to exhibit scatter similar to other mechanical properties of waste, reflecting variability in sample composition, testing methods and the extent of degradation of the tested samples. The degradation of waste constituents over time is likely to cause changes in mechanical properties, potentially leading to instability and/or serviceability concerns. While for conventional landfills, it has been observed that waste does not become significantly weaker over time; in bioreactor landfills, which are subjected to rapid stabilization techniques, there may be changes in the stress-deformation behaviour of waste with increasing degradation. This paper presents the results of a laboratory test of MSW subjected to accelerated degradation in a large one-dimensional compression cell. The evolution of compressibility and at-rest lateral pressure of waste during degradation is explored and the results compared with similar published results from the literature. The mechanism of secondary compression in waste is explained. The findings from this study address the third objective of this research: to measure the evolution of compressibility behaviour of MSW with degradation and verify the mechanism of secondary compression in waste.

[†]A similar version of this chapter is under review for possible publication as a research paper in the *Journal of Geotechnical and Geoenvironmental Engineering*, ASCE.

Citation: M. K. Singh and I. R. Fleming “Evolution of compressibility behaviour of Municipal waste during degradation”.

Abstract

This paper presents the results of a laboratory test of municipal solid waste subjected to accelerated degradation and one-dimensional compression. Incremental vertical stresses were applied to simulate staged construction of a landfill. Degradation was quantified by methane yield, leachate quality and loss of volatile solids. Lateral and vertical stress, pore pressure and vertical settlement were continuously monitored during the 150 day duration of the experiment. Data were collected regarding the evolution of the at-rest lateral earth pressure, the compressibility and the constrained modulus. The results show a significant influence of degradation on compressibility parameters (C_{ce} and $C_{\alpha e}$). The K_0 value did not change significantly during degradation and it is proposed that it might be considered a constant regardless of applied stresses or age. The mechanism of compression and development of lateral stresses with time are discussed.

5.1 Introduction

The condition of MSW inside a landfill changes over time due to degradation, compression, decomposition and creep. The mechanical properties of MSW therefore, may also change over time, potentially leading to stability and/or serviceability concerns. While there is not, at present, a consensus regarding the net effect of degradation on the global stability of waste slopes, there is some basis to suggest that the waste in many conventional landfills does not become significantly weaker over time (Kavazanjian 2008). However, in modern bioreactor landfills, subject to rapid biodegradation and exhibiting high moisture content, there may be changes in the stress-deformation

response of the waste material over time. Given that these facilities incorporate significant buried infrastructure representing a substantial financial investment, it is reasonable to consider how the relevant material properties might change during the course of degradation.

The mechanical properties required to evaluate stress-deformation behaviour are Young's modulus (E') and Poisson's ratio (ν'), the later can also be expressed in terms of at-rest lateral earth pressure (K_0). The published literature regarding the elastic properties of waste is relatively sparse. Various authors (Kavazanjian 2006, Dixon and Langer 2006, Landva et al. 2000, Dixon et al. 1999, Carvalho and Vilar 1998, Matasovic and Kavazanjian 1998, Beaven and Powrie 1995 and Sharma et al. 1990) have measured the elastic properties of waste using various techniques. The evolution of elastic properties as a result of degradation, however, is not well understood. Knowledge of the change in the mechanical properties of MSW over time is important as it governs the deformation behaviour of the waste.

The mechanism of settlement in landfills is complex due to the heterogeneous composition of municipal waste. This complexity is further exacerbated due to the large variation in compressibility and degradation potential of waste constituents. There is significant loss of mass as a result of degradation and loss of volume due to collapse of the macro and micro-structure of the waste (McDougall and Pyrah 2004, Stoltz and Gourc 2008). As a result, an equilibrium void ratio is seldom reached in waste and the landfill continues to settle and deform for a very long time. Large and differential vertical settlements can damage the integrity of the landfill cover resulting in excessive infiltration of surface water and consequent increased generation of leachate. This can

also lead to unwanted escape of landfill gases to the atmosphere. Lateral deformations, on the other hand, can substantially damage gas collection systems installed in landfills for mitigating greenhouse gas emissions and for implementation of waste to energy program (Singh et al. 2007). Given these facts, post-closure settlements in landfills have often been recognized as the greatest concern especially for bioreactor landfills (McDougall 2008).

Though long-term deformations in a landfill can not be prevented, it may be possible to mitigate adverse effects by designing its various components to withstand the anticipated deformations. In order to be able to do this, it will be necessary to understand the change in mechanical properties over time. This paper explores the evolution of elastic and compressibility behaviour of MSW during accelerated degradation. The results from this study are compared with similar published results from the literature. The present study is an extension of previous work done by Singh and Fleming (2008).

5.2 Compressibility and Elastic properties of MSW

5.2.1 Compressibility

The mechanism of compression of MSW in response to applied normal stress is somewhat different from soils and has been discussed by various authors (Van Impe and Bouazza 1996, Gasparini et al. 1995, Wall and Zeiss 1995, Morris and Woods 1990 and Sowers 1973). Broadly speaking, waste settlement is a combined outcome of mainly two phases: initial compression and delayed or secondary compression. The initial compression occurs immediately following application of external load either by dozers/compactors or due to the self weight of overlying waste. A majority of crushing,

distortion, squeezing and raveling of waste constituents occurs during this stage and the initial compression can continue for the first few days of waste placement depending upon landfill operating practices. Due to short-term settlements, the initial compression is of limited interest to engineers except when considering piggy-back expansion (Kavazanjian 2006).

Secondary compression, on the other hand, is of great interest to engineers and takes place as a combined action of two different mechanisms which occur as a result of mechanical and degradation processes. Laboratory tests conducted by Al-Khafaji and Andersland (1981) on organic soils suggest that secondary compression produced by the degradation process exceeds that caused by simple creep. Similar behaviour might also be expected in waste but to a greater degree, given the higher proportion of organic material in waste when compared to organic soils. The two mechanisms of secondary compression are indistinguishable and it is difficult to identify their precedence over each other. It was hypothesized by McDougall et al. (2004) that these two mechanisms proceed simultaneously as an episodic process of gradual weakening of the waste structure due to degradation and its collapse at a point when the structure becomes too weak to resist overburden stresses. This process is then followed by the mechanical processes of raveling of constituents into the collapsed structure.

For soils, compressibility is conveniently described using compression indices expressed in terms of void ratio. However, the meaning and significance of void ratio as it applies to MSW is somewhat complicated (McDougall 2008). Given the inadequate information regarding the void ratio of waste, the compressibility of waste has often been described in terms of primary compression ratio (C_{ce}) and secondary compression ratio

($C_{\alpha e}$) which are expressed in terms of axial strains rather than void ratio. The value of C_{ce} is obtained from the slope of the straight line virgin compression part of the $\varepsilon_a - \log \sigma'_v$ curve using equation [1],

$$C_{ce} = \frac{\Delta \varepsilon_a}{\Delta \log(\sigma'_v)} \quad [1]$$

where $\Delta \varepsilon_a$ is the change in axial strain per log cycle of change in vertical effective stress [$\Delta \log(\sigma'_v)$]. Similarly, the secondary compression ratio ($C_{\alpha e}$) is computed as the slope of the $\varepsilon_a - \log(\text{time})$ curve, expressed as:

$$C_{\alpha e} = \frac{\Delta \varepsilon_a}{\Delta \log(t)} \quad [2]$$

For soils, the compression indices and compression ratios are related by the expressions: $C_c = (1 + e_0)C_{ce}$ and $C_{\alpha} = (1 + e_0)C_{\alpha e}$, where e_0 is the initial void ratio and C_c and C_{α} are compression indices expressed in terms of void ratio. While the applicability of this relationship for waste is somewhat unclear, various researchers (Vilar and Carvalho 2004, Hossain et al 2003 and Gabr and Valero 1995) have made assumptions of the value of e_0 in arriving at the values for C_c and C_{α} for waste.

A review of published data shows a typical range of C_{ce} and $C_{\alpha e}$ values lying between 0.1 to 0.92 and 0.0005 to 0.22 respectively. While some of the scatter in these values is expected because of the heterogeneous nature of MSW, the authors suggest that most of the observed scatter in the data may be attributed to the use of different sizes and types of equipment and samples of varying age, unit weight and moisture content.

5.2.2 Lateral stresses and At-rest lateral pressure

Knowledge of the lateral stresses that will develop in waste over time is critical to anticipating lateral deformations, especially those developed along side slopes. Lateral stresses are also an important consideration in the design of vaults and conduits, retaining walls, and deep foundations installed for post-closure development (Kavazanjian 2006). Determination of lateral stresses requires an estimate of K_0 , the ratio of the lateral to the vertical effective stresses under the conditions of no lateral deformation.

Published data on K_0 values for MSW are sparse. Measurements of K_0 from in-situ testing (e.g. Dixon et al. 1999), laboratory testing (e.g. Singh and Fleming 2008, Kavazanjian 2006, Towhata et al. 2004 and Landva et al. 2000) and by indirect estimation from measurement of Poisson's ratio (e.g. Zekkos 2005, Matasovic and Kavazanjian 1998 and Houston et al. 1995) suggest a range of possible K_0 values from 0.1 to 1.0 with values between 0.3 to 0.5 being common. However, the influence of waste degradation on K_0 with time has not been documented.

5.2.3 Constrained Modulus

Large one-dimensional compression cells have been used to estimate the constrained modulus (E'_0) of MSW (e.g. Singh and Fleming 2008, Beavan and Powrie 1995). In situ tests have also been used to obtain estimates of the shear modulus of MSW using shear wave velocity measurements (Kavazanjian et al. 1996), pressuremeter tests (Dixon et al. 1999), or high pressure dilatometer and self boring pressuremeter tests (Dixon and Langer 2006).

5.3 Experimental set-up

5.3.1 Dual-purpose laboratory compression cell

The experimental set-up used in this study is a dual-purpose large laboratory compression cell (LCC) designed and fabricated at the University of Saskatchewan, Canada (Figure 5-1). The purpose of the LCC is to study changes in the mechanical behaviour of waste subjected to accelerated degradation under controlled conditions. Incremental vertical stresses were applied to simulate the staged construction of a landfill.

The LCC is a 442 mm internal diameter and 600 mm high stainless steel cell with a wall thickness of 6.8 mm. The wall thickness of the cell was chosen so as to enable measurement of lateral stresses from less than 10 kPa to approximately 100 kPa while satisfying the K_0 condition. The cell is mounted on a 600 mm x 600 mm x 50 mm aluminum plate bolted to the bottom rail of a 1.83 m tall steel girder frame. An air-jack manufactured by Hydro-line, Inc having a piston diameter of 200 mm and capable of applying a maximum vertical stress of 260 kPa to the top of the waste, is attached to the top rail of the steel girder frame. The piston rod of the airjack has a diameter of 75 mm with a stroke length of 330 mm. A regulated supply of nitrogen is used in the airjack to maintain a desired vertical stress in the waste sample. The constant pressure system was able to maintain vertical stresses within $\pm 5\%$ of the targeted stress.

The plunger used for consolidating the waste is 442 mm in diameter and 38 mm thick, and was constructed by butting two aluminum plates each 19 mm thick together. The lower aluminum plate of the plunger has uniformly distributed holes 5 mm in diameter to facilitate biogas escape into a cavity which is provided between the two

aluminum plates. An outlet is provided on the upper aluminum plate to collect the biogas from this cavity via a one-way valve. The plunger is sealed against the cell wall by two O-rings spaced vertically at 20 mm. The overall system is thus sealed and leachate may be introduced and gas collected as the system is operated.

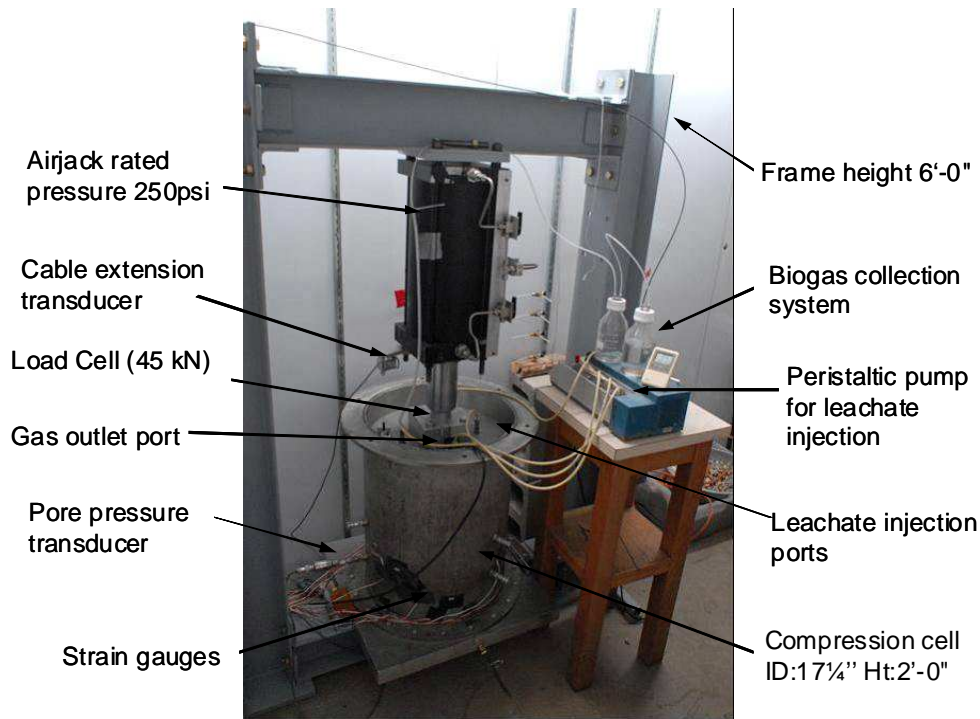


Figure 5-1 Dual purpose landfill compression cell (LCC) used in the present study

Four leachate injection ports, each with a hollow shaft are provided on the top aluminum plate of the plunger. The hollow shafts extend 75 mm beyond the bottom plate of the plunger so as to prevent leachate back-up into the gas cavity. The injection ports are evenly spaced for providing uniform distribution of leachate inside the cell. A peristaltic pump is used to inject leachate at a desired flow rate. The rubber tubing which is used to transport leachate from peristaltic pump to injection ports was capable of withstanding liquid pressures up to 275 kPa which was deemed necessary for pumping

leachate into compacted waste. An outlet is provided in the bottom aluminum plate for collecting leachate coming out of the waste.

5.3.2 Instrumentation

The instrumentation attached to the LCC comprises a load cell (to measure the vertical stress), a cable extension transducer (to measure vertical settlement of the sample), a pore pressure transducer and six strain gauges to measure the lateral stress of the consolidating waste against the sidewall of the compression cell.

A pancake-type load cell (45 kN capacity) was placed at the center of the top aluminum plate of the plunger and rigidly fastened to the piston rod and the plunger by means of a bracket assembly. The cable extension transducer is attached to a hook on the top plate of the plunger to record waste settlement. Six quick-connect ports in two tiers, horizontally spaced at 120° on the lower middle outer surface of the cell, are provided for pore pressure measurements. The six strain gauges are mounted on the outer surface of the LCC in two levels (75 mm and 150 mm from the base of the cell) and are spaced 120° apart horizontally. They are 3.0 mm foil type strain gauges (Tokyo Sokki Kenkyujo Co., Ltd.; Type: FCA-3-350-17-3L) built as a single unit of orthogonally placed two strain gauges. Two such built-in units of strains gauges, one at each level are connected so as to provide a full bridge circuit. Such assembly of strain gauges increases the accuracy in the determining lateral stresses. The data acquisition was accomplished with a USB-based DAQ module with 8 channels of 12-bit analog input using LabView v.8.0 software (National Instruments Inc. Ltd, Texas USA). .

5.3.3 Calibration

The calibration of the load cell, cable extension transducer, and pore pressure transducer was carried out using the procedure followed in geotechnical engineering. A different procedure was followed for calibration of the strain gauges which was required for inferring lateral stresses.

Lateral stresses (or K_0) in waste have been measured using different methods such as self-boring pressuremeters (Dixon et al. 1999), split ring consolidometers (Landva et al. 2000), vertical and horizontal stress cells (Dixon et al. 2004); and ultra thin tactile pressure sensors (Kavazanjian 2006). However, the technique used in the present study allows for continuous measurements of lateral stresses while the MSW is degrading, and is adapted from a method used by Edil and Dhowian (1981) to measure lateral stresses in peat soils. The calibration of strain gauges for inferring lateral stresses was done for three different sample heights. For each sample height, the compression cell was filled with de-aired water and increments of vertical stresses were applied. The response of the strain gauges to each increment of vertical stresses for each of the three sample heights was recorded in terms of change in strain gauge resistance. A linear relationship was obtained between the change in strain gauge resistance and the change in applied vertical stress for each sample height. The calibration constant for each of the three sample heights were not significantly different and, therefore, an average calibration constant was used for inferring the lateral stresses.

The measurement of hydrostatic pressure discussed above was also used for determining the actual vertical stresses transferred to the waste sample. A calibration curve was plotted between theoretical vertical stress (obtained from load cell reading) and

the hydrostatic pressure measured by pressure transducers in order to account for the sidewall friction generated between the plunger O-rings and the LCC wall. During calibration, piston friction on the sidewall was a constant value of 1.5 kN and an excellent linear fit was found between theoretical vertical stress and actual vertical stress. This work, serves to verify the vertical stress applied only at the top of the sample. The vertical stress at the bottom may be somewhat less because of sidewall friction between the waste and the vertical cylindrical walls of the compression cell.

5.4 Description of the MSW sample tested

The MSW sample used in the present study was slightly different from that reported by Singh and Fleming (2008) and was obtained from an excavation near the surface of the Spadina landfill in Saskatoon, Canada. The waste was less than one year old as clearly evident from the presence of recovered newspaper. The overall composition was dominated by food waste, diapers, papers, newspaper, wood pieces and plastic. Metals and aluminum constituted less than 5% by weight, perhaps reflecting recycling practice in the City. The waste was highly odorous typical of very young waste. Approximately 165 kg of waste was collected in pails, sealed and brought to the laboratory. Large chunks of wood and metals (approximately greater than 75 mm) were discarded during sampling.

5.5 Procedure

A representative sample of waste, approximately 100 kg, was prepared by thoroughly mixing and subdividing the bulk sample many times. Representative triplicate sub

samples, each 2.0 to 2.5 kg, were analyzed separately for moisture content and volatile solids. The compression cell was filled with the representative MSW in layers to achieve a total height of 580 mm, equivalent to an initial bulk unit weight of 9 kN/m^3 . The initial compacted unit weight considered in the present study is typical of most landfills where good initial compaction of waste is practiced (Zekkos et al. 2006).

The LCC was placed in a temperature controlled room maintained at $35 \pm 2^\circ\text{C}$. A geotextile filter overlying a layer of 20 mm nominal size gravel was placed at the base of the LCC to prevent clogging of the drainage line. Similarly, a 20 mm thick gravel layer overlying a wire mesh was placed on top of the waste to provide a headspace for gas collection. The plunger was mounted on the top of the cell and a small vertical stress (approximately 10 kPa) was applied to the plunger to bring the bottom of the plunger in direct contact with the sample without actually applying any vertical stress to the sample. As discussed above, this is the minimum pressure required to move the plunger inside the cell due to sidewall friction. The compression cell, filled with waste, was allowed to sit in this state for 24 hours. During this period, the baseline instrumentation response was recorded and thereafter, the increments of vertical stresses were applied by raising the pressure in the air-jack. The response of strain gauges, pore pressure transducer, cable extension transducers, and load cell were logged continuously. For each instrument, the average of all the values logged each day was computed. Five different data sets were recorded to document the complete stress history of the waste sample: time, lateral stresses, vertical stress, vertical displacement and pore water pressure.

The biodegradation of waste in the LCC was enhanced by leachate recirculation. The leachate injection rate for the first seven days, was approximately 700 ml-day^{-1} after

which it was reduced to 160 ml-day⁻¹ injected every alternate day. It took eight days for the waste to reach its field capacity, assuming that the liquid was distributed uniformly and there were no preferential flow paths inside the sample. No seeding was done in this experiment and the characteristics of the leachate and biogas, therefore, represents solely the biochemical properties of waste present inside the LCC. The overall composition of the waste was evaluated in terms of its volatile solid content for comparison with the composition of the sample after several months of accelerated degradation in the LCC.

The moisture content of the sample, both before and after incubation, was determined by drying the sample at 60⁰ C to a constant weight. For determining volatile solids (VS), the residue left after moisture content determination was ignited at 550⁰ C to a constant weight. Because of the large sample size, the time taken for both moisture and VS determination was more than 24 and 12 hrs respectively. Leachate samples were analyzed intermittently. Biogas samples were collected using tedlar bags for analysis of the gas composition. The gas production rate was estimated using the water displacement method.

5.6 Results and Discussion

The experiment commenced with a first increment of vertical stress equal to 22 kPa. The subsequent increments of vertical stresses were 44, 84 and 180 kPa. Each increment of vertical stress was maintained for at least 30 days except for $\sigma_v = 180$ kPa, for which the duration was 60 days. The time-settlement profile for the entire duration of experiment

(Figure 5-2) represents the combined effect of degradation and increments of vertical stresses on the overall settlement behaviour of waste.

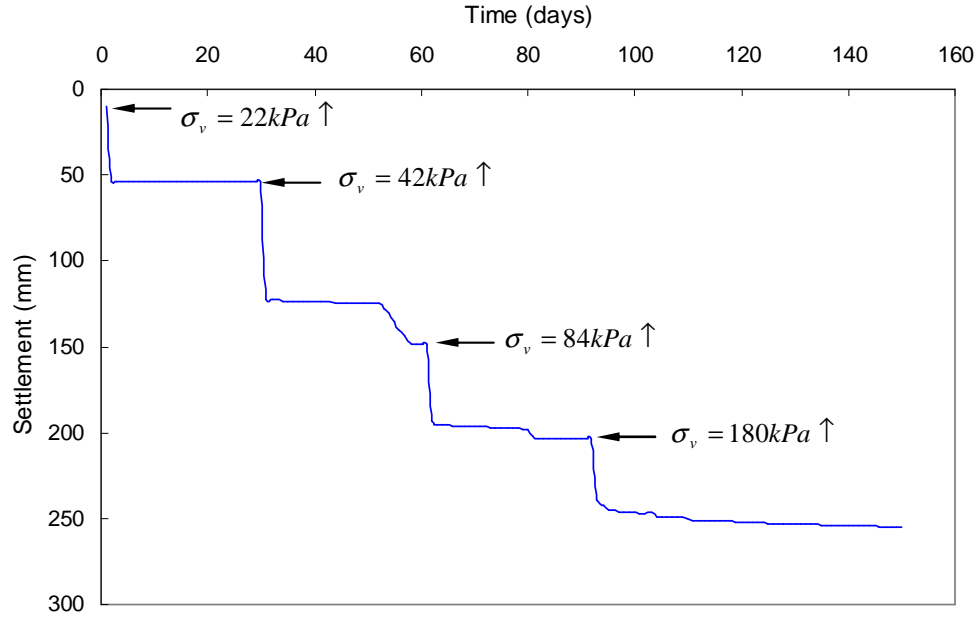


Figure 5-2 Time-settlement curve for the entire duration of the experiment (present study)

5.6.1 Degree of degradation of the waste sample during the experiment

The degree of degradation of the waste sample was assessed from cumulative methane production, leachate quality and the volatile solids remaining after degradation. BMP values for MSW typically lie between 54-108 L-kg⁻¹ of waste (Themelis and Ulloa, 2007). In an earlier study by Singh and Fleming (2004), the biochemical methane potential (BMP) of the waste from the Spadina landfill was estimated to be 60 L-CH₄ kg⁻¹ of waste and the volatile content of the waste was estimated as 55%.

The cumulative CH₄ production over the entire testing was 30 L-CH₄ kg⁻¹ of waste (Figure 5-3). This represents approximately 30-50% degradation of the waste sample, consistent with the estimate of loss of volatile solids during this study (Table 5-1). The

volatile solids decreased from 56.6% before incubation to 27.2% after incubation. As a result of degradation, an estimated 3.5 kg of solids were removed from the system (in the form of gas, condensate and dissolved solids in leachate) representing approximately 6% of initial total solids. The cumulative gas production (Figure 5-3) and biogas composition (Figure 5-4) were stable during the period monitored.

Table 5-1 Biochemical characterization of waste used in this study

| | Before incubation | After incubation |
|-----------------------------------|--|------------------|
| Wet wt (kg) | 82.4 | 86.9 |
| Average Water Content (%) | 30.6 | 38.3 |
| Average VSS Content (%) | 56.6 | 27.2 |
| Weight of dry solids(kg) | 57.2 | 53.6 |
| Loss of Solids during degradation | 3.5 kg which corresponds to 6% of initial total solids | |

The leachate quality was assessed in terms of pH, chemical oxygen demand (COD) and ammonia. The pH of the leachate fluctuated between 6.5 and 8.5 during the first week of the controlled experiment, and was then stable around 7.5 indicative of favorable conditions for methanogenesis. Figure 5-5 shows the removal of COD and ammonia during various stages of degradation. More than 90% of COD and ammonia were removed from the system during the experiment.

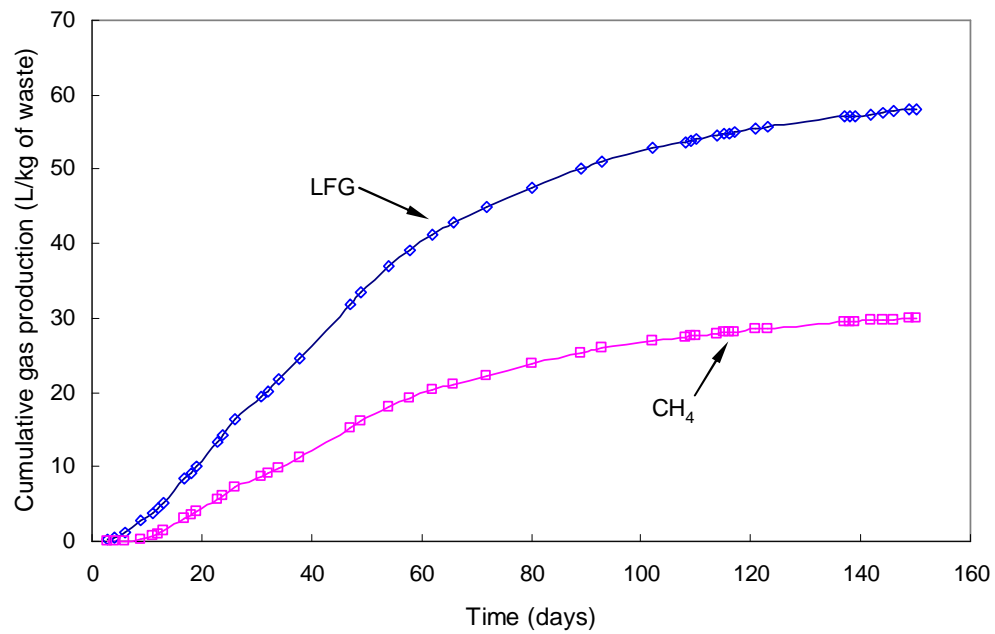


Figure 5-3 Cumulative gas production for the entire duration of experiment

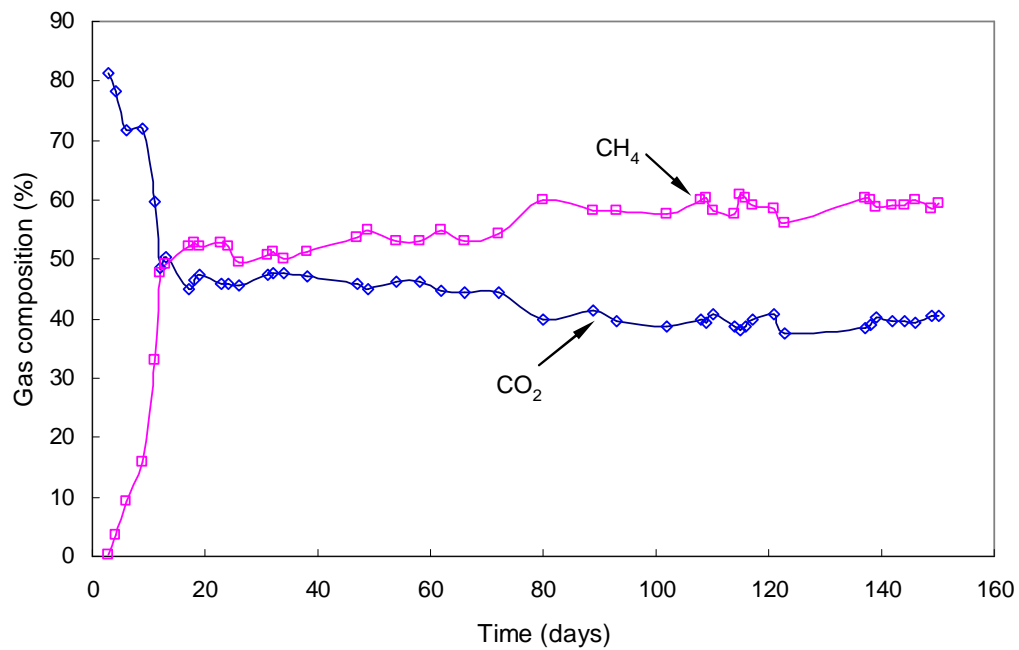


Figure 5-4 Biogas composition measured during the entire duration of experiment

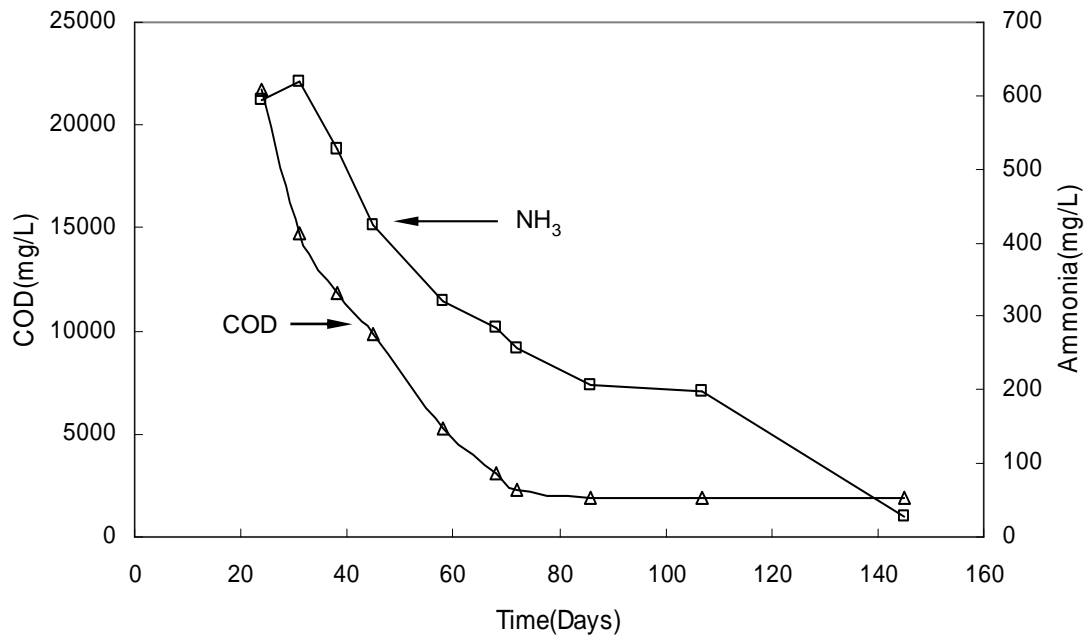


Figure 5-5 Depletion of leachate COD and ammonia during degradation

5.6.2 At-rest lateral earth pressure

Figure 5-6 shows the variation in effective stresses measured during the entire duration of the experiment. Drainage continued without any problems with clogging during the entire test run. During the first two months of loading, the observed pore water pressures were insignificant, possibly due to the low vertical stress and high void ratio. A temporary localized high pore pressure on day-90 can be seen in Figure 5-6 and corresponds to the start of last increment of vertical stress (= 180kPa). This high pore pressure however, soon dissipated.

Four increments of vertical stress were used to investigate the long-term effect of degradation on K_o . At each increment of vertical stress, K_o was estimated as the ratio of the average daily horizontal effective stress to the average daily vertical effective stress.

The daily average value of K_0 was observed to have some fluctuation during each stage of loading; however the moving average of K_0 was found to be stable and close to 0.40 for the entire duration of the experiment.

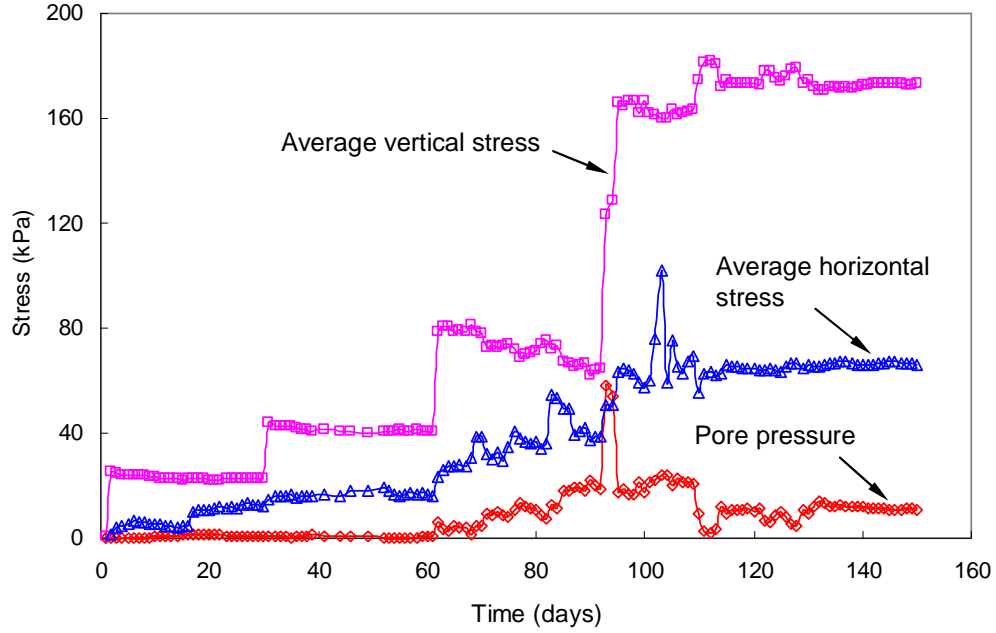


Figure 5-6 Variation of effective stresses during the test duration

Figure 5-7 shows the change in horizontal effective stress ($\Delta\sigma'_h$) vs. change in vertical effective stress ($\Delta\sigma'_v$) for each load step obtained from the present study as well as from Singh and Fleming (2008). The values of σ'_h and σ'_v used here are the average value of stresses for the entire duration of each load step and thus accounts for degradation as well. The at-rest earth pressure coefficient (K_0) is obtained as the slope of the regression line fitted to experimental data from this study. The value of K_0 obtained in Figure 5-7 is very close to that obtained from moving average method. The moving average of K_0 was obtained from the ratio of daily average values of σ'_h and σ'_v and is

in good agreement with published studies by Landva et al. (2000) and Singh and Fleming (2008).

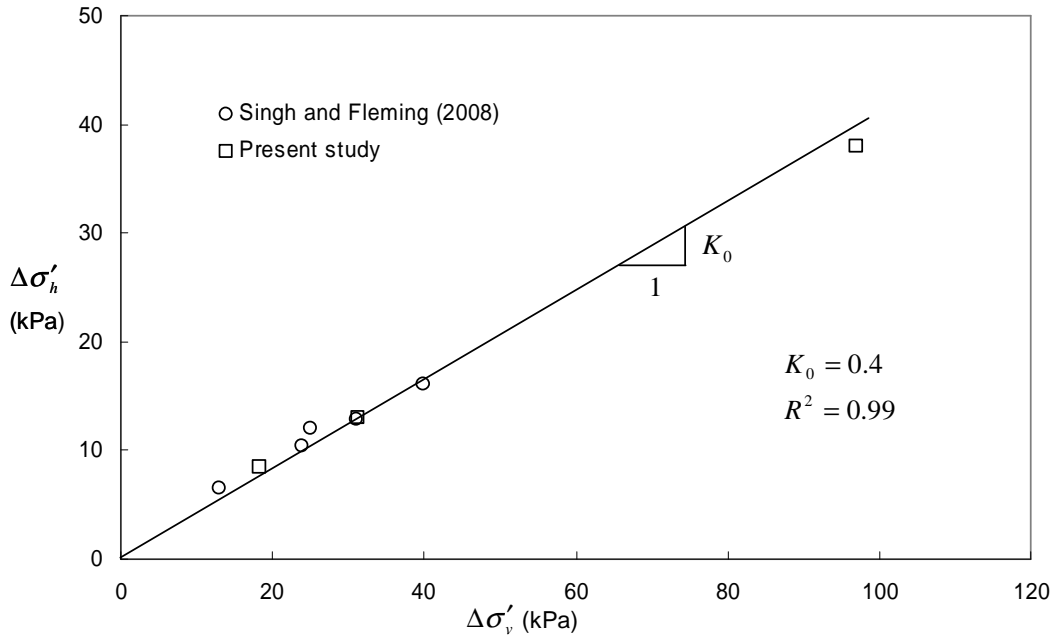


Figure 5-7 Estimation of K_0

A K_0 of 0.40 corresponds to a Poisson's ratio of 0.29, which is also consistent with values of Poisson's ratio obtained by Matasovic and Kavazanjian (1998). Lateral stress measurement using a pressuremeter (Dixon et al. 1999) provided a varying K_0 from 0.2 to 1.0. Towhata et al. (2004) measured K_0 from triaxial compression tests and obtained a value of 0.25 to 0.35 for vertical stresses of 250 kPa. Kavazanjian (2006) used ultra-thin tactile pressure sensors in estimating K_0 of waste and reported values of 0.3 for a moderately-compacted sample ($\gamma = 9.6 \text{ kN/m}^3$) and 0.2 for densely compacted sample ($\gamma = 11 \text{ kN/m}^3$).

In soil mechanics, K_o is widely accepted as a unique elastic constant. The present study suggests that it is also a unique elastic constant for MSW regardless of applied stresses and age.

5.6.3 Constrained Modulus

In this paper, the stiffness of the refuse has been quantified in terms of the constrained modulus which is defined as:

$$E'_0 = \frac{\Delta\sigma'_v}{\Delta\epsilon_a} \quad [3]$$

Figure 5-8 presents the values of the constrained modulus obtained from the present study. The values shown in Figure 5-8 are the values of E'_0 measured at the end of each 30 to 60 day load step and therefore these values incorporate the effect of degradation.

The data from previous short-term tests by Singh and Fleming (2008) are also plotted in Figure 5-8. The results from this study are consistent with the findings of Beaven and Powrie (1995) for the selected range of vertical stress used in this study. A closer look at Figure 5-8 suggests that, though there is a general increase in E'_0 with increasing vertical stress, the value of E'_0 shows some decrease when compared with values obtained in short-term tests by Singh and Fleming (2008) and this may be a result of degradation. However, at this stage this cannot be conclusively explained.

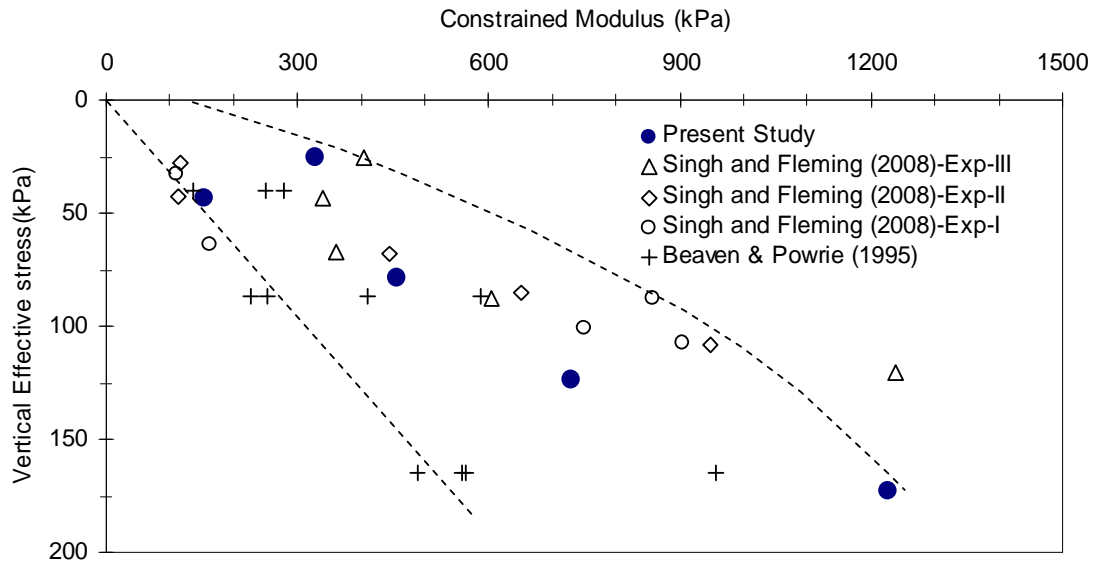


Figure 5-8 Constrained modulus measured in present study and from published literature

5.6.4 Compressibility

The primary compression, as discussed earlier, takes place immediately at the instance of load application and continues for some time. The primary compression is accompanied with significant changes in axial strains and this was observed in this study to occur during the first twenty four hours of load increment. The commencement of secondary compression was assumed to take place after primary compression has occurred. This was also evidenced from the record of axial strain which did not change by more than 1% after primary compression has occurred. Similar assumptions have also been made by other researchers such as Landva et al. (2000).

Figure 5-9 shows a plot of $\varepsilon_a - \log \sigma'_v$ obtained from this study. The value of ε_a and σ'_v are the average of the values measured during first twenty four hours of load increments. The value of primary compression ratio obtained in this way also

incorporates the effect of degradation. A best-fit line drawn through the data points gives an overall value of C_{ce} as 0.48. The authors are of the view that the value of C_{ce} estimated in this manner is more representative of waste since the processes of degradation (in lower lifts) and initial settlement due to overburden (in upper lifts) cannot be distinguished in a landfill.

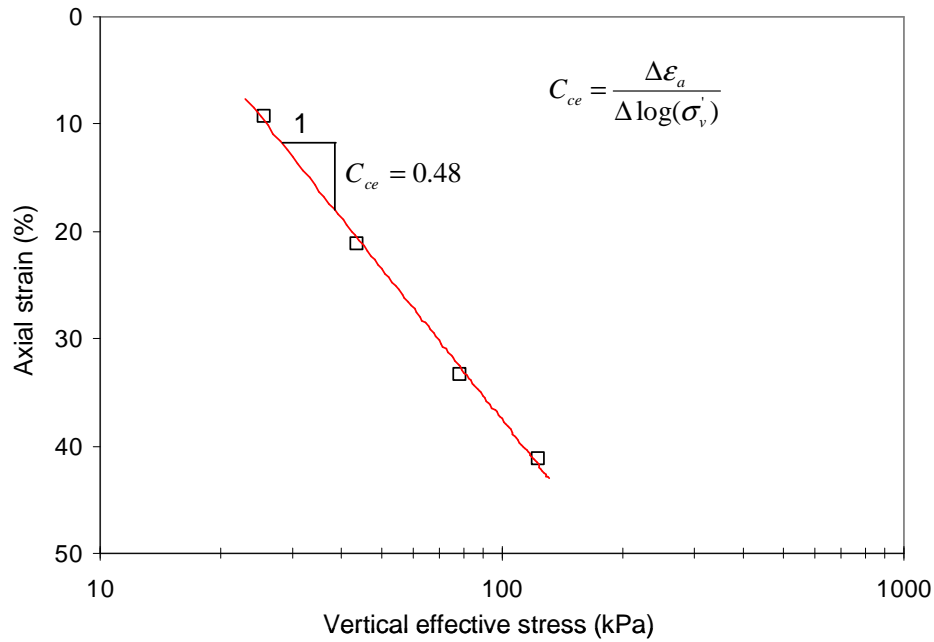


Figure 5-9 Primary compression ratio (C_{ce}) measured in this study

Hossain et al. (2003) observed an increase in the value of C_c from 0.16 to 0.37 as a result of degradation. It is worth mentioning here that these authors used shredded waste sample(s) with a maximum particle size of approximately 10 mm x 20 mm, tested in a 63.5 mm diameter oedometer. Vilar and Carvalho (2004) obtained values of C_c between 0.52 and 0.92 for 15 year old auger cuttings of degraded waste. The authors' question whether size reduction or shredding of waste may exhibit increased biodegradation due to large available surface area and increased nutrient access for biological activity (Wall and

Zeiss, 1995) and suggest that compression indices determined using such shredded waste should be used with caution.

Figure 5-10 to Figure 5-13 shows $\varepsilon_a - \log(t)$ curves for different stages of loading obtained from this study. The data for the first 24 hours of load increment, representing initial compression, have been demarcated clearly in these figures to elaborate the two-stage compression behaviour of MSW that was observed. It is evident from Figure 5-10 to Figure 5-13 that, there does not appear to be a smooth transition from initial compression to the onset of secondary compression and is thus consistent with the hypothesis that the mechanism of initial compression is a combined effect of distortion, bending, crushing and reorientation of waste constituents.

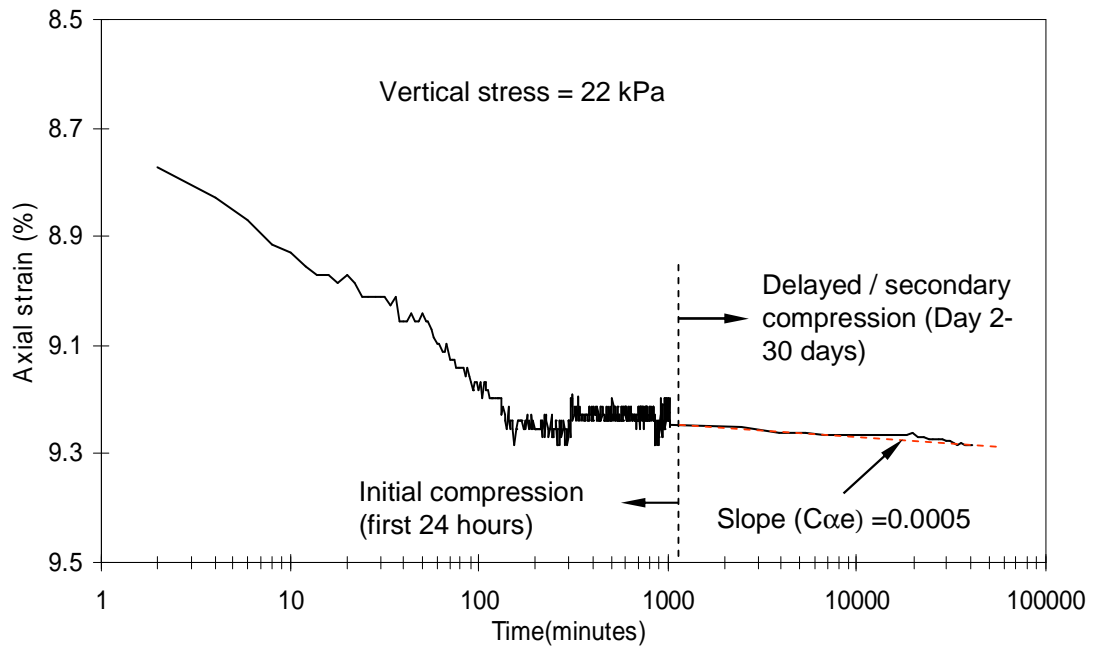


Figure 5-10 Secondary compression for $\sigma_v = 22kPa$

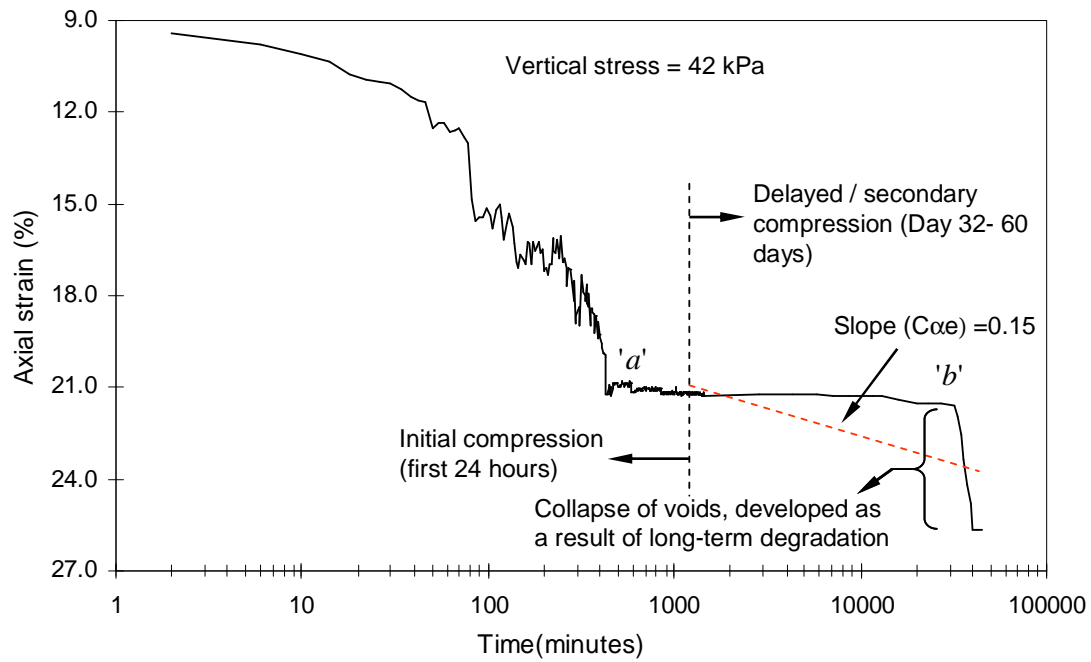


Figure 5-11 Secondary compression for $\sigma_v = 42kPa$

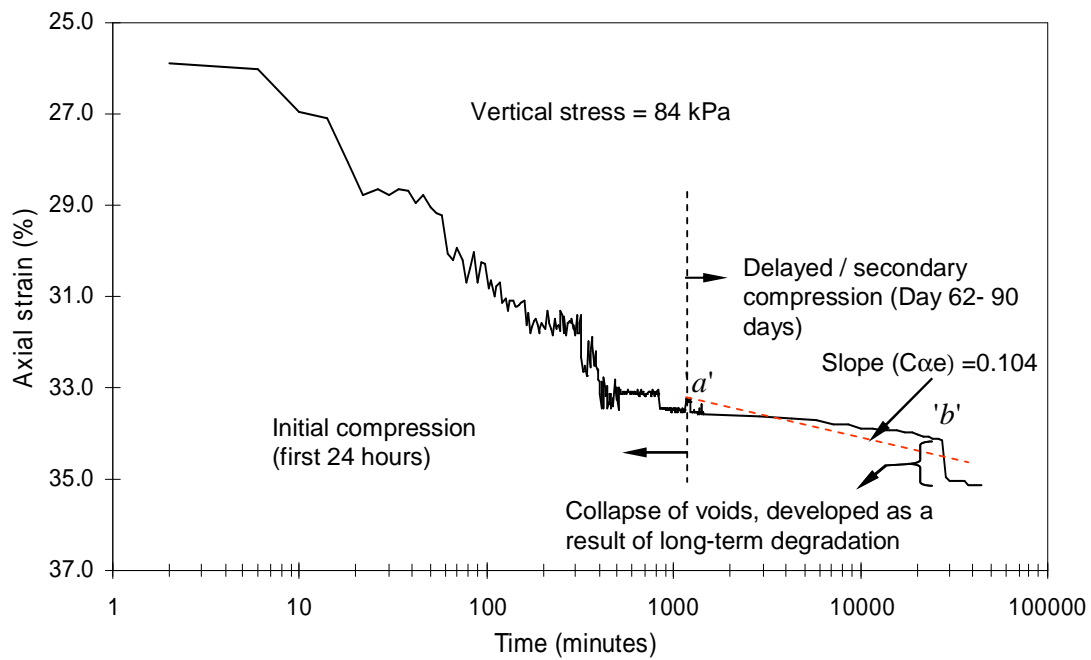


Figure 5-12 Secondary compression for $\sigma_v = 84kPa$

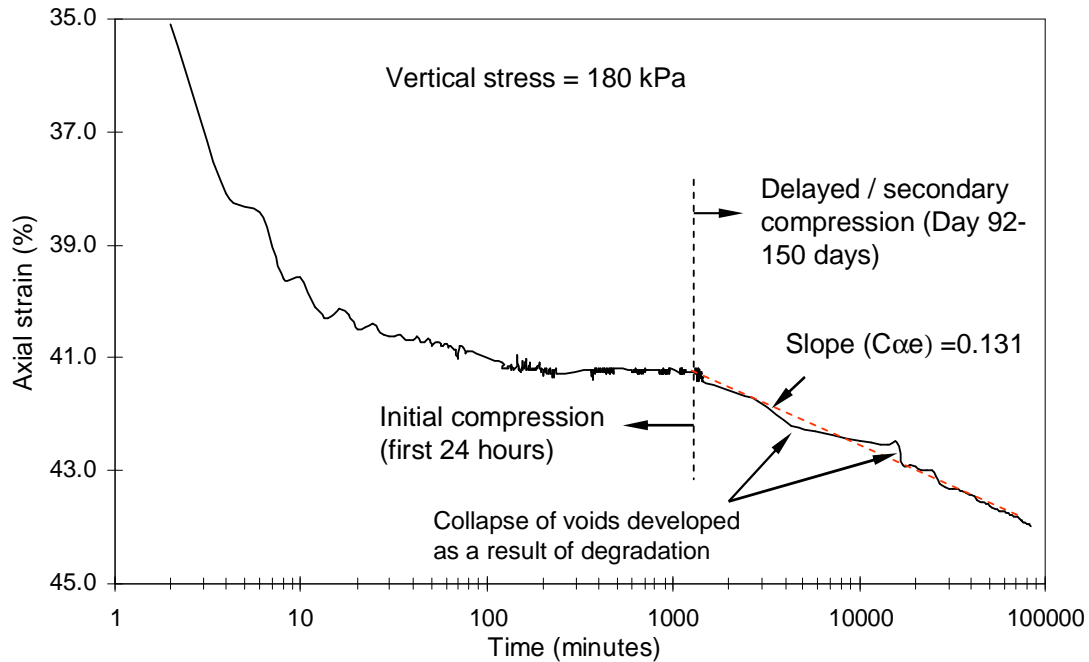


Figure 5-13 Secondary compression for $\sigma_v = 180\text{kPa}$

The secondary compression, as discussed earlier, began after 24 hours of load application and therefore in Figure 5-10 to Figure 5-13, for times beyond 24 hours up to the next increment of loading, the recorded data has been smoothed by presenting the daily average value. It appears from Figure 5-10 and Figure 5-11 that at small vertical loads (representing near surface waste); the secondary compression is not very significant except for an abrupt “collapse” observed near the end of the 42 kPa load step which is further discussed below. However, as the vertical stress is increased (as a result of placement of successive lifts of waste) and with the progression of degradation, the secondary compression becomes more prominent.

The values of $C_{\alpha e}$ as shown in Table 5-2 for various stages of loading and degradation were obtained by drawing a best fit line to secondary compression data (beyond 24 hours up to the next load increment). The pattern suggests a general increase

in the value of $C_{\alpha e}$ with an increase in vertical stress and degradation, though not in a linear fashion. Such a change in $C_{\alpha e}$ as a result of degradation has also been reported by Manassero et al. (1997) from their observations of landfill settlement in Spain and Greece. However, these observations are not in agreement with the results of Wall and Zeiss (1995) and Landva et al. (1984) who suggested that there is no significant difference between secondary compression rates in older and more recent landfills. Contrary to a suggestion by Sowers (1973), Gabr and Valero (1995) suggested that secondary compression is less dependent on initial void ratio and depends more on conditions favorable for degradation.

Table 5-2 Secondary compression ratio estimated in this study

| Vertical stress (kPa) | Duration of loading (days) | $C_{\alpha e}$ |
|--------------------------|-------------------------------|----------------|
| 22 | 30 | 0.0005 |
| 44 | 30 | 0.150 |
| 84 | 30 | 0.104 |
| 180 | 60 | 0.131 |

A brief overview of the testing details and results of compressibility of waste from published studies is shown in Table 5-3. A general observation from Table 5-3 reveals that these studies were conducted either as short term studies with vertical stress increasing over a very short period of time, or as long term studies at a constant vertical stress. In either case, the waste settlement behaviour as simulated and observed in the present study is somewhat different from published studies.

A possible mechanism for the degradation-induced compression of MSW is associated with ‘phase change’ of materials during the process of degradation

Table 5-3 Compressibility indices of MSW from published studies

| Reference | Primary | | Secondary | | Remarks |
|----------------------------------|-----------|-----------------------|----------------|-----------------------|---|
| | C_{ce} | C_c | $C_{\alpha e}$ | C_{α} | |
| Vilar and Carvalho (2004) | 0.18-0.23 | 0.52-0.92 | 0.012-0.016 | 0.021-0.044 | auger cuttings; 15 year old waste; test cell 365mm in diameter; $\gamma = \text{kN/m}^3$; loading duration 7-15 days but no consideration for degradation; max. vertical stress =640 kPa |
| Hossain et al. (2003) | | | | | |
| (a) With accelerated degradation | | 0.16-0.37 | | 0.08-0.22 | test cell 63.5mm in diameter; shredded waste(10mm x 20mm); loading duration 70 days; constant vertical stress 95 kPa; |
| (b) Degradation inhibited | | 0.16-0.25 | | 0.07-0.12 | |
| Landva et al. (2000) | 0.17-0.24 | | 0.01-0.016 | | test cell 600 mm diameter; sample 5 year old+ additional artificial degradation; degraded for 9 years; constituents > 150mm were shredded; vertical stress 46-260 kPa; loading duration 1-32 days |
| Gabr and Valero (1995) | | 0.4-0.9 | | 0.009-0.03 | test cell 63mm diameter; particle size < 6.3mm; sample-auger cuttings representative of 15-30 year old waste; initial void ratio 1.0-3.0; No consideration for vertical stress and test duration |
| Wall and Zeiss (1995) | | | | | |
| (a) With accelerated degradation | 0.25 | | 0.033-0.056 | | test cell 570mm in diameter designed to perform as both lysimeter and consolidometer; particle size reduced by shredding; loading duration 229 days at a constant average vertical stress of 10kPa. |
| (b) Degradation inhibited | 0.21 | | 0.037-0.049 | | |
| Sowers (1973) | | 0.15-0.55 times e_o | | 0.03-0.09 times e_o | Compression indices related to initial void ratio |
| Present study | 0.42 | | | 0.0005 -0.15 | test cell 400mm diameter; 1 year old waste degraded for 150 days in purpose compression cell(Bioreactor +Consolidometer); loading duration 60 days+leachate injection; vertical stress 22-180 kPa; primary compression ratio reduced from 0.58 to 0.27 under the application of incremental vertical stresses and simultaneous degradation. A best fit representing all stages of loading gave a value of 0.42. |

(McDougall et al. 2004 and McDougall and Pyrah 2004). These authors suggested that the solids decomposition results in an enlarged void space without significant overall volumetric reduction. The solid skeleton progressively weakens due to degradation and reaches a point where it can no longer support the overburden and a collapse occurs. Densification due to collapse temporarily improves the material strength and the ability to resist further deformation. Continued decomposition will produce further episodes of void enlargement and collapse.

The development and collapse of voids during degradation is likely a major contributory factor to secondary compression in MSW. The settlement mechanism suggested by McDougall et al. (2004) and McDougall and Pyrah (2004) is well demonstrated in Figure 5-10 to Figure 5-13. Referring to Figure 5-11 and Figure 5-12, from points *a* to *b*, the waste skeleton seems to be getting weaker as a result of degradation, however with minor distortion and raveling. At point *b* the waste structure becomes sufficiently weak to sustain vertical stresses and the voids developed due to degradation collapses which is marked by an abrupt increase in axial strain at point *b*. The authors expect that additional such episodes of void collapse might have been observed, had the waste been allowed to degrade at each vertical stress for a longer period.

From the pattern in C_{ae} values obtained from this study and based on Figure 5-10 to Figure 5-13, some important observations can be made regarding the settlement behaviour of MSW with particular emphasis to bioreactor landfills. It is likely that significant differential settlements may be expected during the early phases of the landfill operation (typically 10-15 years). During this period, the majority of the readily-

degradable waste constituents will be volatilized, thereby creating a collapsible structure. The collapse of these voids will result into an uneven settlement of the waste surface. Further degradation will gradually reduce the size of constituents available for collapse and the secondary settlement will become uniform and linear in the later phase of degradation. The use of a single value of $C_{\alpha e}$ for settlement calculation may thus provide unrealistic estimates of settlement in waste.

5.7 Conclusions

A dual-purpose compression cell has been designed and fabricated to study the evolution of compressibility and elastic properties of municipal solid waste subjected to accelerated degradation under the application of incremental vertical stresses. Approximately 30-50% degradation of the waste sample was achieved during the experiment which was quantified from the estimates of volatile solids removed and cumulative methane produced.

The evolution of at-rest lateral earth pressure of MSW was quantified from the estimates of lateral stresses developed during the course of degradation. It is proposed that K_0 of waste is a unique elastic parameter and is not influenced by applied stresses and degradation. The constrained modulus was estimated to lie between 300 kPa to 1200 kPa for the range of applied vertical stresses and appears to be slightly influenced by degradation; however, this cannot be conclusively stated at this time.

The cumulative settlement during this study was estimated as 255 mm constituting approximately 44% of the initial height of the sample. The experiment yielded a value for

the primary compression ratio which is high compared to published values in which degradation had not been considered. This observation suggests that degradation increases the compressibility of waste. The primary compression ratio (C_{ce}) was observed to decrease from 0.58 to 0.27 for successive increments of vertical stresses.

The secondary compression is significantly effected by degradation and accounted for approximately 21.5% (50 mm) of the overall settlement observed in this study. The contributions of secondary settlement at individual load steps were 0.2% (22 kPa); 10.7% (44 kPa); 4.2% (84 kPa) and 6.5% (180 kPa). The secondary compression ratio ($C_{\alpha e}$) was observed to increase from 0.0005 to 0.15 for various load increments. Use of a single value of $C_{\alpha e}$ may therefore result in unrealistic settlement estimates of landfills. Given these observations, it is suggested that enhancing waste degradation may result in an increase in the compressibility of waste.

A significant finding is that the data from this study tend to confirm that the mechanism of secondary compression in MSW occurs as an episodic process of void formation and later collapse of these voids. The differential settlements observed in landfills are an outcome of the mechanism as discussed above. The overall settlement will depend upon the constituent size; its degradation potential; and the existence of favorable conditions for its degradation. Long-term laboratory or field studies on a larger scale are required to substantiate these observations and to understand the influence of pre-compression, re-compaction, and lateral stresses (three-dimensional compression) on the compression indices and on the mechanism of settlement.

5.8 References

- Al-Khafaji, A. W. N., and Andersland, O. B. 1981. Compressibility and strength of decomposing fibre-clay soils. *Geotechnique*, 31(4): 497-508.
- Beaven, R.P. and Powrie, W. 1995. Hydrogeological and geotechnical properties of refuse using a large scale compression cell. *Proc. 5th International Waste Management and Landfill Symposium, Sardinia*, 745-760.
- Carvalho, M.de.F. and Vilar, O.M. 1998. In situ tests in urban waste Sanitary landfill. *Environmental Geotechnics*, Seco e Pinto, ed., Balkema, Rotterdam, 121-126.
- Dixon, N. and Langer, U. 2006. Development of a MSW classification system for the evaluation of mechanical properties. *Waste Management*, 26: 220-232.
- Dixon, N., Jones, D.R.V. and Whittle, R.W. 1999. Mechanical properties of household waste: In-situ assessment using pressuremeter. *Proc. 7th International Waste Management and Landfill Symposium, Sardinia*, 453-460.
- Edil, T.B. and Dhowian, A.W. 1981. At rest lateral pressure of peat soils. *Journal of Geotechnical Engineering, ASCE*, 107(GT2): 721-738.
- Gabr, M.A. and Valero, S.N. 1995. Geotechnical Properties of Municipal Solid Waste. *Geotechnical Testing Journal*, 18(2): 241-251.
- Gasparini, P.A., Saetti, G.F. and Marastoni, M. 1995. Experimental research on MSW compaction degree and its change with time. *Proc. 5th International Waste Management and Landfill Symposium, Sardinia*, 833-842.
- Hossain, M.S., Gabr, M.A. and Barlaz, M.A. 2003. Relationship of compressibility parameters to municipal solid waste decomposition. *Journal of Geotechnical and Geoenvironmental Engineering, ASCE*, 129(12): 1151-1158.
- Houston, W.N., Houston, S.L., Liu, J.W., Elsayed, A. and Sanders, C.O. 1995. In-situ testing methods for dynamic properties of MSW landfills. *Geotechnical Special Publication, ASCE*, 54: 73-82.

- Kavazanjian, E, Jr. 2008. The Impact of degradation on MSW shear strength. Geotechnical Special Publication, ASCE, 177: 224-231.
- Kavazanjian, E, Jr. 2006. Waste mechanics: Recent findings and unanswered questions. Geotechnical Special Publication, ASCE, 148: 34-54.
- Kavazanjian, E., Jr., matasovic, N., Stokoe, K. and Bray, J.D. 1996. In-situ shear wave velocity of solid waste from surface wave measurements. Proc., 2nd International Congress on Environmental Geotechnics, Osaka, Japan, Balkema, 1: 97-104.
- Landva, A.O., Valsangkar, A.J. and Pelkey, S.G. 2000. Lateral earth pressure at rest and compressibility of municipal solid waste. Canadian Geotechnical Journal, 37: 1157-1165.
- Landva, A.O., Weisner, W.R. and Burwash, W.J. 1984. Geotechnical engineering and refuse landfills. 6th International Conference on Waste Management, Canada.
- Manassero, M., Van Impe, W. F., and Bouazza, A. 1996. Waste Disposal and Containment. Proc. 2nd International Congress on Environmental Geotechniques, Osaka, Japan, A.A. Balkema, 3:1425-1474.
- Matasovic, N. and Kavazanjian, E. Jr. 1998. Cyclic characterization of OII landfill solid waste. Journal of Geotechnical and Geoenvironmental Engineering, ASCE, 124(3): 197-210.
- McDougall, J.R. 2008. Geomechanics and Long-term landfill settlement. Geotechnical Special Publication, ASCE, 177: 192-199.
- McDougall, J. R., and Pyrah, I. C. 2004. Phase relations for decomposable soils. Geotechnique, 54(7): 487-493.
- McDougall, J. R., Pyrah, I. C., Yuen, S. T. S., Monteiro, V. E. D., Melo, M. C., and Juca, J. F. T. 2004. Decomposition and settlement in landfilled waste and other soil-like materials. Geotechnique, 54(9): 605-609.
- Morris, D. V. and Woods, C. E. 1990. Settlement and Engineering considerations in Landfill and final cover design. Geotechniques of Waste Fills – Theory and

- Practice, ASTM, STP 1070, A. Landva and G.D. Knowles, Eds., Philadelphia, P.A., 9-21.
- Sharma, H.D., Dukes, M.T., Olsen, D.M. 1990. Geotechniques of Waste Fills – Theory and Practice, ASTM, STP 1070, A. Landva and G.D. Knowles, Eds., Philadelphia, P.A., 57-70.
- Singh, M.K. and Fleming, I.R. 2004. Evaluation of existing and potential methane generation at the city of Saskatoon landfill. Draft report, submitted to Saskatchewan Power Corporation, Regina, SK, Canada.
- Singh, M.K. and Fleming, I.R. 2008. Estimation of the Mechanical Properties of MSW during degradation in a laboratory compression cell. Geotechnical Special Publication, ASCE, 177: 200-207.
- Singh, M.K., Fleming, I.R. and Sharma, J.S. 2007. Development of a practical method for the estimation of maximum lateral displacement in Large Landfills. Practice Periodical of Hazardous, Toxic, and Radiactive Waste Management, ASCE (Accepted)
- Sowers, G. F. 1973. Settlement of waste disposal fills. Proc. 8th International Conference of Soil Mechanics and Foundation Engineering, Moscow, 2, A. A. Balkema, 207-210.
- Stoltz, G. and Gourc, J.P. 2008. Variation of fluid conductivity with settlement of domestic waste. Geotechnical Special Publication, ASCE, 177: 272-279.
- Themelis, N.J. and Ulloa, P.A. 2007. Methane generation in landfills. Renewable Energy, 32: 1243-1257.
- Towhata, I., Kawano, Y., Yonai, Y., and Koelsch, F. 2004. Laboratory tests on dynamic properties of municipal wastes. Proc. 11th Conference in Soil Dynamics and Earthquake Engineering and 3rd International Conference on Earthquake Geotechnical Engineering, 1: 688-693.
- Van Impe, W.F. and Bouazza, A. 1996. Densification of domestic waste fills by dynamic compaction. Canadian Geotechnical Journal, 33: 879-887.

- Vilar, O.M. and Carvalho, M.F. 2004. Mechanical properties of municipal solid waste. *Journal of Testing and Evaluation*, ASTM. 32(6): 1-12.
- Wall, D.K. and Zeiss, C. 1995. Municipal landfill biodegradation and settlement. *Journal of Environmental Engineering*, 121(3): 214-224.
- Zekkos, D.P., Bray, J.D., Kavazanjian, E., Matasovic, N., Rathje, E.M., Riemer, M.F., Stokoe, K.H. 2006. Unit weight of municipal solid waste. *Journal of Geotechnical and Geoenvironmental Engineering*, ASCE, 132(10):1250-1261.
- Zekkos, D.P. 2005. Evaluation of static and dynamic properties of municipal solid waste. PhD thesis, Department of Civil and Environmental Engineering, University of California, Berkley.

CHAPTER 6 A DESIGN CHART FOR ESTIMATION OF HORIZONTAL DISPLACEMENT IN MUNICIPAL LANDFILLS

Preface[†]

It is evident that ensuring the serviceability of buried collection pipes and other infrastructure installed in a landfill is a crucial task, especially given the increasing trend towards bioreactor landfills. It is, therefore, important to be able to estimate horizontal displacement within a landfill and design the buried collection pipes accordingly in order to mitigate such effects. It is hypothesized that prior knowledge during the design process of the likely magnitude of such lateral displacements would enable engineers to choose materials and/or designs aimed at mitigating such serviceability issues, particularly relating to the gas collection system. This paper proposes an easy-to-use design chart to estimate the maximum expected lateral displacement within a landfill using the height and the sideslope of the landfill. The design chart is developed using results of a finite element parametric study. The input parameters were obtained from laboratory testing data and an extensive numerical modelling exercise. The validity of the design chart is assessed using field monitoring results from the Brock West landfill in Ontario, Canada. The work presented herein addresses the fourth objective of this research: to develop a simple design chart for predicting lateral deformations in landfills.

[†]A similar version of this chapter is under review for possible publication as a research paper in *Waste Management*.

Citation: M. K. Singh, J. S. Sharma and I. R. Fleming “A design chart for estimation of horizontal displacement in municipal landfills”.

Abstract

This paper describes the development of a design chart for the estimation of maximum horizontal displacement within a municipal landfill using the height and the sideslope of the landfill. The design chart is based on the results of a finite element parametric study in which the behaviour of the municipal solid waste was modeled using a non-linear elastic hyperbolic model. The model input parameters, i.e. non-linear stiffness, shear strength and unit weight of MSW, were obtained from laboratory testing data and an extensive stochastic numerical modelling exercise. Non-linear variations of unit weight as well as Young's modulus of MSW with depth were incorporated in the finite element analyses. The validity of the design chart was assessed using field monitoring results from a large landfill located in Ontario, Canada.

6.1 Introduction

In recent years, there has been an unprecedented global increase in urban population. According to a report by the Population Division of the Department of Economic and Social Affairs of the United Nations Secretariat (UN 2006), 47 per cent of the world's population lived in large cities at the end of the last century. The report also predicts that more than half of the world's population will be urban by the year 2010 (UN 2006). This trend of increasing urban population has resulted in a significant increase in waste production and has made it necessary for the municipalities to use landfill space more efficiently. Sanitary landfills are now being forced to accept greater quantities of municipal solid waste (MSW) per unit area of landfill footprint by increasing landfill

height, employing steeper sideslopes, enhancing MSW degradation, or by ‘piggyback’ expansion of existing landfills. Concurrently, there has also been an increase in the use of closed landfills for the generation and collection of landfill gas (LFG) from decomposing waste. As a result, engineered systems for the collection of LFG are being installed in many landfills. Such gas collection systems also help to minimizing the impact of the landfill on the air quality and to capture emission of greenhouse gases.

These trends of higher and steeper landfills along with the installation of gas collection systems have made it challenging to ensure both the stability of the landfilled waste mass and the serviceability of the installed gas collection infrastructure. It can be argued that the stability of a landfill can be ensured as long as the landfill is adequately engineered and is monitored regularly for significant changes in operating conditions. It is, however, quite difficult to ensure the serviceability of buried collection pipes, etc. A landfill may not fail catastrophically because of increases in height or because of waste degradation; however, it is always possible for the waste to undergo large lateral deformations, impairing the function of the gas collection system. It is important, therefore, to be able to estimate the maximum horizontal displacement within a landfill in order to mitigate such effects.

This study presents an easy-to-use design chart for the estimation of the maximum expected lateral displacement within a landfill using the height and the sideslope of the landfill. The design chart is developed using results of a finite element parametric study in which the behaviour of the municipal solid waste is modeled using a non-linear elastic hyperbolic model. The design chart incorporates non-linear variation in unit weight as well as Young’s modulus of MSW with depth. Mechanical properties of MSW used for

the development of this design chart (i.e. non-linear stiffness, shear strength and unit weight of MSW) were obtained using a substantial database of laboratory testing data as well as through stochastic numerical modelling. The validity of the design chart is established using field monitoring results from Brock West landfill located in Ontario, Canada.

6.2 Approach

The design chart proposed in this study is based on the results of a series of finite element analyses conducted using a stress-deformation finite element program SIGMA/W, which is a component of the GeoStudio 2007 suite of software (GSI, 2007). A typical finite element analysis involved the simulation of a staged increase in the height of a landfill at a given sideslope angle. Only half of the landfill was modeled because of the symmetry along the vertical axis. The foundation soil was modeled as a 10-m thick layer of linear elastic material (Young's modulus = 20 MPa; Poisson's ratio = 0.33). The stress-deformation behaviour of MSW was modeled using a non-linear elastic hyperbolic (NLEH) model. A brief description of the NLEH model is provided in the next section.

The mechanical properties required by the NLEH model (namely shear strength parameters, elastic properties and unit weight) were obtained in two different ways: (a) statistical analysis of data available in the literature as well as data from laboratory testing of MSW conducted by the authors; and (b) stochastic modelling of the mechanical behaviour of MSW using 'unit cell' finite element simulations. Details of these two methods are provided in the subsequent sections. Non-linear variations with depth for both Young's modulus and the unit weight were incorporated in the finite element

analyses. Details of how these variations were obtained are also given in the subsequent sections.

6.3 Non-linear elastic hyperbolic (NLEH) model

A non-linear elastic hyperbolic (NLEH) model (Kondner 1963, Duncan and Chang 1970) is used to model the non-linear deviatoric stress vs. axial strain response of MSW (Figure 6-1). The NLEH model is deemed appropriate for modelling the stress-deformation behaviour of MSW because it can simulate decreasing stiffness with increasing axial strain as well as increasing initial stiffness with increasing confining stress. Detailed formulation of the NLEH model can be found in Kondner (1963) and Duncan and Chang (1970) and only a brief summary of the NLEH model is presented here.

The stress-strain relationship for the NLEH model can be expressed as:

$$(\sigma'_1 - \sigma'_3) = \frac{\varepsilon_a}{\left[\frac{1}{E_i} + \frac{\varepsilon_a R_f}{(\sigma'_1 - \sigma'_3)_f} \right]} \quad [1]$$

where $(\sigma'_1 - \sigma'_3)$ is the deviatoric stress, ε_a is the axial strain, E_i is the initial tangent Young's modulus, $(\sigma'_1 - \sigma'_3)_f$ is the deviatoric stress at failure, and R_f is a factor that relates the deviatoric stress at failure to the ultimate (asymptotic) value of deviatoric stress $(\sigma'_1 - \sigma'_3)_{ult}$ as:

$$(\sigma'_1 - \sigma'_3)_f = R_f (\sigma'_1 - \sigma'_3)_{ult}$$

The value of R_f is always less than unity.

Following Janbu (1963) and Duncan and Chang (1970), the initial tangent Young's modulus can be considered a function of the effective confining stress (or minor principle effective stress):

$$E_i = KP_a \left(\frac{\sigma'_3}{P_a} \right)^n \quad [2]$$

where P_a is the atmospheric pressure (equals 101.3 kPa), σ'_3 is the effective confining stress, K is a modulus number representing the value of initial tangent Young's modulus normalized with atmospheric pressure (i.e E_i / P_a) at σ'_3 equals 101.3 kPa and n represents the rate of change of E_i with σ'_3 . The larger the value of n , the more rapidly E_i increases with increasing σ'_3 .

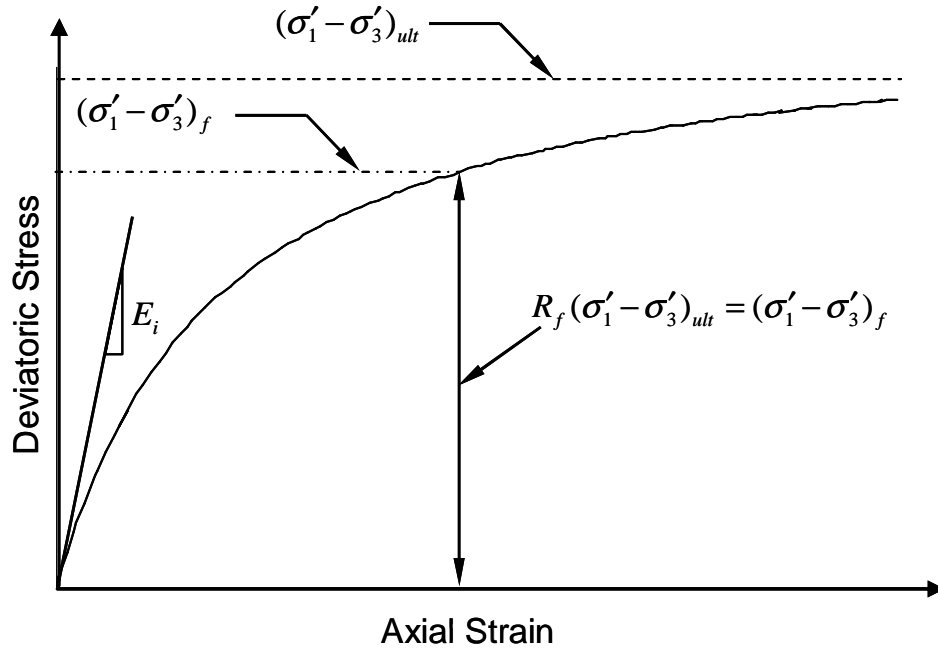


Figure 6-1 Stress-strain curve for the non-linear elastic hyperbolic (NLEH) model

The deviatoric stress at failure can be related to the shear strength parameters – cohesion intercept c' and angle of shearing resistance ϕ' – using the Mohr-Coulomb failure criterion:

$$(\sigma'_1 - \sigma'_3)_f = \frac{2c' \cos \phi' + 2\sigma'_3 \sin \phi'}{1 - \sin \phi'} \quad [3]$$

The tangent Young's modulus E_t for any stress state may then be determined by differentiating Equation (1) with respect to axial strain ε_a and substituting Equation (2) and equation (3) in the resulting equation.

$$E_t = \left[1 - \frac{R_f (1 - \sin \phi') (\sigma'_1 - \sigma'_3)}{2c' \cos \phi' + 2\sigma'_3 \sin \phi'} \right]^2 KP_a \left(\frac{\sigma'_3}{P_a} \right)^n \quad [4]$$

Equation (4), which describes the non-linear variation of the tangent Young's modulus with deviatoric stress (or axial strain) for a NLEH model using the five input parameters: K , n , c' , ϕ' , and R_f , is used in the finite element analyses conducted for the development of the design chart.

6.4 Mechanical properties of MSW

Modelling the mechanical behaviour of MSW using the NLEH model requires five input parameters (K , n , c' , ϕ' , and R_f) for the complete description of its stress-strain behaviour. Additionally, the unit weight of MSW (γ) is required to determine the vertical and horizontal effective stress profiles within the landfill.

Lower- and upper-bound values of parameters K , n and R_f were obtained from statistical analysis of these parameters estimated from triaxial stress-strain data available in the literature as well as data obtained from extensive laboratory testing of MSW carried out by the authors using large samples of MSW taken from two different landfills in Canada (Singh et al. 2008). Lower- and upper-bound values of parameters c' and ϕ' were obtained from the results of stochastic modelling of the mechanical behaviour of MSW using ‘unit cell’ finite element analyses as well as statistical analysis of data available in the literature. The profiles of unit weight vs. depth corresponding to low, typical and high values of unit weight were obtained using data available in the published literature.

6.4.1 Estimation of Young’s modulus

Using large-scale tests on MSW, the Young’s modulus of MSW has been found to increase with depth and increasing confining stress (Beaven and Powrie 1995; Castelli and Maugeri 2008; Singh and Fleming 2008; Singh and Fleming 2008a). Accordingly, a power function first proposed by Janbu (1963) for a wide range of geomaterials ranging from plastic clays to soft rocks and given by Equation (5) is used to capture the stress dependence of Young’s modulus of MSW:

$$E = KP_a \left(\frac{\sigma'_3}{P_a} \right)^n \quad [5]$$

Equation (2), which relates initial tangent Young’s modulus E_i to the effective confining stress, is simply a special case of Equation (5). It is worth mentioning here that municipal waste was likely not a material considered by Janbu (1963) when proposing

Equation (5). A practical advantage in using this formulation is that it is coded into some stress-deformation finite element software such as SIGMA/W (GSI, 2007). Equation (5) implies that as σ'_3 approaches 0, E_i should also approach 0; this is consistent with the authors' laboratory compression cell testing data (Singh and Fleming 2008; Singh and Fleming 2008a) and data from a large-scale compression cell in the UK (Beaven and Powrie 1995) as shown in Figure 6-2.

Figure 6-2 Modulus of MSW from large compression cell

Unlike soils, MSW shows significant variability in terms of composition and undergoes chemical and biological degradation with time. It is likely, therefore, that Young's modulus of MSW may also depend on the composition and the state of degradation of MSW; however, no evidence has been found in published literature in support of this hypothesis. Hence, in the present study, the Young's modulus of MSW is assumed to vary only with the effective confining stress according to Equation (5). It is

also assumed that the effective confining stress can be estimated from the effective vertical stress σ'_v and the at-rest coefficient of earth pressure K_0 using

$$\sigma'_3 = K_0 \sigma'_v \quad [6]$$

Substitution of Equation (6) into Equation (5) results in:

$$E = KP_a \left(\frac{K_0 \sigma'_v}{P_a} \right)^n \quad [7]$$

K_0 was obtained from one-dimensional compression tests on MSW samples using a 400-mm diameter dual-purpose landfill bioreactor and compression cell (LCC) capable of measuring changes in horizontal stress. Further details of the LCC and the estimation of K_0 from measured changes in horizontal stress can be found in Singh and Fleming (2008a). A constant value of K_0 equal to 0.40 was used in the finite element analyses, corresponding to a value of 0.29 for the Poisson's ratio of MSW and consistent with published values of K_0 (e.g. Landva et al. 2000) and ν' (e.g. Matasovic and Kavazanjian 1998; Dixon et al. 1999; Kavazanjian 2006) for MSW.

Values of K , n and R_f were obtained from laboratory testing of MSW conducted by the authors as well as laboratory testing data from published literature (Singh et al. 2008). The authors' laboratory testing program comprised triaxial testing of large-diameter samples of intact as well as recompacted MSW samples. Published triaxial test data were extracted from Jessberger and Kockel (1993), Kockel (1995), Grisolia et al. (1995), Machado et al. (2002), Caicedo et al. (2002), and Vilar and Carvalho (2004) by digitization of their deviatoric stress vs. axial strain curves. Equation (4) was then used

for the analysis of data from triaxial tests in order to obtain K , n and R_f values. More than 50 individual triaxial compression tests representing 12 different test series were evaluated using this approach. The values estimated for the parameters K , n and R_f are presented in Table 6-1. Upper and lower limits on the mean values of K , n and R_f at 90% confidence level are also shown in Table 6-1. Further details regarding this testing and analysis can be found in Singh et al. (2008). The estimated values of K , n and K_0 were used in Equation (7) to establish a lower and upper bound of typical modulus profile with depth for MSW.

6.4.2 Estimation of Unit weight

The unit weight of MSW is a function of the effective confining stress, which increases as the height of the landfill is increased. This increase in unit weight with increasing landfill height may have a significant effect on the stress-deformation behaviour of MSW because it influences the stress distribution within the waste body. It is important, therefore, to account for the variation of unit weight with depth in order to obtain accurate estimates of the maximum lateral deformation within a landfill.

Published data on the in-situ unit weight of MSW show considerable scatter from one site to another. Higher values of unit weight are generally associated with landfills having a greater proportion of daily or interim cover soil and landfills with higher moisture content (Zekkos et al. 2006); however, information on cover soil content and moisture content is often not reported in published literature and this could be one of the reasons for the scatter in the reported unit weight values. It is worth noting that regardless

of the scatter in reported unit weight values, the trend of unit weight values increasing with depth has been observed consistently (Zekkos et al. 2006).

Table 6-1 Summary of hyperbolic model parameters K , n and R_f for MSW estimated from laboratory test results (after Singh et al. 2008)

| Reference Study | | Estimated hyperbolic parameters | | |
|---|----|---------------------------------|-----------|-------------|
| | | n | K | $*R_f$ |
| Vilar and Carvalho (2004) | CD | 0.83 | 29 | 0.70 |
| | CU | 1.05 | 28 | 0.91 |
| Machado et al. (2002) | | 1.26 | 25 | 0.72 |
| Caicedo et al. (2002) | | 0.31 | 68 | 0.90 |
| Jessberger and Kockel (1993) | | 0.39 | 42 | 0.33 |
| Kockel (1995) | | 0.76 | 55 | 0.55 |
| Grisolia et al. (1995) | | 0.61 | 12 | 0.53 |
| Authors study using samples from Spadina landfill, Saskatoon, Canada | R | 0.65 | 34 | 0.68 |
| | I | 0.53 | 75 | 0.87 |
| | LC | 0.56 | 44 | 0.86 |
| Authors study using samples from Brockwest landfill, Ontario, Canada | R | 0.87 | 93 | 0.92 |
| | I | 1.12 | 58 | 0.82 |
| Mean | | 0.75 | 47 | 0.73 |
| Standard deviation | | 0.29 | 24 | 0.18 |
| Standard error of mean | | 0.08 | 7 | 0.05 |
| using confidence level of 90% for the mean of the hyperbolic parameters | | | | |
| Upper confidence limit | | 0.88 | 58 | 0.82 |
| Lower confidence limit | | 0.61 | 36 | 0.64 |

Note: R - Recompacted, I - Intact, LC - statically compacted in compression cell

* Average value from a series of tests for each study

Published data on the unit weight of MSW from various American landfills, such as the OII landfill (Kavazanjian et al. 1999) and the Tri-Cities landfill (Zekkos et al. 2006) indicate a non-linear relationship between the unit weight and the effective confining stress. Profiles of unit weight vs. depth suggested by Kavazanjian (1995) and later revised by Kavazanjian (1999) have been cited frequently in the literature. Zekkos et al. (2006) have proposed a hyperbolic relationship between the unit weight and the depth of the landfill represented by Equation (8) below:

$$\gamma = \gamma_i + \frac{z}{\alpha + \beta z} \quad [8]$$

where γ_i is the near-surface in-place unit weight (in kN/m³), z is the depth (in m), and α (in m⁴/kN) and β (in m³/kN) are hyperbolic curve-fitting parameters. Parameter α represents the near-surface rate of increase of unit weight with depth; its value typically lies between 0 and 10. Parameter β is the inverse of the difference between the maximum (asymptotic) unit weight of MSW and γ_i ; its value typically lies between 0 and 1.

Based on the compaction effort and the amount of daily cover soil present within a landfill, Zekkos et al. (2006) have recommended three sets of γ_i , α and β values corresponding to low, typical and high values of unit weight (Figure 6-3). These three sets of γ_i , α and β values were used in this study as input for the finite element analyses. Using the unit weight vs. depth profiles shown in Figure 6-3, a unit weight value corresponding to the overburden stress at full height of the landfill was assigned at

mid-height of each layer of MSW. This approach has also been suggested by Penman et al. (1971) for the estimation of deformations in heterogeneous embankments.

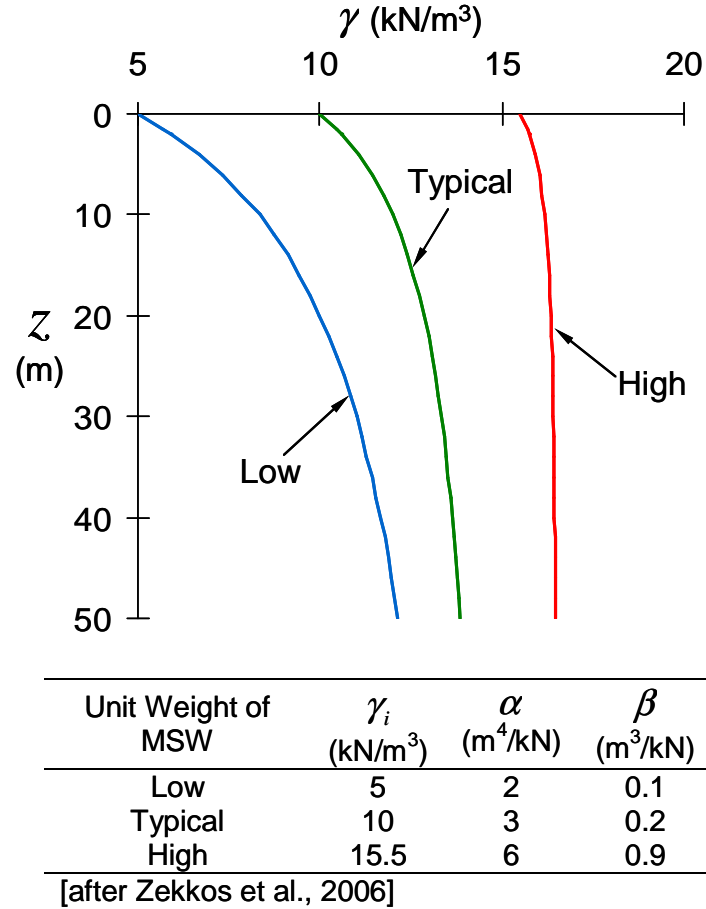


Figure 6-3 Range of values of unit weight profiles used in the development of the design chart

6.4.3 Estimation of shear strength parameters

The values of shear strength parameters c' and ϕ' were estimated using statistical analysis of data obtained from large triaxial tests on intact and recompacted MSW samples (150 mm and 200 mm diameter) conducted by the authors; along with data from published studies on laboratory and field testing of MSW. The estimated values of c' and

ϕ' are presented in Table 6-2. Upper and lower confidence limits on the mean value of c' and ϕ' at 90% confidence level are also shown in Table 6-2.

Table 6-2 Summary and statistical analysis results of shear strength parameters for MSW estimated from published literature

| Reference | Shear Strength Parameters | | Method of estimation |
|---------------------------------|---------------------------|-------------|--|
| | c' (kPa) | ϕ' (°) | |
| Cowland et al. (1993) | 10 | 25 | Back analysis of deep trench cut in waste |
| Caicedo et al. (2002) | 67 | 23 | Large DS, pressure phicometer |
| Edincliler et al. (1996) | 27 | 42 | DS |
| Eid et al. (2000) | 25 | 35 | Large DS and back analysis of failed slopes |
| Gabr & Valero (1995) | 17 | 34 | Small CU triaxial (values at 20% axial strain) |
| Grisolia et al. (1995) | 2-3 | 15-20 | Large Triaxial (at 10-15% axial strain) |
| Grisolia et al. (1995) | 10 | 30-40 | Large Triaxial (at 10-15% axial strain) |
| Harris et al. (2006) | 9-14 | 20-29 | DSS, DS, Large CU triax |
| Houston et al. (1995) | 5 | 33-35 | Large DS on undisturbed samples |
| Jessberger and Kockel (1995) | 0 | 31-49 | Both large and small Triaxial |
| Kavazanjian et al. (1995) | 24 | 0 | For normal stress up to 30 kPa |
| Kavazanjian et al. (1995) | 0 | 30 | For normal stress more than 30 kPa |
| Landva & Clark (1986) | 10-23 | 24-42 | DS on waste from various Canadian landfills |
| Landva & Clark (1990) | 0-23 | 24-41 | DS |
| Mahler & De Lamare Netto (2003) | 2.5-4 | 21-36 | DS |
| Mazzucato et al. (1999) | 43 | 31 | Large DS |
| Pelkey et al. (2001) | 0 | 26-29 | Large DS |
| Siegel et al. (1990) | 0 | 39-53 | DS. At 10 % shear displacement; c' assumed zero |
| Stoll (1971) | 0 | 24-42 | Small triaxial |
| Vilar & Carvalho (2002) | 39.2 | 29 | At natural water content (20% strain) |
| Vilar & Carvalho (2002) | 60.7 | 23 | Saturated sample(20% strain) |
| Whitian et al. (1995) | 10 | 30 | Large DS |
| Zekkos et al. (2007) | | 36-41 | Triax- for confining pressure of 200 kPa |
| Zwanenburg et al. (2007) | | 35-37 | Large Triaxial |
| Singh et al. (2007) | 0-8.4 | 35-47 | Large Triaxial (I and R from Brock West landfill) |
| Singh et al. (2008) | 16-36 | 21-41 | Large Triaxial from Spadina landfill (I, R and statically compacted and degraded in LCC) |
| Mean | 16 | 31 | |
| Standard deviation | 18 | 9 | |
| Standard error of mean | 3 | 2 | |
| Upper confidence limit | 22 | 34 | |
| Lower confidence limit | 11 | 29 | |

Note: DS- Direct Shear test, CU- Consolidated undrained triaxial test, I -Intact, R-Recompacted
LCC- dual purpose landfill compression cell and bioreactor

Shear strength parameters were also estimated from stochastic modelling. The purpose of conducting stochastic modelling was to justify the use of an ‘equivalent’ homogeneous material model (NLEH model) as an analogue to multi-component system for simulating the overall bulk stress-deformation behaviour of MSW. A brief overview of stochastic modelling work carried out by the authors is provided in following section.

Determination of c' and ϕ' using stochastic numerical modelling was a three-step process. The first step involved characterization of MSW into four major constituent groups on the basis of their similarity in influencing the overall mechanical behaviour of MSW. Accordingly, four major constituent groups were identified with each group containing material with similar mechanical properties. Table 6-3 lists the assigned material properties to each constituent group. It was noted that not all constituents classified under Group D provide reinforcing effect; therefore, the Group D constituents were further classified into two subgroups: (a) those providing reinforcing effect such as plastics, corrugated boards, textiles, tires and rubber; and (b) those not providing any reinforcing effect such as newspaper and constituents smaller than 40 mm. Linear elastic bar elements were used to model those constituents classified under Group D that are capable of providing reinforcing effect. The second step involved stochastic modelling using the Monte Carlo method by conducting finite element ‘unit cell’ simulations. A typical finite element unit cell used for conducting stochastic modelling is shown in Figure 6-4.

Four random variables were defined as: (i) proportions of individual constituent groups; (ii) elastic properties of the individual constituent groups; (iii) shear strength properties of the individual constituent groups; and (iv) relative positioning of the

individual constituent groups within MSW matrix. The Monte Carlo method was used for generating the random variables. Random variations in relative proportions and positioning of the constituents were achieved by manipulating the material properties of individual finite elements. Such manipulation was accomplished by editing SIGMA/W input files, which have XML-compatible structure.

Table 6-3 Elastic and shear strength properties and relative proportions of MSW constituent groups used in stochastic modelling

| Group | Property | Constituents | Range (% by weight) | Elastic parameters | | Shear strength parameters | |
|-------|--------------------------------|--|------------------------|--------------------|-----------|---------------------------|----------------|
| | | | | E' (MPa) | ν' | c' (kPa) | ϕ' (°) |
| A | Rigid and incompressible | Metals, glass, wood, ceramic | 5-17 | 75-110 | 0.26-0.49 | 20-30 | 33-39 |
| B | Soil-like material | Demolition waste, cover soil, ash | 6-25 | 10-20 | 0.25-0.33 | 0 | 25-30 |
| C | Degradable & compressible | Food, yard & animal waste | 16-43 | 0.5-0.7 | 0.05-0.15 | 2-7 | 25-30 |
| D | Reinforcing & tensile elements | Paper, cardboard, flexible & rigid plastics, tires | 16-60 | 1.5-3 | 0.28-0.32 | 4-8 | 22-28 |

The third step involved the extraction of c' and ϕ' values from the results of each set of three simulations conducted at 100 kPa, 200 kPa and 300 kPa effective cell pressures. The stress paths leading up to the t_{ult} -point for each of the three effective cell pressures were plotted and a Mohr-Coulomb failure line was fitted through the points. The values of cohesion intercept c' and angle of friction ϕ' were obtained from the slope and the intercept of the fitted Mohr-Coulomb failure line. Further details about stochastic numerical modelling and estimation of shear strength parameters can be found in Singh et al. (2007a).

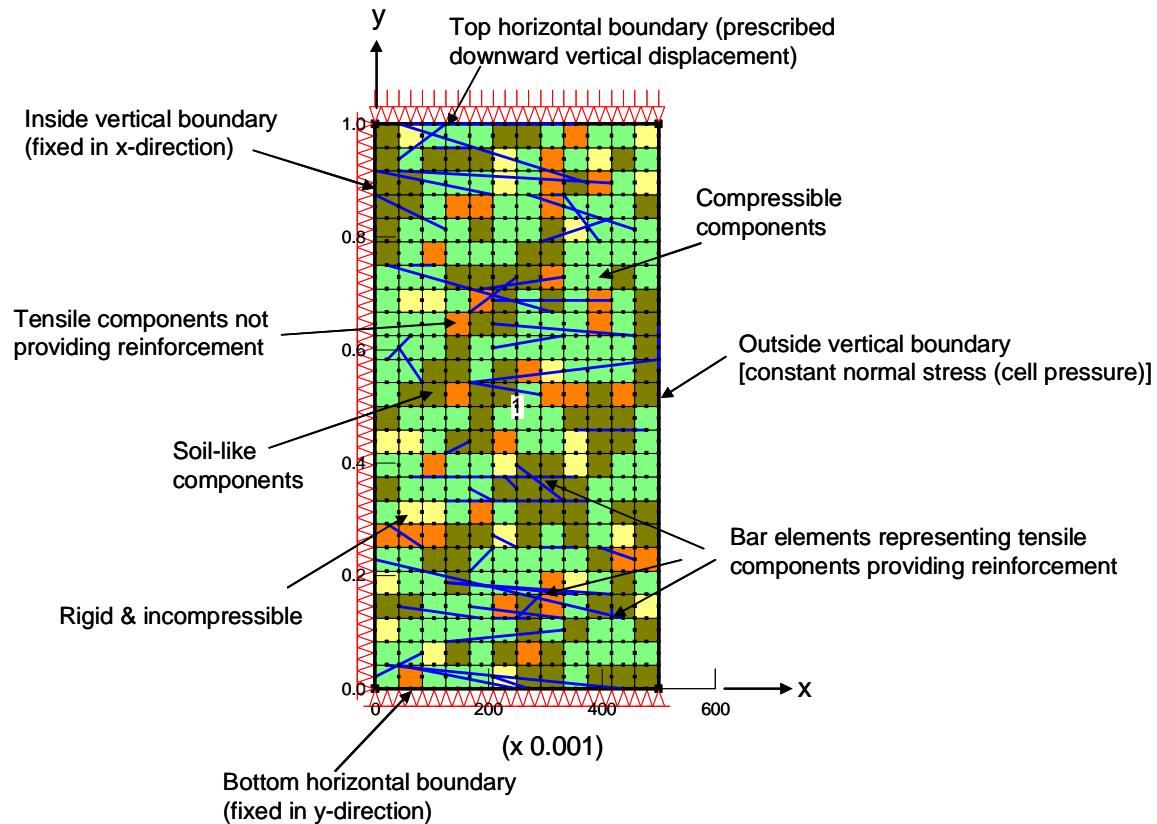


Figure 6-4 A typical finite element 'unit cell' mesh used in the stochastic modelling of MSW behaviour

The mean values of 'equivalent' shear strength parameters c' and ϕ' estimated using stochastic modelling are presented in Table 6-4. For comparison, weighted mean values of c' and ϕ' are presented in Table 6-4. These weighted mean values were obtained by multiplying the values of c' and ϕ' for each constituent group by the proportion of that constituent group.

Statistical analysis of stochastic modelling results confirmed that the values of c' and ϕ' were normally distributed. Upper and lower confidence limits on the mean values of c' and ϕ' at 90% confidence level are also shown in Table 6-4. It can be seen from Table 6-4 that the mean values of c' and ϕ' obtained from stochastic modelling are

higher than their weighted values. This could be attributed to the interlocking of waste components in the matrix, resulting in higher overall shear strength. It should be pointed out that such interlocking is likely influenced by the variations in shape of the waste components, which was not modelled in the present study. As such, further work is required to confirm the increase in shear strength of MSW due to interlocking effect.

Table 6-4 Summary and statistical analysis results of shear strength parameters for MSW estimated from stochastic modelling

| | Shear Strength Parameter | |
|---|--------------------------|-------------|
| | c' (kPa) | ϕ' (°) |
| Estimated Mean | 16.4 | 33 |
| Weighted Mean | 3.2 | 26.1 |
| Standard deviation | 8 | 5 |
| Standard error of mean | 1 | 1 |
| using confidence level of 90% for the mean of the strength parameters | | |
| Upper confidence limit | 18 | 34 |
| Lower confidence limit | 14 | 32 |

Results from stochastic modelling and comparison of data presented in Table 6-2 and Table 6-4 reveal some important observations. It is interesting to note that while individual constituent groups were modeled using an elastic-perfectly plastic constitutive model and, therefore, had well-defined yield (failure) points, the overall stress-strain behaviour as shown in Figure 6-5 did not exhibit a well-defined yield point and resembled the stress-strain response of a NLEH model.

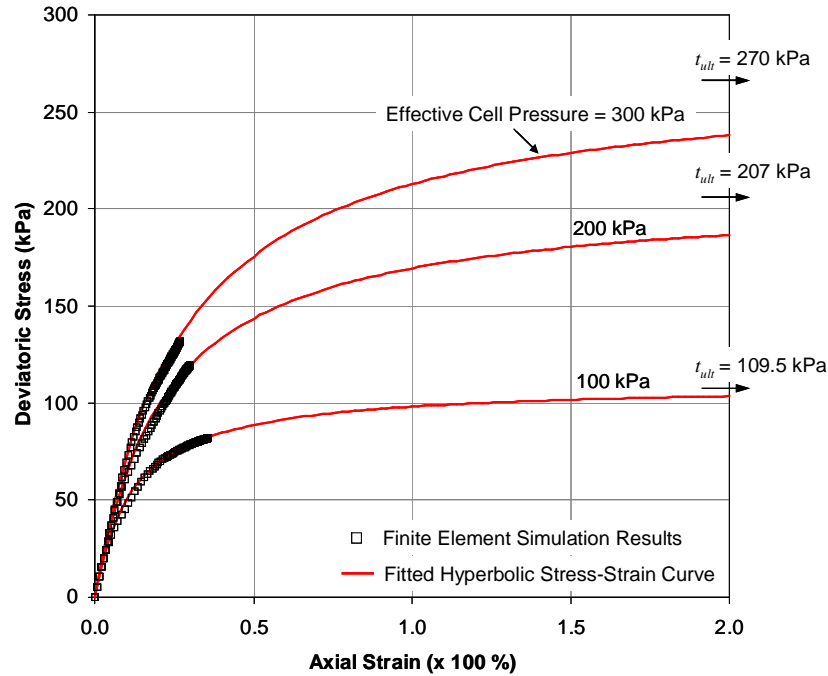


Figure 6-5 Method of estimation of t_{ult} by extrapolating numerical results using hyperbolic curves

The mean values of c' and ϕ' from real test data (Table 6-2) are quite close to mean values of c' and ϕ' from stochastic modelling (Table 6-4), although the values of c' and ϕ' from real test data show greater deviation from the mean values. This deviation could be because of differences in testing protocols, sample type, unit weight, waste composition and age and interpretation of results. Furthermore, the upper and lower confidence limits of c' and ϕ' from stochastic modelling lie within the upper and lower confidence limits from real test data. These findings suggest that a multi-component composite material may be modeled as an “equivalent” homogeneous material exhibiting a non-linear hyperbolic stress-strain behaviour and, therefore, validate the use of a NLEH model to simulate the overall or ‘equivalent’ stress-strain behaviour of MSW.

6.4.4 Range of material properties of MSW for the development of design chart

The range of material properties, obtained from the analyses presented above and bound by the lower and upper confidence limits at 90% confidence level, are presented in Table 6-5 and used in the development of design chart.

Table 6-5 Range of hyperbolic model input parameters used in the development of the design chart

| Parameter | K | n | R_f | c' (kPa) | ϕ' (°) |
|-------------------------------------|-----|------|-------|------------|-------------|
| Upper confidence limit ^a | 58 | 0.88 | 0.82 | 22 | 34 |
| Lower confidence limit ^a | 36 | 0.61 | 0.64 | 11 | 29 |

^aUsing confidence level of 90% for the mean

6.5 Parametric study

6.5.1 Methodology

The parametric study involved conducting finite element simulations of landfill at five different heights, seven different side slopes, and three different unit weight profiles as presented in Table 6-6. Each simulation was done using both the lower- and the upper-bound values of the five input parameters: K , n , c' , ϕ' , and R_f given in Table 6-5. A total of 210 finite element simulations were conducted. For all the simulations, the bottom width of the landfill was kept constant and the foundation soil was modeled using a 10-m thick layer of linear elastic material ($E' = 20$ MPa; $\nu' = 0.33$). The results of these

simulations are presented in the next section in terms of the effect of each parameter on the value of maximum horizontal displacement ($\delta_{h_{\max}}$) within the landfill.

Table 6-6 Range of parameters used in the parametric study for the development of the design chart

| Parameter | Range |
|---------------------------|-----------------------------------|
| Height (m) | 20, 30, 40, 50, 60 |
| Sideslope (Cot θ) | 2.0, 2.5, 3.0, 3.5, 4.0, 4.5, 5.0 |
| Unit weight | Low, Typical, High |

[Note: θ - Inclination of sideslope with horizontal]

6.6 Results

6.6.1 Effect of height and sideslope on lateral deformation

The effect of height of the landfill H on the lateral deformation ($\delta_{h_{\max}}$) was studied by conducting five simulations with same side-slope but different H values. The effect of the side-slope of the landfill $\cot(\theta)$ on $\delta_{h_{\max}}$ was studied by conducting seven simulations with same H but with different $\cot(\theta)$ values. The results are presented in Figure 6-6. As seen from Figure 6-6(a), increasing the height of the landfill resulted in an increase in $\delta_{h_{\max}}$. Also, the rate of increase of $\delta_{h_{\max}}$ with respect to H was greater for higher landfills, which can be attributed to reduction in stiffness with increasing deviatoric stress.

A landfill with gentler side-slope (i.e. higher $\cot(\theta)$) results in lower δh_{\max} as seen from Figure 6-6(b). This is an expected result since gentler side slopes have higher stiffness because of lower deviatoric stresses.

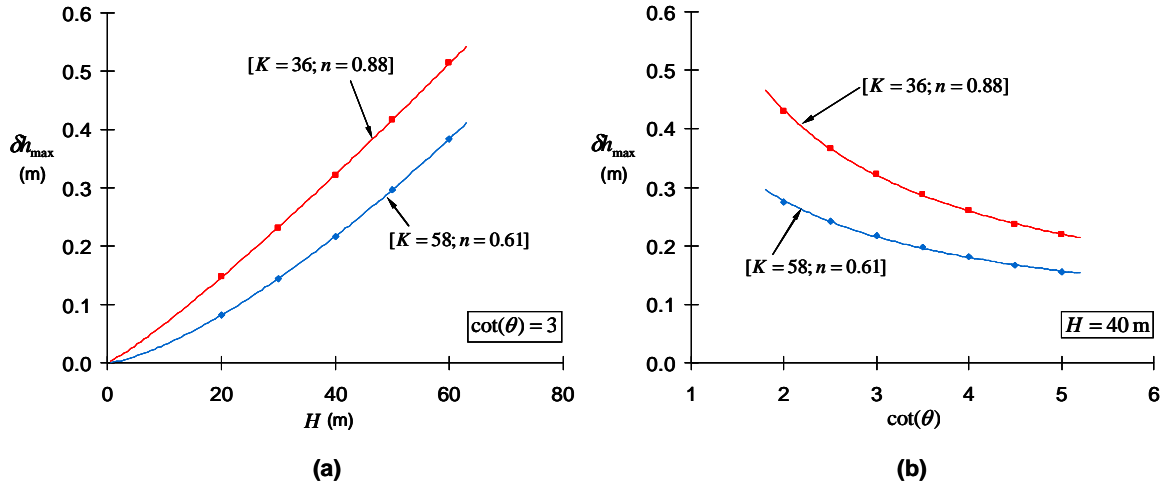


Figure 6-6 Effect of (a) height of the landfill H , and (b) horizontal stretch of the side slope of the landfill $\cot(\theta)$ on maximum horizontal displacement δh_{\max}

6.6.2 Effect of mechanical properties of MSW

6.6.2.1 Effect of K, n and R_f

Table 6-7 lists the values of maximum horizontal displacement δh_{\max} for eight different combinations of lower- and upper-bound values of parameters K , n , and R_f ($H = 20$ m; $\cot(\theta) = 4$ for the landfill). It is evident from Table 6-7 that R_f has no effect on the magnitude of maximum horizontal displacement. One explanation for this could be that at full height, the stress state of the entire landfill is sufficiently far from failure. It is also worth noting that the lowest value of δh_{\max} is obtained for the combination of an upper-bound value of K and a lower-bound value of n whereas the highest value of δh_{\max} is

obtained for the combination of lower-bound value of K and an upper-bound value of n . This result may appear to be counter-intuitive because the highest values of δh_{\max} should correspond to lower-bound values of both K and n and vice versa; however, the result makes perfect sense when examined in the light of the magnitude of effective confining stress σ'_3 . It was noted from the results of the finite element analyses that the magnitude of σ'_3 at the location of maximum horizontal displacement within the landfill was between 10 and 60 kPa (depending on the height of the landfill). At values of σ'_3 less than 100 kPa, it is the combination of lower-bound K and upper-bound n that gives the lowest value of Young's modulus and, therefore, the highest value of δh_{\max} (Figure 6-7).

6.6.2.2 Effect of c' and ϕ'

Values of c' and ϕ' appear to have no effect on the magnitude of δh_{\max} . The magnitude of δh_{\max} obtained from simulations using lower-bound values of c' and ϕ' was the same as that obtained from simulations using upper-bound values of c' and ϕ' , which indicated that at full height, the stress state within the landfill is sufficiently far from failure. It was decided, therefore, to use the lower-bound values of c' and ϕ' for all simulations.

6.6.2.3 Effect of Unit weight

Figure 6-8 shows the variation of δh_{\max} with near-surface in-place unit weight γ_i for a 40 m high landfill with 3H to 1V side slopes for the two combinations of K and n that yield the highest and lowest values of Young's modulus.

Table 6-7 Magnitudes of maximum horizontal displacement for various combinations of parameters K , n and R_f ($H = 20$ m; $\cot(\theta) = 4$)

| n | K | R_f | δh_{\max} (m) |
|------|-----|-------|--------------------------|
| 0.61 | 36 | 0.64 | 0.08 |
| 0.61 | 36 | 0.82 | 0.08 |
| 0.61 | 58 | 0.64 | 0.06 |
| 0.61 | 58 | 0.82 | 0.06 |
| 0.88 | 58 | 0.64 | 0.07 |
| 0.88 | 58 | 0.82 | 0.07 |
| 0.88 | 36 | 0.64 | 0.11 |
| 0.88 | 36 | 0.82 | 0.11 |

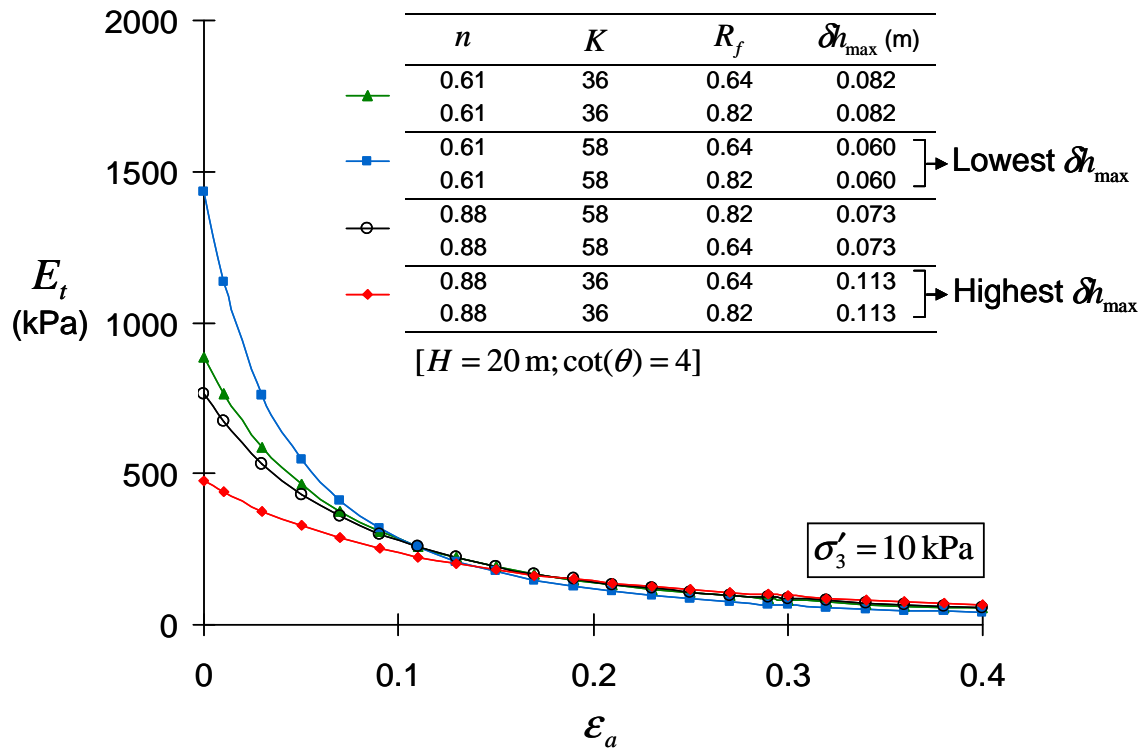


Figure 6-7 Effect of combinations of parameters K , n and R_f on maximum horizontal displacement δh_{\max} for effective confining stress $\sigma'_3 < 100$ kPa

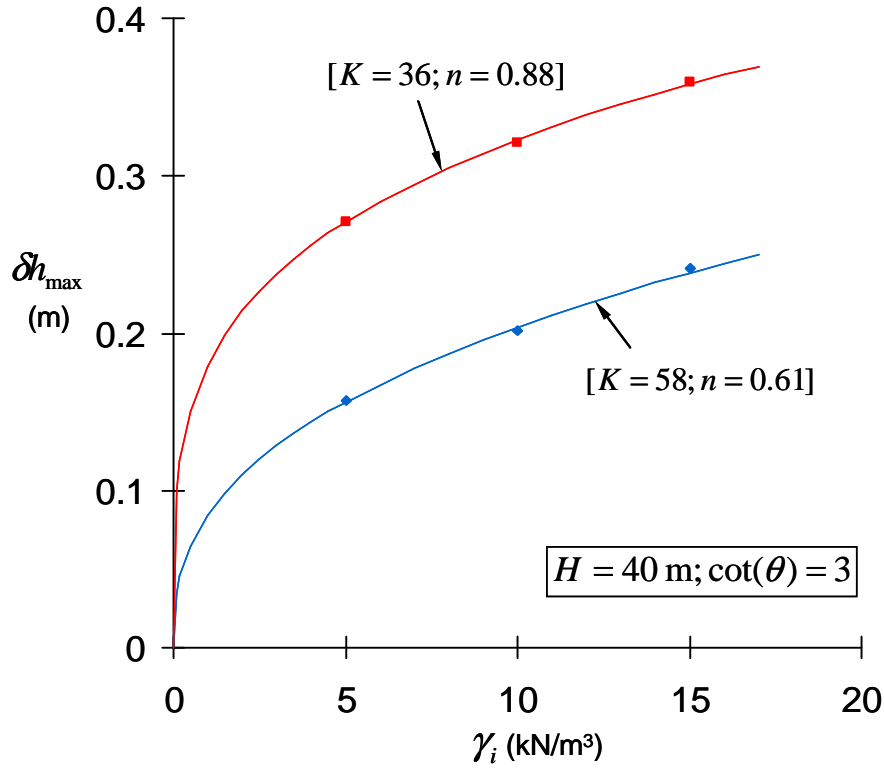


Figure 6-8 Effect of unit weight (represented by near-surface unit weight γ_i) on maximum horizontal displacement

It can be seen from Figure 6-8 that δh_{\max} increases as γ_i increases; however, the rate of increase of δh_{\max} with respect to γ_i is smaller for higher values of γ_i . An increase in unit weight results in an increase in overburden stress, resulting in more horizontal displacement; however, an increase in overburden stress also results in increase in effective confinement, resulting in higher stiffness and a reduction in horizontal displacement. Consequently, the rate of increase in δh_{\max} with respect to γ_i drops at higher values of γ_i .

6.7 Design Chart

6.7.1 Presentation

It was shown in Figure 6-6 that δh_{\max} increases as the height of the landfill H is increased and decreases as the side-slope of the landfill decreases (i.e. increasing $\cot(\theta)$). Regression analysis of the δh_{\max} vs. H and δh_{\max} vs. $\cot(\theta)$ results revealed that δh_{\max} is directly proportional to H and inversely proportional to the square root of $\cot(\theta)$. When the results of finite element analyses are plotted in terms of δh_{\max} and the ratio $H / \sqrt{\cot(\theta)}$, they appear to plot on two unique curves corresponding to the upper-bound and lower-bound combinations of parameters K and n as shown in Figure 6-9.

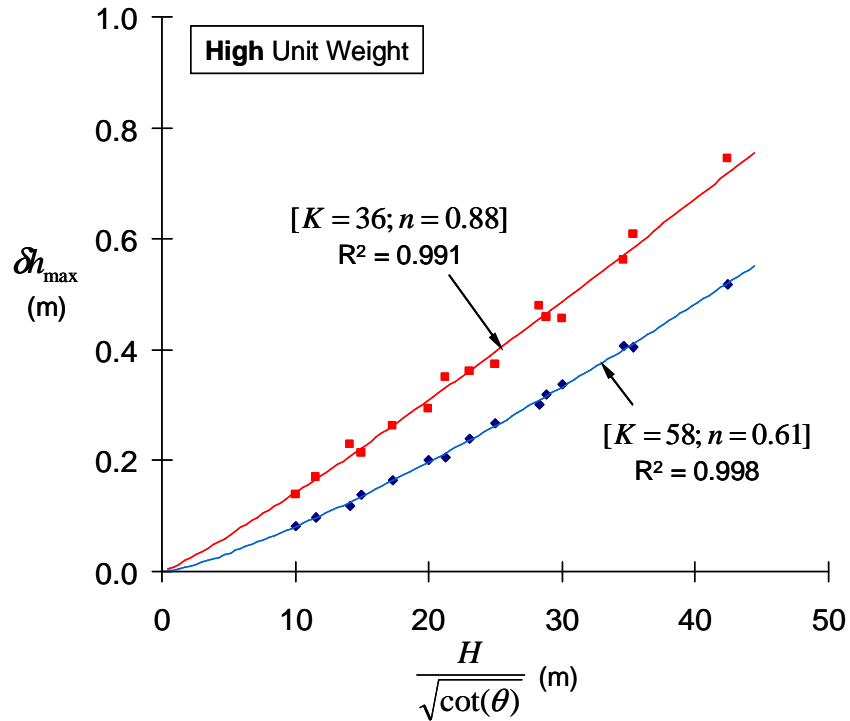


Figure 6-9 Results of the parametric study plotted in $\delta h_{\max} - (H / \sqrt{\cot(\theta)})$ space (all analyses with high density)

The goodness of fit for the two curves was excellent as indicated by R^2 values very close to 1. It was decided, therefore, to present the design chart in terms of three sets of upper-bound and lower-bound δh_{\max} vs. $H/\sqrt{\cot(\theta)}$ curves (one set each for low, typical and high unit weight) as shown in Figure 6-10. For each curve shown in Figure 6-10, R^2 value was greater than or equal to 0.99. The proposed design chart is easy to use and results in quick estimates of the lowest and highest values of the maximum horizontal displacement expected in a landfill of height H and horizontal stretch of sideslope $\cot(\theta)$.

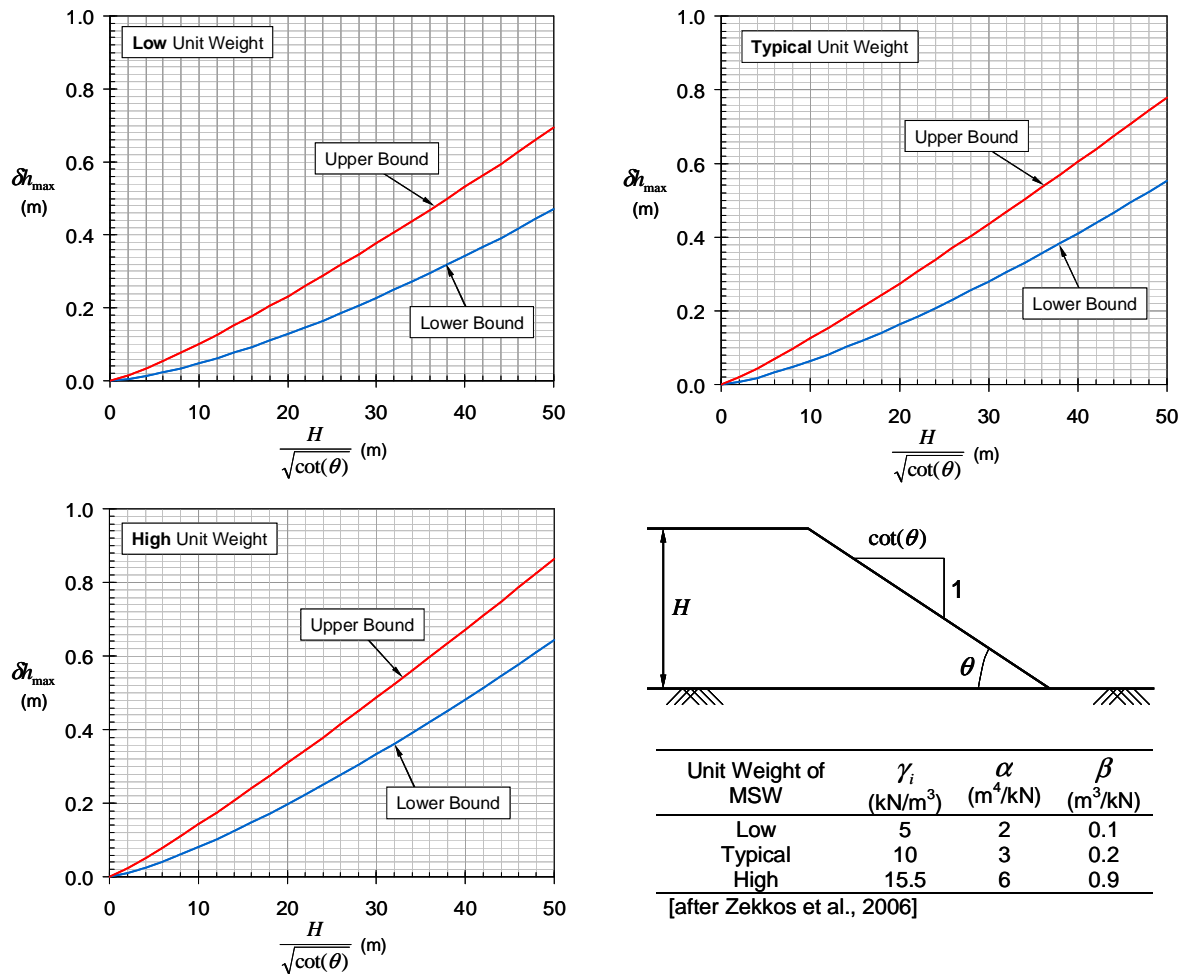


Figure 6-10 Design chart for the estimation of maximum horizontal displacement δh_{\max}

6.7.2 Validation

The validity of the proposed design chart can be established using records of the height of the landfill and its maximum horizontal displacement; however, such records are rarely kept and it is very difficult to find these in published literature. The authors have been involved with continuous monitoring of horizontal displacements at the Brock West landfill in Ontario, Canada. The monitoring of horizontal displacements of the south slope of the landfill began in 2004 after it was noticed that a few of the gas laterals were severely distorted (Figure 6-11).



Figure 6-11 A distorted gas lateral located on the south slope of the Brock West landfill, Ontario

Although horizontal displacement of the south slope was occurring prior to 2004, there are no documented records of these displacements. Data from four inclinometers installed on the south slope showed an increase in horizontal displacement from 0.04 m in October 2004 to 0.23 m in September 2006. Using the design chart, the expected range of maximum horizontal displacement at Brock West landfill ($H = 60$ m; $\cot(\theta) = 4$;

Typical unit weight) is 0.28 m to 0.44 m. Given that, the horizontal displacements are ongoing at this landfill, this range of maximum horizontal displacement estimated using the proposed design chart is quite reasonable.

6.8 Conclusions

In this paper, an easy-to-use design chart for the estimation of maximum horizontal displacement within a landfill using only the height and the horizontal stretch of the side slope of the landfill has been presented. The design chart was developed using results of a finite element parametric study in which the behaviour of the municipal solid waste was modelled using a non-linear elastic hyperbolic model. The development of the design chart took into account non-linear variation in unit weight as well as Young's modulus of MSW with depth. Mechanical properties of MSW used in the development of the design chart, i.e. non-linear stiffness, shear strength and unit weight of MSW, were obtained using statistical analysis of laboratory testing data as well as using stochastic numerical modelling. For each mechanical property, upper and lower confidence limits at 90% confidence level were used to establish the range of expected maximum horizontal displacement. The range of maximum horizontal displacement estimated using the proposed design chart were reasonably close to measured maximum horizontal displacement at the Brock West landfill site in Ontario, Canada. The design chart is easy to use and provides landfill engineers with quick estimates of maximum horizontal displacements within a landfill, which are crucial for ensuring satisfactory functioning of ancillary services such as the gas collection system.

6.9 References

- Beaven, R.P. and Powrie, W. 1995. Hydrogeological and geotechnical properties of refuse using a large scale compression cell. Proc. 5th International Waste Management and Landfill Symposium, Sardinia, 745-760.
- Caicedo, B., Yamin, L., Giraldo, E. and Coronado, O. 2002. Geomechanical properties of municipal solid waste in Dona Juana sanitary landfill. Proc. 4th International Congress on Environmental Geotechnics, Brazil, 1: 177-182.
- Castelli, F., and Maugeri, M. 2008. Experimental analysis of waste compressibility. Geotechnical Special Publication, ASCE, 177: 208-215.
- Cowland, J.W., Tang, K.Y. and Gabay, J. 1993. Density and strength properties of Hong Kong refuse. Proc. 4th International Waste Management and Landfill Symposium, Sardinia, 1433-1446.
- Dixon, N., Jones, D.R.V. and Whittle, R.W. 1999. Mechanical properties of household waste: In-situ assessment using pressuremeter. Proc. 7th International Waste Management and Landfill Symposium, Sardinia, 453-460.
- Dixon, N. and Langer, U. 2006. Development of a MSW classification system for the evaluation of mechanical properties. Waste Management, 26: 220-232.
- Duncan, J.M. and Chang, C.Y. 1970. Nonlinear analysis of stress and strain in soils. Journal of the Soil Mechanics and Foundation Engineering Division, ASCE, 96 (SM5): 1629-1653.
- Edinçliler, A. Benson, C. H. and Edil, T. B. 1996. Shear strength of municipal solid waste. Interim Report - Year 1, Environmental Geotechnics Report 96-2, Department of Civil and Environmental Engineering, University of Wisconsin, Madison.
- Eid, H.T., Stark, T.D., Evans, W.D. and Sherry, P.E. 2000. Municipal solid waste slope failure – I: Waste and foundation soil properties. Journal of Geotechnical and Geoenvironmental Engineering, ASCE, 126(5): 397-407.

- GSI, 2007. SIGMA/W 2007 Stress-deformation analysis software. Geo-Slope International (GSI). See <http://www.geo-slope.com/products/sigmaw2007.aspx> [accessed on April 4, 2008].
- Gabr, M.A. and Valero, S.N. 1995. Geotechnical Properties of Municipal Solid Waste. *Geotechnical Testing Journal*, ASTM, 18(2): 241-251.
- Grisolia, M., Napoleoni, Q. and Tancredi, G. 1995. Contribution to a technical classification of MSW. *Proc. 5th International Waste Management and Landfill Symposium*, Sardinia, 703-710.
- Harris, J.M., Shafer, A.L., DeGroff, L., Hater, G.R., Gabr, M. and Barlaz, M.A. 2006. "Shear strength of degraded reconstituted municipal solid waste". *Geotechnical Testing Journal*, ASTM, 29(2):1-8.
- Houston, W.N., Houston, S.L., Liu, J.W., Elsayed, A. and Sanders, C.O. 1995. In-situ testing methods for dynamic properties of MSW landfills. *Geotechnical Special Publication*, ASCE, 54: 73-82.
- Janbu, N. 1963. Soil compressibility as determined by oedometer and triaxial tests. *Proc. 3rd European Conference on Soil Mechanics*, Wiesbaden, Germany, 1:19-25.
- Jessberger, H.L. and Kockel, R. 1993. Determination and assessment of the mechanical properties of waste materials. *Proc. 4th International Waste management and Landfill Symposium*, Sardinia, 1383-1392.
- Kavazanjian, E. 2006. Waste mechanics: Recent findings and unanswered questions. *Geotechnical Special Publication*, ASCE, 148: 34-54.
- Kavazanjian, E. 1999. Seismic design of solid waste containment facilities. *Proc. 8th Canadian Conference on Earthquake Engineering*, Vancouver, 51- 89.
- Kavazanjian, E. 1995. Evaluation of MSW properties for seismic analysis. *Geotechnical Special Publication*, ASCE , 46: 1126-1141.
- Kavazanjian, E., Matasovic, N. and Bachus, R.C. 1999. Large diameter static and cyclic laboratory testing of municipal solid waste. *Proc. 7th International Waste Management and Landfill Symposium*, Sardinia.

- Kockel, R. 1995. Scherfestigkeit von Mischabfall im Hinblick auf die Standsicherheit von Deponien. PhD thesis, Mitteilungen Heft 133, Leichtweiß-Institut für Wasserbau, Technische Universität Braunschweig.
- Kondner, R.L. 1963. Hyperbolic stress-strain response: Cohesive soils. *Journal of the Soil Mechanics and Foundation Division, ASCE*, 89(SM1): 115-141.
- Landva, A.O. and Clark, J.I. 1986. Geotechnical testing of wastefills. *Proc. 39th Canadian Geotechnical Conference, Ottawa*, 371-385.
- Landva, A.O. and Clark, J.I. 1990. Geotechnics of MSW fills. *Geotechnics of MSW Fills – Theory and Practice*. A. Landva and G.D. Knowles (Eds.), ASTM STP 1070, 86-103.
- Landva, A.O., Valsangkar, A.J. and Pelkey, S.G. 2000. Lateral earth pressure at rest and compressibility of municipal solid waste. *Canadian Geotechnical Journal*, 37: 1157-1165.
- Machado, S.L., Carvalho, M.F. and Vilar, O.M. 2002. Constitutive model for municipal solid waste. *Journal of Geotechnical and Geoenvironmental Engineering, ASCE*, 128(11): 940-951.
- Mahler, C. F. and De Lamare Netto, A. 2003. Shear resistance of mechanical biological pre-treated domestic urban waste. *Proc. 9th International Waste Management and Landfill Symposium, Sardinia (on CD Rom)*.
- Manassero, M., Van Impe, W. F. and Bouazza, A. 1997. Waste Disposal and Containment. *Proc. 2nd International Congress on Environmental Geotechnics, Osaka*, 3: 1425-1474.
- Matasovic, N. and Kavazanjian, E. 1998. Cyclic characterization of OII landfill solid waste. *Journal of Geotechnical and Geoenvironmental Engineering, ASCE*, 124(3): 197-210.
- Mazzucato, A., Simonini, P. and Colombo, S. 1999. Analysis of block slide in a MSW landfill. *Proc. 7th International Waste management and Landfill Symposium, Sardinia*.

- Pelkey, S.A., Valsangkar, A.J. and Landva, A. 2001. Shear displacement dependent strength of municipal solid waste and its major constituents. *Geotechnical Testing Journal*, ASTM, 24(4): 381-390.
- Penman, A.D.M., Burland, J.B. and Charles, J.A. 1971. Observed and predicted deformations in a large embankment dam during construction. *Proc. Institution of Civil Engineers*, 49(May), 1-21.
- Siegel, R.A., Robertson, R.J. and Anderson, D.G. 1990. Slope stability investigation at a landfill in Southern California. *Geotechnics of Waste Fills – Theory and Practice*. A. Landva and G.D. Knowles (Eds.), ASTM STP 1070, 259-284.
- Singh, M.K. and Fleming, I.R. 2008. Estimation of the mechanical properties of MSW during degradation in a laboratory compression cell. *Geotechnical Special Publication*, ASCE, 177: 200-207.
- Singh, M.K. and Fleming, I.R. 2008a. Evolution of compressibility behaviour of municipal solid waste during degradation. Manuscript submitted to *Journal of Geotechnical and Geoenvironmental Engineering*, ASCE.
- Singh, M.K., Fleming, I.R. and Sharma, J.S. 2008. Application of a nonlinear stress-strain model to municipal solid waste. Manuscript submitted to *Géotechnique*.
- Singh, M.K., Sharma, J.S. and Fleming, I.R. 2007. Shear strength testing of intact and recompacted samples of municipal solid waste. Manuscript submitted to *Canadian Geotechnical Journal*.
- Singh, M.K., Fleming, I.R. and Sharma, J.S. 2007a. Estimation of mechanical properties of municipal solid waste using stochastic modelling. *Proc. 11th International Waste Management and Landfill Symposium*, Sardinia. (on CD-Rom).
- Stoll, O.W. 1971. Mechanical properties of milled refuse. *ASCE National Water Resources Engineering Meeting*, Phoenix, Arizona, 11-15.
- Thomas, S., Aboura, A.A., Gourc, J.P., Gotteland, P., Billard, H., Delineau, T., Gisbert, T., Ouvry, J.F. and Vuillemin, M. (1999). An in-situ waste mechanical

experimentation on a French landfill. Proc. 7th International Waste Management and Landfill Symposium, Sardinia.

UN. 2006. World Population Prospects: The 2004 Revision and World Urbanization Prospects: The 2005 Revision. Report by Population Division of the Department of Economic and Social Affairs of the United Nations Secretariat.

Vilar, O.M. and Carvalho, M.F. 2002. Shear strength properties of municipal solid waste. Proc.4th International Conference on Environmental Geotechnics, Lisse, The Netherlands, 59-64.

Vilar, O.M. and Carvalho, M.F. 2004. Mechanical properties of municipal solid waste. Journal of Testing and Evaluation, ASTM, 32(6):1-12.

Withiam, J.L., Tarvin, P.A., Bushell, T.D., Snow, R.E. and German, H. W. 1995. Geotechnical Special Publication, ASCE, 46: 1005-1019.

Zekkos, D.P., Bray, J.D., Kavazanjian, E., Matasovic, N., Rathje, E.M., Riemer, M.F. and Stokoe, K.H. 2006. Unit weight of municipal solid waste. Journal of Geotechnical and Geoenvironmental Engineering, ASCE, 132(10): 1250-1261.

Zwanenburg, C., Knoeff, J.G. and Hounjet, M.W.A. 2007. Geotechnical characterization of waste. Proc.11th International Waste Management and Landfill Symposium, Sardinia. (on CD Rom).

CHAPTER 7 SUMMARY AND CONCLUSIONS

This thesis presented a detailed examination of the mechanical properties of municipal solid waste and investigated the deformation mechanism in landfills, particularly those facilities equipped for rapid stabilization, recovery of landfill gas to mitigate greenhouse gas emissions and to generate power. Four research objectives were identified as: (1) develop a method for obtaining intact samples of waste and examine the significance of using intact versus recompacted samples in characterizing the stress-deformation behaviour of MSW; (2) characterize MSW shear strength and Young's modulus of elasticity from interpretation of triaxial test results and determine the parameters of a non-linear constitutive model as applied to MSW; (3) measure the evolution of compressibility behaviour of MSW with degradation and verify the mechanism of secondary compression in waste and; (4) develop a simple design chart for predicting lateral deformations in landfills. A comprehensive research plan was carried out, which broadly consisted of a review of the literature, field investigation, experimental and numerical modelling work.

An exhaustive review of the literature was carried out to understand the existing state of practical and theoretical knowledge and to identify significant knowledge gaps. This review focused primarily on the shear strength and elastic properties of waste which are required to address stability and serviceability issues in a landfill. Various sampling methods and the types of waste samples tested were also explored.

It has been observed from this review of literature that, often the samples for testing have been prepared by recompaction of waste obtained from excavation pits or from auger cuttings obtained from boreholes. It is very likely that such recompaction of waste might possibly disturb the structure of waste matrix and the orientation and entanglement of tensile/ reinforcing elements in the waste matrix. It was hypothesized that such rearrangement of waste constituents in recompacted samples might exhibit stress-strain behaviour which may be different from intact samples of waste. A method for obtaining large diameter (150mm and 200mm) intact samples of waste from deep within the landfill was developed and was successfully used to obtain intact samples from several landfills.

Consolidated undrained (CU) triaxial tests with pore pressure measurements were conducted on intact as well as recompacted samples of waste in order to evaluate stress-strain behaviour. The data were presented in terms of stress paths in $q - p'$ space and the shear strength parameters were interpreted from effective stress paths followed during shearing. The pattern of stress paths exhibited by these samples is typical of cross-anisotropic soils which exhibit a coupling between volumetric and distortional effects under undrained loading. Although, intact and recompacted samples yielded similar shear strength parameters, their pre-failure response was different. This observation is quite significant from the viewpoint of evaluating serviceability conditions within a landfill and supports the use of intact samples for establishing deformation characteristics of MSW.

The shear strength parameters estimated from stress paths drawn in $q - p'$ space, are comparable with published values. Slope stability analyses conducted using these

site-specific shear strength parameters suggests that inadequate shear strength does not adequately explain the observed movement at the Brock West landfill. It can therefore be concluded that short of failure, there may be lateral deformation sufficient to cause problems for a landfill and particularly for its buried infrastructure, and it is, therefore, important to understand the stress-deformation behaviour of MSW

From evaluation of numerous triaxial test results, both from the published literature as well as those conducted as part of this research program, it was observed that the stress-deformation behaviour of MSW can be approximated by a non-linear elastic constitutive model (such as an hyperbolic model), at least within the range of strains (0-20%) typically considered by researchers for interpretation of test data. Such an argument is supported by the fact that MSW shows large pre-failure deformations. The parameters of this model (K , n and R_f) were obtained through a statistical analysis of the data from over 50 triaxial tests carried out as part of this research and taken from the published literature. Considering the wide variability in sample composition, age, unit weight and confinement used in these tests; the estimated values of K , n and R_f were specified by an upper and a lower bound value using a 90% confidence limit. The suggested upper and lower bound values of K , n and R_f are 58 and 36; 0.88 and 0.61; and 0.82 and 0.64 respectively. It is proposed by the author that this approach provides a practical way to capture the inherent variability of material properties and accounts for the wide variability in sample composition, testing methods, degree of compaction and the effect of degradation, which are pertinent to waste.

The degradation of waste over time is expected to bring changes in its mechanical properties, potentially leading to stability and/or serviceability concerns. There is little information in the literature at this time regarding the evolution of the mechanical behaviour of waste with time and increased degree of degradation. The results from a long-term degradation test conducted using the large dual-purpose compression cell revealed that K_0 is not influenced by degradation and may be considered a constant with a value in the order of 0.4. The constrained modulus, however, appears to exhibit a slight decrease with degradation when compared with corresponding values obtained from short-term tests conducted in this study. The compressibility indices were observed to undergo significant change due to degradation, and therefore, the use of a single compressibility index may provide unrealistic estimates of settlement in landfills.

A significant finding is that the data gathered from the long term compression/degradation test tend to confirm that the mechanism of secondary compression in MSW involves an episodic process of void formation due to degradation with subsequent collapse of these voids and rearrangement of the material structure with consequent settlement.

The various aspects of this research program were ultimately compiled and used as the basis for a parametric study of horizontal deformations in a landfill slope. The resulting predictions were used to develop an easy-to-use design chart for the estimation of the maximum expected lateral displacement within a landfill. The parametric study was carried out using finite element simulations of a landfill slope in which the stress-deformation behaviour of the municipal solid waste followed a non-linear elastic hyperbolic model with upper and lower bound values for the non-linear modulus

parameters. Other key properties of MSW required to develop this design chart, (i.e. the shear strength parameters and the unit weight), were obtained using a substantial database of laboratory testing data as well as through stochastic numerical modelling. The design chart incorporates non-linear variation with depth of both the unit weight and the Young's modulus. A brief "reality check" for the resulting design chart was carried out using field monitoring results from the Brock West Landfill.

7.1 Contribution of this research to the state of Practical and Theoretical knowledge

The work presented in this thesis has enhanced the fundamental understanding of the mechanical behaviour of waste, particularly relating to pre-failure deformation and serviceability issues. The specific contributions of the proposed research are:

- (i) This study has confirmed that recompacted samples of waste may be used to obtain reasonable estimates for the shear strength parameters of municipal waste. This finding is particularly significant in light of the challenges inherent in collecting large intact samples of waste.
- (ii) An approach based upon effective stress paths obtained from shearing of samples in a CU triaxial test is proposed for estimating the shear strength parameters of waste which also established the fact that the mechanical behaviour of saturated MSW samples can be explained using the principle of effective stress.

- (iii) It is proposed that a non-linear hyperbola is an appropriate constitutive model for the stress-deformation behaviour of municipal solid waste. This finding has practical significance in terms of the ability to easily predict deformations in landfills, particularly given that this constitutive model is incorporated into various widely available numerical modelling software packages. Upper and lower bound values are established for the required input parameters for the hyperbolic model.
- (iv) A constant value of $K_o=0.4$ is proposed for municipal solid waste regardless of age or applied stress.
- (v) Test data confirm that the mechanism of secondary compression in waste involves an episodic process of void formation and growth during degradation followed by collapse of voids and rearrangement of the internal structure of the waste and consequent reduction in the void ratio.

7.2 Recommendations for future research

Waste mechanics will continue to evolve at least for foreseeable future as new research comes into and the database of its mechanical properties builds up. Some of the issues pertaining to serviceability still require in-depth study. The following research recommendations are suggested:

- (i) There is a need to develop a systematic framework for interpretation of waste mechanical properties.

- (ii) Further long-term degradation studies are required to verify compressibility behaviour of MSW as observed in this study.
- (iii) The mechanism of secondary compression as observed and understood in this study needs further verification.
- (iv) A systematic experimental study is required to understand the effect of accelerated degradation on waste shear strength.
- (v) The role of tensile/reinforcing constituents in mobilizing shear strength need to be explored further using a three dimensional numerical tool.
- (vi) The numerical modelling carried out in this study can also be extended to numerically verify the effect of degradation on waste shear strength and compressibility.
- (vii) Field monitoring of lateral deformations in landfills is generally missing in published literature. Such data could be used for validation of the design chart proposed in this study.

APPENDIX A

Articles published / submitted to Journals for possible publication

- Singh, M.K. and Fleming, I.R. 2008. Estimation of the Mechanical Properties of MSW during Degradation in a Laboratory Compression Cell. Geotechnical Special Publication, ASCE, 177: 200-207.
- Gharabaghi, B., Singh, M.K., Inkratas, C., Fleming, I.R. and McBean, E. 2008. Comparison of Slope Stability in two Brazilian Municipal Landfills. Waste Management (In Press).
- Singh, M.K., Fleming, I.R. and Sharma, J.S. 2007. Development of a practical method for the estimation of maximum lateral displacement in Large Landfills. Practice Periodical of Hazardous, Toxic, and Radioactive Waste Management, ASCE. (Accepted)
- Singh, M.K., Fleming, I.R. and Sharma, J.S. 2008. Application of a non-linear stress-strain model to Municipal Solid Waste. Geotechnique. (Under Review)
- Singh, M.K., Sharma, J.S. and Fleming, I.R. 2008. A design chart for estimation of horizontal displacements in municipal landfills. Waste Management. (Under Review)
- Singh, M.K. and Fleming, I.R. 2008. Evolution of Compressibility behaviour of Municipal waste during degradation. Journal of Geotechnical and Geoenvironmental Engineering, ASCE. (Under Review)
- Singh, M.K., Sharma, J.S. and Fleming, I.R. 2007. Shear Strength Testing of Intact and Recompacted samples of Municipal Solid Waste. Canadian Geotechnical Journal. (Under Review)

Refereed Conference Proceedings

- Singh, M.K., Fleming, I.R., Sharma, J.S. 2007. Estimating Mechanical Properties of Municipal Waste using Stochastic Modelling. Proc. 11th International Waste Management and Landfill Symposium, Sardinia, Italy.

Non-Refereed Conference Proceedings

Singh, M.K., Sharma, J.S., Fleming, I.R. 2006. Estimation of Elastic Properties of Municipal Solid Waste using Stochastic Modelling. Proceedings, 59th Canadian Geotechnical Conference, October 1-4, Vancouver, BC, Canada.

Singh, M.K., Fleming, I.R., Deewale, P. 2005. Slope Stability Analysis of Brock West Landfill. Proceedings, 58th Canadian Geotechnical Conference, September 18-21, Saskatoon, SK, Canada.